Power Counting Rules for Next-to-Leading Order Hard Thermal Loop Theory

by

Alex Mirza

A Thesis submitted to the Faculty of Graduate Studies of

The University of Manitoba

in partial fulfilment of the requirements of the degree of

MASTER OF SCIENCE

Department of Physics and Astronomy

University of Manitoba

Winnipeg

Canada

Abstract

The goal of this thesis is to determine power counting rules at next-to-leading order (NLO) in the hard thermal loop (HTL) resummation. The original paper by Braaten and Pisarski discusses NLO HTL resummation and argues that there are potentially three types of contributions. We start by studying these terms in the specific case of the boson and fermion self energies in QED and QCD, as these quantities have been calculated in previous literature. For the real and imaginary parts of the fermion and gluon self energies, one needs to calculate only one type of term, as the other two are found to be subleading. However, for the real and imaginary parts of the photon self energy, all types of terms need to be calculated.

Contents

List of Tables

List of Figures

Chapter 1

Introduction

In the first chapter of this thesis we provide an introduction to finite temperature field theory and the hard thermal loop resummation. The first section involves a discussion of zero temperature field theory, specifically scalar field theory and quantum electrodynamics (QED). The next section provides a brief introduction to the imaginary time and real time formalisms of thermal field theory. The real time formalism is then discussed in detail. A discussion of the different bases used to define propagators is included. In the third section, the hard thermal loop resummation techniques of Braaten and Pisarski [1] are introduced. In the fourth and final section of this chapter the hard thermal loop resummation is applied at leading order to a QED plasma. We use the techniques described in the previous section to obtain physical information about the plasma.

1.1 Zero Temperature Field Theory

We consider scalar, electron and photon fields. The generalization to QCD is straightforward. The scalar fields are the easiest to study, as electron fields involve Dirac matrices and photon fields depend on the gauge of the calculations and have Lorentz structure [2].

1.1.1 Scalar Fields

For scalar fields in ϕ^4 theory, the Lagrangian is [3]

$$L = \frac{1}{2}(\partial_\mu \phi)^2 - \frac{1}{2}m^2\phi^2 - \frac{\lambda}{4!}\phi^4. \tag{1.1.1}$$

In (1.1.1), the first two terms combine to form the free Lagrangian, while the last term is the interaction Lagrangian. The equation of motion can be derived from the free Lagrangian in (1.1.1), and is the Klein-Gordon equation,

$$(\partial^\mu \partial_\mu - m^2)\phi(X) = 0. \tag{1.1.2}$$

The inverse of the bare propagator in momentum space is obtained by taking the Fourier transform of (1.1.2):

$$\Delta_0^{-1}(P) = P^2 - m^2 + i\epsilon. \tag{1.1.3}$$

The imaginary term is included to regulate the singularity that would otherwise occur at $P^2 = m^2$ and corresponds to time ordered boundary conditions. The bare propagator is obtained by inverting (1.1.3):

$$\Delta_0(P) = \frac{1}{P^2 - m^2 + i\epsilon}. \tag{1.1.4}$$

The normalization is chosen so that in a Feynman diagram, an internal line corresponds to i times the propagator. In scalar ϕ^4 theory, the vertex is equal to $-i\lambda$.

The self energy Π is defined to represent the interactions that the scalar particle has with the medium in which it is propagating. We define the dressed propagator to be

$$\begin{aligned}\Delta(P) &= \frac{1}{\Delta_0^{-1}(P) - \Pi} = \frac{\Delta_0(P)}{1 - \Pi\Delta_0(P)} = \Delta_0(P)\sum_n (\Pi\Delta_0(P))^n \\ &= \Delta_0(P) + \Delta_0(P)\Pi\Delta_0(P) + \Delta_0(P)\Pi\Delta_0(P)\Pi\Delta_0(P) + ...\end{aligned} \tag{1.1.5}$$

Based on this definition of the dressed propagator, the self energy is equal to i times the corresponding Feynman diagram. The Dyson-Schwinger equation [4] is obtained by inversion of (1.1.5),

$$\Delta^{-1}(P) = \Delta_0^{-1}(P) - \Pi(P). \tag{1.1.6}$$

1.1.2 QED

In this section we consider the photon and electron propagators at zero temperature. This is an extension of the work done for scalars, and details of the analysis can be found in appendix B. Consider the QED Lagrangian at zero temperature in the Feynman gauge [2]:

$$L = \bar{\psi}(i \not{\partial} - m)\psi - \frac{1}{4}F_{\mu\nu}F^{\mu\nu} - e\bar{\psi}\gamma^{\mu}\psi A_{\mu} + \frac{1}{2}(\partial_{\mu}A^{\mu})^2 \tag{1.1.7}$$

$$F_{\mu\nu} = \partial_{\mu}A_{\nu} - \partial_{\nu}A_{\mu}. \tag{1.1.8}$$

Here, A_{μ} and A_{ν} are the photon fields, ψ is the electron field and $\overline{\psi}$ its Dirac conjugate, and $F_{\mu\nu}$ is the field strength tensor. The first two terms of (1.1.8) represent the Lagrangians of free electrons and photons, respectively; the third term represents the interaction between photons and electrons, and the last term is the gauge fixing term. Note that $\not{\partial} = \gamma^{\mu}\partial_{\mu}$, where γ represent the Dirac matrices [2].

The resulting propagator for photons in momentum space is obtained from the second term of (1.1.8) in a manner described in appendix B and is

$$\begin{aligned} D^0_{\mu\nu}(P) &= -\frac{\left[g_{\mu\nu} - (1-\zeta)\frac{P_{\mu}P_{\nu}}{P^2}\right]}{P^2} \\ &= -\frac{g_{\mu\nu}}{P^2}. \end{aligned} \tag{1.1.9}$$

Note that ζ is the gauge fixing term. In the second line of (1.1.9) we have chosen to use the Feynman gauge ($\zeta = 1$), as the resulting propagator has a particularly simple form.

Similar to (1.1.6) for scalars, the effective photon propagator is

$$D_{\mu\nu}(P)^{-1} = (D^0_{\mu\nu})^{-1}(P) - \Pi_{\mu\nu}(P) \tag{1.1.10}$$

where $\Pi_{\mu\nu}(P)$ is the self energy of the photon. Due to (1.1.10), the photon self energy is i times the corresponding bubble diagram.

The propagator for non-interacting fermion fields in momentum space is obtained from the first term of

(1.1.8) and is

$$S_0(P) = (\not{P} - m + i\epsilon)^{-1} = \frac{\not{P} + m}{P^2 - m^2 + i\epsilon}. \tag{1.1.11}$$

Note that the denominator of the fermion propagator in the second term of (1.1.11) is the same as that of the scalar propagator. Both forms are useful depending on the calculation being performed. The effective fermion propagator is defined analogously to (1.1.6):

$$S^{-1}(P) = S_0^{-1}(P) - \Sigma(P). \tag{1.1.12}$$

As in the case of scalars and photons, the fermion self energy is defined to be i times the corresponding diagram.

It is important to note that in QED, photon and electron propagators are matrices. The photon-electron vertex is also a matrix, and is given by $-ie\gamma_\mu$, where e is the QED coupling constant and γ^μ is a gamma matrix.

The extension from QED to QCD can be found in [2]. The gluon and quark propagators are equal to the analogous ones in QED (photons, electrons) up to constants. There is an additional propagator for ghosts.

1.2 Thermal Field Theory

1.2.1 Real Time and Imaginary Time Formalisms

Consider scalar fields. In finite temperature field theory, there are two formalisms that can be used to calculate amplitudes of different diagrams [5]. Note that the time paths in both formalisms satisfy the Kubo-Martin-Schwinger (KMS) condition, which states that the imaginary component of the time must lie in the interval $[0, \beta]$ [6], where $\beta = \frac{1}{T}$.

The imaginary time formalism (ITF) uses a purely imaginary time path (see figure 1.1). The Feynman rules are similar to those in zero-temperature field theory. The main difference is that instead of integrating over the zeroth component of the momentum, a sum over discrete frequencies (the Matsubara frequencies, $k_0 = 2\pi inT$) is performed [6]. Once the integration and summation are complete, an analytic continuation is

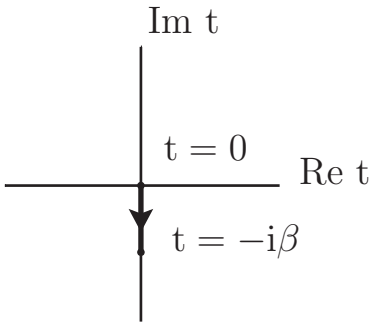

Figure 1.1: The imaginary time integration contour

performed to get the physical result. However, the analytic continuation can be a very complicated process. Another disadvantage to the ITF is that since the time variable is exchanged for temperature the formalism cannot be used in non-equilibrium scenarios [4].

The real time formalism (RTF) involves integrating over a path that includes branches parallel and anti-parallel the real time axis, as shown in figure 1.2 (C_1 and C_2). Due to the fact that we can integrate along either the top path or bottom path of (1.2), the resulting propagator is a matrix. This is known as the doubling of degrees of freedom. We will be using the closed time path ($\sigma = 0$) since in this case the propagator has a particularly simple form. Thus, the branches C_1 and C_2 lie along the real time axis. The RTF can be used to study non-equilibrium scenarios. While it can be more complicated for some calculations, the RTF is the simpler formalism to use for our purposes.

1.2.2 The (1-2) basis

The propagator in the real time formalism is a (2×2) matrix due to the doubling of degrees of freedom discussed in the previous subsection. We now look at one basis in which we can perform calculations: the (1-2) basis. The components of the matrix correspond to the branches on which the particle starts and finishes: Δ_{11} and Δ_{22} correspond to the particle traveling along C_1 and C_2, respectively, while Δ_{12} and Δ_{21} involve the particle traveling from C_1 to C_2 and C_2 to C_1, respectively. The propagator in the (1-2) basis in

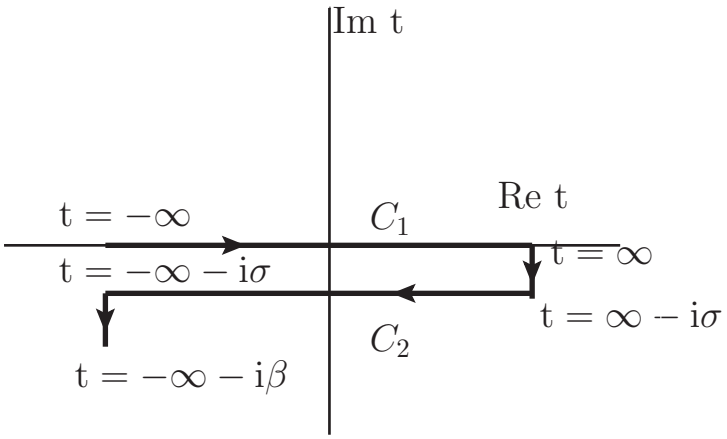

Figure 1.2: The real time integration contour

position space is [7]:

$$\Delta^0(X,Y) = \begin{bmatrix} -i\langle T(\theta(X)\theta(Y))\rangle & -i\langle\theta(Y)\theta(X)\rangle \\ -i\langle\theta(X)\theta(Y)\rangle & -i\langle\tilde{T}(\theta(X)\theta(Y))\rangle \end{bmatrix} \tag{1.2.1}$$

where T and $\tilde{T}$ are the time ordering and anti-time ordering operators, respectively, The (11) component of (1.2.1) is the standard time-ordered propagator seen in zero temperature field theory. The (22) component has time running in the opposite direction, hence the anti-time ordering operator. The (12) and (21) cases do not involve time ordering since times on C_2 are always later than C_1.

The momentum space scalar propagator in the real time formalism is [4]:

$$\Delta^0(K) = \begin{bmatrix} \frac{1}{K^2-m^2+i\epsilon} & 0 \\ 0 & \frac{-1}{K^2-m^2-i\epsilon} \end{bmatrix} - 2\pi i\delta(K^2-m^2) \begin{bmatrix} n_B(|k_0|) & \Theta(-k_0)+n_B(|k_0|) \\ \Theta(k_0)+n_B(|k_0|) & n_B(|k_0|) \end{bmatrix}. \tag{1.2.2}$$

The function $n_B(k_0)$ is the boson distribution function and is defined appendix A.

For fermions and photons, the propagators in the (1-2) basis have the same structure as the scalar propagator and differ by multiplication with an operator:

$$S_0(K) = (\not{K}+m)\tilde{\Delta}(K), \quad \tilde{\Delta}(K) = \Delta(K)|_{n_B(k_0)\to -n_F(k_0)} \tag{1.2.3}$$

$$D^0_{\mu\nu}(K) = -g_{\mu\nu}\Delta(K)|_{m\to 0} \tag{1.2.4}$$

where $n_F(k_0)$ is the Dirac distribution for fermions and is defined in appendix A.

The vertices at finite temperature also have a tensor structure of the form $\Gamma^0_{ijk}, \{i,j,k\} \in \{1,2\}$. One can show that the only non-zero components in scalar theory in the (1-2) basis are:

$$\Gamma^0_{111} = -i\lambda$$

$$\Gamma^0_{222} = i\lambda. \tag{1.2.5}$$

Note that the (111) component is the zero temperature vertex in scalar theory. In QED, the vertices have the same form, but with $\lambda \to e\gamma^\mu$, where e is the QED coupling constant and γ^μ is a Dirac matrix.

The Feynman rules are:

1) Each internal line is $\to i$ times propagator corresponding to that line.

2) The non-zero vertices are $\Gamma_{111} = -\Gamma_{222} = -i\lambda$ in scalar theory, and in QED $\lambda \to e\gamma^\mu$. All other Γ_{ijk} are zero. There are additional vertices in QCD [2].

3) Each loop of momentum $K_i \to \int \frac{d^4k_i}{(2\pi)^4}$ as in zero temperature theory [8].

4) Symmetry factors are the same as they are in zero-temperature theory.

1.2.3 Keldysh Basis

We again consider only scalar fields to start. We can write the propagator (1.2.2) in a different basis. This is useful since the components of the (1-2) basis are not all independent:

$$\Delta_{11} + \Delta_{22} - \Delta_{12} - \Delta_{21} = 0. \tag{1.2.6}$$

A particularly useful choice is the Keldysh basis, which consists of retarded, advanced and symmetric components:

$$\Delta_R = \Delta_{11} - \Delta_{12}$$

$$\Delta_A = \Delta_{11} - \Delta_{21}$$

$$\Delta_S = \Delta_{11} + \Delta_{22}. \tag{1.2.7}$$

The inversion of (1.2.6) and (1.2.7) gives useful expressions for the (1-2)-basis elements:

$$\begin{aligned}
\Delta_{11} &= \frac{1}{2}[\Delta_S + \Delta_A + \Delta_R] \\
\Delta_{12} &= \frac{1}{2}[\Delta_S + \Delta_A - \Delta_R] \\
\Delta_{21} &= \frac{1}{2}[\Delta_S - \Delta_A + \Delta_R] \\
\Delta_{22} &= \frac{1}{2}[\Delta_S - \Delta_A - \Delta_R].
\end{aligned} \tag{1.2.8}$$

The Keldysh basis elements for bare scalar propagators in momentum space are:

$$\begin{aligned}
\Delta_R^0(K) &= \frac{1}{K^2 - m^2 + i\mathrm{sgn}(k_0)\epsilon} \\
\Delta_A^0(K) &= \frac{1}{K^2 - m^2 - i\mathrm{sgn}(k_0)\epsilon} \\
\Delta_S^0(K) &= -2\pi i\delta(K^2 - m^2)\mathrm{sgn}(k_0)(1 + 2n_B(k_0)).
\end{aligned} \tag{1.2.9}$$

The usefulness of the Keldysh basis is immediately apparent: only the symmetric propagator is temperature dependent, and there are fewer non-zero components. Not all the elements of the Keldysh basis are independent, as they can be related by the KMS condition

$$\Delta_S^0(K) = N(k_0)[\Delta_R^0(K) - \Delta_A^0(K)] \tag{1.2.10}$$

where $N(k_0)$ can be either $N_B(k_0) = 1 + 2n_B(k_0)$ or $N_F(k_0) = 1 - 2n_F(k_0)$, depending on the statistics of the propagator. The self energies in the Keldysh basis can be defined in a similar manner to (1.2.8):

$$\begin{aligned}
\Pi_R &= \Pi_{11} + \Pi_{12} \\
\Pi_A &= \Pi_{11} + \Pi_{21} \\
\Pi_S &= \Pi_{11} + \Pi_{22}.
\end{aligned} \tag{1.2.11}$$

The KMS condition for self energies is

$$\Pi_S = N(k_0)(\Pi_R - \Pi_A). \tag{1.2.12}$$

Another advantage of the Keldysh basis is that the Dyson equation has the same form as at zero tem-

perature (see (1.1.6)). Consider first the propagator in the (1-2) basis and look at Δ_{11}. From (1.1.5):

$$\begin{aligned}\Delta_{11} &= \Delta^0_{11} + \Delta^0_{1x}\Pi_{xy}\Delta^0_{y1} + ... \\ &= [\Delta^0_{11} + \Delta^0_{11}\Pi_{11}\Delta^0_{11}] + \Delta^0_{11}\Pi_{12}\Delta^0_{21} + \Delta^0_{12}\Pi_{21}\Delta^0_{11} + \Delta^0_{12}\Pi_{22}\Delta^0_{21} + ...\end{aligned}$$

In comparison, the retarded propagator has the form

$$\begin{aligned}\Delta_R &= \Delta_{11} - \Delta_{12} \\ &= \Delta^0_{11} + \Delta^0_{11}\Pi_{11}\Delta^0_{11} + \Delta^0_{11}\Pi_{12}\Delta^0_{21} + \Delta^0_{12}\Pi_{21}\Delta^0_{11} + \Delta^0_{12}\Pi_{22}\Delta^0_{21} \\ &\quad - [\Delta^0_{12} + \Delta^0_{11}\Pi_{11}\Delta^0_{12} + \Delta^0_{12}\Pi_{21}\Delta^0_{12} + \Delta^0_{11}\Pi_{12}\Delta^0_{22} + \Delta^0_{12}\Pi_{22}\Delta^0_{22}] + ... \\ &= \Delta^0_R + \Delta^0_{11}(\Pi_{11}\Delta^0_R + \Pi_{12}(\Delta^0_{21} - \Delta^0_{22})) + \Delta^0_{12}(\Pi_{21}\Delta^0_R + \Pi_{22}(\Delta^0_{21} - \Delta^0_{22})) + ... \\ &= \Delta^0_R + \Delta^0_{11}(\Pi_{11}\Delta^0_R - \Pi_{12}\Delta^0_R) + \Delta^0_{12}(\Pi_{21}\Delta^0_R - \Delta^0_{22}\Delta^0_R) \\ &= \Delta^0_R + \Delta^0_R\Pi_R\Delta^0_R + ...\end{aligned} \tag{1.2.13}$$

It is easy to see that including higher order terms we obtain $\Delta_R = \frac{1}{(\Delta^0_R)^{-1} - \Pi_R}$, in contrast with the result from the (1-2) basis where $\Delta_{11} \neq \frac{1}{(\Delta^0_{11})^{-1} - \Pi_{11}}$.

Now consider QED. In the Feynman gauge, the Keldysh representation of the fermion and photon propagators are proportional to the scalar propagator:

$$S_i(K) = \not{K}\Delta_i(K)|_{n_B \to -n_F}, \quad i \in \{R, A, S\} \tag{1.2.14}$$

$$D^j_{\mu\nu}(K) = -g_{\mu\nu}\Delta^j(K)|_{m=0}, \quad j \in \{R, A, S\}. \tag{1.2.15}$$

One major disadvantage associated with the Keldysh basis is that the vertices have more complicated structures. There is no need to give the explicit expressions for the vertices, as we can avoid using them. For 1-loop self energies (see appendices) we start in the (1-2) basis and obtain the corresponding expression with Keldysh propagators using (1.2.8). For more complicated calculations (such as for two loop diagrams or diagrams with greater than two external legs) we will use the Mathematica program described in [9] to obtain the integral expression of the diagram.

1.3 Hard Thermal Loop Resummation

1.3.1 Introduction to HTL Resummation

Initially, calculations of quantities in thermal field theory were performed using the standard perturbative loop expansion. However, these calculations yielded gauge dependent results for physical quantities, in particular the gluon damping rate [10], indicating that perturbation theory breaks down. This is caused by the presence of a new dimensionful scale (the temperature). The solution to this problem is the hard thermal loop (HTL) resummation, which entails resumming infinite sets of diagrams .

We define two different momentum scales: 'hard' momenta, which are of order T, and 'soft' momenta, which are of order gT. In a diagram, if any of the external legs are hard, then regular perturbation theory can be applied: if all external legs are soft, perturbation theory must be reorganized.

In this section we calculate the retarded leading order HTL self energies for scalars, photons and electrons. The leading order contribution to any diagram with all legs soft comes from the hard region of integration of the internal loop momentum. Calculations at leading order can be done by taking the momentum in the loop (k_0, k) to be much greater than the momenta of the legs (q_0, q). We will now consider three self energy diagrams at leading order HTL in the high temperature limit and the corresponding effective propagators. The self energies are the scalar self energy (figure 1.3), the photon self energy (figure 1.4), and the electron self energy (figure 1.5). We will discuss the corresponding diagrams in QCD later in this section. We consider the retarded part of the self energies and effective propagators, and from this point suppress the subscript R. The advanced self energies follow from the substitution $i\epsilon \to -i\epsilon$, while the symmetric self energy can be calculated directly from (1.2.12).

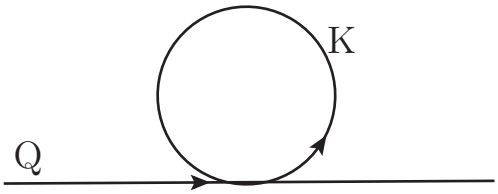

Figure 1.3: The scalar self energy diagram

1.3.2 Scalar Propagator

The calculation of the scalar self energy is done in appendix C1. The result is

$$\Pi = \frac{\lambda T^2}{24}. \tag{1.3.1}$$

Now consider the full propagator defined in (1.1.5). Each term in the sum is a factor of $\frac{\Pi}{Q^2}$ times the previous one. Since we have assumed the external legs are soft ($Q \approx gT$), the order of each term in the series will be the same. Thus, for soft Q the bare propagator cannot be used and we must use the HTL resummed propagator instead. Therefore, from (1.1.5), the leading order HTL propagator in scalar ϕ^4 theory is

$$\Delta(Q) = \frac{1}{Q^2 - m^2 - \Pi}. \tag{1.3.2}$$

1.3.3 QED Propagators

We consider the effective photon propagator at finite temperature. From the analysis presented in appendix B,

$$D_{\mu\nu}(Q) = -\frac{P^T_{\mu\nu}(Q)}{Q^2 - \Pi_T} - \frac{P^L_{\mu\nu}(Q)}{Q^2 - \Pi_L} - \frac{P^0_{\mu\nu}(Q)}{Q^2}. \tag{1.3.3}$$

The calculations of Π_L and Π_T, the longitudinal and transverse photon self energies, in the first order HTL approximation, are done in appendices C2.1 and C2.2. Using $\omega_p = \frac{eT}{3}$ (see appendix A for a list of mass scales used in this thesis),

$$\Pi_L(Q) = 3\omega_p^2 \frac{Q^2}{q^2}\left[\frac{q_0}{2q}\ln\left(\frac{q_0 + q + i\epsilon}{q_0 - q + i\epsilon}\right) - 1\right] \tag{1.3.4}$$

$$\Pi_T(Q) = \frac{3\omega_p^2}{2}\left[\frac{q_0^2}{q^2} - \frac{q_0 Q^2}{2q^3}\ln\left(\frac{q_0 + q + i\epsilon}{q_0 - q + i\epsilon}\right)\right]. \tag{1.3.5}$$

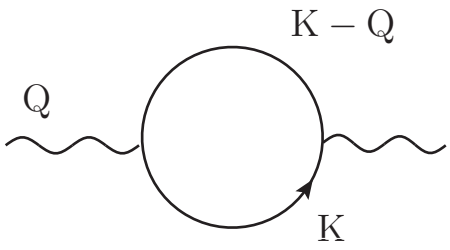

Figure 1.4: The photon self energy diagram

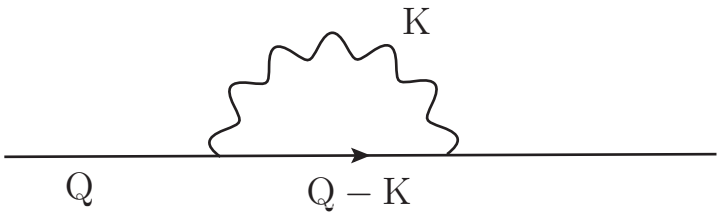

Figure 1.5: The fermion self energy diagram

Unlike the HTL scalar self energy, both (1.3.4) and (1.3.5) depend on the external momentum.

The effective fermion propagator is studied in appendix B. Using $P_{\pm}(Q) = \frac{1}{2}(\gamma_0 \pm \vec{\gamma}\cdot\hat{q})$ and the form of the fermion self energy from (B.22) of appendix B, the effective fermion propagator is

$$\begin{aligned}
&\Sigma(Q) = \Sigma^{(0)}(Q)\gamma_0 - \Sigma^{(s)}\vec{\gamma}\cdot\hat{q} \\
&\Sigma_{\pm}(Q) = \Sigma^{(0)}(Q) \pm \Sigma^{(s)}(Q) \\
&S(Q) = \Delta_+(Q)P_-(Q) + \Delta_-(Q)P_+(Q) \\
&\Delta_+(Q) = \frac{1}{q_0 - q - \Sigma_+(Q)}, \qquad \Delta_-(Q) = \frac{1}{q_0 + q - \Sigma_-(Q)}.
\end{aligned} \tag{1.3.6}$$

The leading order fermion self energy is calculated in appendix C3. Using $m_F^2 = \frac{e^2T^2}{8}$, the fermion self energy is found to be

$$\Sigma(P) = \frac{m_F^2}{q}\left[\frac{1}{2}\ln\left(\frac{q_0+q+i\epsilon}{q_0-q+i\epsilon}\right)\gamma_0 - \left[\frac{q_0}{2q}\ln\left(\frac{q_0+q+i\epsilon}{q_0-q+i\epsilon}\right) - 1\right]\hat{q}\cdot\vec{\gamma}\right]. \tag{1.3.7}$$

The calculation of the QCD gluon self energy is similar to the photon self energy. However, in addition to the calculation of the diagram in figure 1.4, there are three additional diagrams: the gluon tadpole (figure

1.3 with gluon lines replacing scalar lines), the diagram in 1.4 with the quark loop replaced with a ghost loop and the diagram with the quark loop replaced with a gluon loop. The quark self energy is given by (1.3.7) up to a constant. In QCD the ghost self energy must also be considered. It is given by a diagram similar to figure 1.5 but with the fermion lines replaced with ghost lines. We will show in the next chapter that the bare ghost propagator is sufficient in leading order HTL resummation.

1.4 Physics from HTL Resummation

Physical information can be extracted from the poles of the resummed propagator. The propagator represents the probability amplitude of a given mode, and when the denominator of the propagator is zero the propagator blows up, indicating that the mode is dominant.

1.4.1 Photons in a Plasma

The poles of the photon propagator are given by the following equations:

$$\begin{aligned} Q^2 - \Pi_T(Q)|_{q_0=\omega_T(q)+i\gamma_T(q)} &= 0 \\ Q^2 - \Pi_L(Q)|_{q_0=\omega_L(q)+i\gamma_L(q)} &= 0 \end{aligned} \tag{1.4.1}$$

where Π_L and Π_T are given in (1.3.4) and (1.3.5). The real parts of the poles are $\omega_{L,T}(q)$ and give the dispersion relations of the longitudinal or transverse waves traveling in the plasma, and the imaginary parts of the poles $\gamma_{L,T}(q)$ give the corresponding damping rates for waves of that mode. Assuming $\frac{\gamma}{\omega} << 1$, (1.4.1) gives

$$\begin{aligned} \omega^2_{L,T}(q) &= q^2 + \mathrm{Re}\Pi_{L,T}(q_0) = \omega_{L,T}(q), q) \\ \gamma_{L,T}(q) &= -\frac{1}{2\omega_{L,T}}\mathrm{Im}\Pi_{L,T}(q_0) = \omega_{L,T}(q), q). \end{aligned} \tag{1.4.2}$$

The equations in (1.4.2) cannot be solved analytically, but approximate solutions for the frequencies $\omega_{L,T}$ can be found in the limit of large and small q. They are:

$$\begin{aligned} q << m: \qquad & \omega_L^2 \approx \omega_p^2 + \frac{3}{5}q^2 \\ & \omega_T^2 \approx \omega_p^2 + \frac{6}{5}q^2 \\ q >> m: \qquad & \omega_L \approx q\bigg(1 + 2\text{exp}\bigg(-\frac{\frac{2}{3}q^2 + \omega_p^2}{\omega_p^2}\bigg)\bigg) \\ & \omega_T^2 \approx q^2 + \frac{3}{2}\omega_p^2. \end{aligned} \tag{1.4.3}$$

The corresponding residues for $q >> m$ are

$$Z_L(q) \approx \frac{2q}{m^2}\text{exp}\bigg(-\frac{q^2+m^2}{m^2}\bigg) \tag{1.4.4}$$

$$Z_T(q) \approx \frac{1}{2q}. \tag{1.4.5}$$

Note the following:

1) For $q \to 0$ the longitudinal and transverse mode frequencies are identically $\omega_p = \frac{eT}{3}$. Therefore, for small 3-momenta q the two modes cannot be distinguished from one another.

2) For large q longitudinal modes decouple (see 1.4.4), and as a result only transverse modes will be present [6]. Note that at zero temperature only transverse modes are present, which makes sense since the low temperature and high momentum limits should be equivalent.

3) At large q, the transverse modes have an effective mass $m_\infty = \frac{e^2T^2}{6}$.

4) The leading order damping rate is zero, as the imaginary parts in (1.4.2) vanish because $\omega_{L,T}(q) > q$ for all q. From the definition of the photon self energies in (1.3.4) and (1.3.5), the only way the result will have an imaginary part is if the argument of the logarithm is less than zero; the condition is $q_0 < 0$. However, from (1.4.3) we see that for large momentum the transverse and longitudinal plasma frequencies are always greater than q. Since $q_0 \to \omega_{T,L}$, there is no damping rate in leading order HTL.

We can also discuss static screening. The static limits of the self energies $\Pi_{L,T}$ are

$$m_E^2 = \Pi_L(q_0 = 0, q \to 0) = 3\omega_p^2$$
$$m_B^2 = \Pi_T(q_0 = 0, q \to 0) = 0. \tag{1.4.6}$$

Consider a charge $\mathcal{Q}$ placed in a medium. The potential felt by this charge is obtained by the Fourier transform of the static propagator $D_{00}(0, q)$:

$$V(r) = \mathcal{Q} \int \frac{d^3q}{(2\pi)^3} \frac{e^{iq\cdot r}}{q^2 + \Pi_L(q_0, q \to 0)} = \frac{\mathcal{Q}}{r} e^{-rm_E} = \frac{\mathcal{Q}}{r} e^{-\frac{r}{r'}}. \tag{1.4.7}$$

The result here is the standard representation of a screened potential [11]. The quantity r' is called the deBye radius, and using (1.4.6) it is given by

$$r' = \frac{1}{m_E} = \frac{1}{\sqrt{3}\omega_p}. \tag{1.4.8}$$

Physically this result corresponds to the screening of a static electric field. There is no screening of static magnetic fields due to the fact that the static limit of the transverse self energy vanishes.

1.4.2 Fermions in the Plasma

Next we will look at the fermion modes. The fermion self energy in the HTL approximation is calculated in appendix C3.

The HTL fermion propagator has the form

$$S(Q) = \frac{1}{2}\Delta_+(Q)(\gamma_0 - \gamma \cdot \hat{q}) + \frac{1}{2}\Delta_-(Q)(\gamma_0 + \gamma \cdot \hat{q}) \tag{1.4.9}$$

where

$$\begin{aligned} \Delta_\pm(Q) &= \frac{1}{q_0 \mp q - \Sigma_\pm(Q)} \\ &= \left(q_0 \mp q - \frac{m_F^2}{2q} \left[(1 \mp \frac{q_0}{q}) \ln \left[\frac{q_0 + q + i\epsilon}{q_0 - q + i\epsilon} \right] \pm 2 \right] \right)^{-1}. \end{aligned} \tag{1.4.10}$$

The dispersion relations for fermions are defined analogous to (1.4.1):

$$q_0 - q - \Sigma_+(Q)|_{q_0 = \omega_+(q) + i\gamma_+(q)} = 0$$
$$q_0 + q - \Sigma_-(Q)|_{q_0 = \omega_-(q) + i\gamma_-(q)} = 0. \tag{1.4.11}$$

From (1.4.9), when the denominator of Δ_+ tends to zero the corresponding mode that dominates is the one that satisfies $\gamma_0 - \gamma \cdot \hat{q} = 0$, and when the denominator of Δ_- tends to zero the corresponding mode that dominates is the one that satisfies $\gamma_0 + \gamma \cdot \hat{q} = 0$. The former condition indicates a positive helicity over chirality ratio, while the latter indicates a negative helicity over chirality ratio. Analogous to (1.4.2), we find that

$$\omega_\pm^2(q) = q^2 + \mathrm{Re}\Sigma_\pm(q_0 = \omega_\pm(q), q)$$
$$\gamma_\pm(q) = -\frac{1}{2\omega_\pm}\mathrm{Im}\Sigma_\pm(q_0 = \omega_\pm(q), q). \tag{1.4.12}$$

From [6],

$$q >> m \qquad \omega_+(q) \approx q + \frac{m_F^2}{q}$$
$$\omega_-(q) \approx q + \frac{2q}{e}\exp\left(-\frac{2q^2}{m_F^2}\right) \tag{1.4.13}$$

$$q << m \qquad \omega_\pm(q) \approx m_F \pm \frac{1}{3}q. \tag{1.4.14}$$

The residues are

$$Z_+(q) \approx 1 + \frac{m_F^2}{2q^2}\left[1 - \ln\left(\frac{2q^2}{m_F^2}\right)\right] \tag{1.4.15}$$
$$Z_-(q) \approx \frac{2q^2}{em_F^2}\exp\left(-\frac{2q^2}{m_F^2}\right). \tag{1.4.16}$$

Note the following:

1) In the vacuum, only fermions with a positive helicity over chirality ratio are present. Equivalently, when the fermion mass approaches zero, the chirality operator approaches the helicity operator, leading to a ratio of +1. Similar to the longitudinal photon case, the residues of the negative ratio modes tend to zero exponentially (decoupling from the medium) (see 1.4.16). This is seen in the plasma frequency at large momentum ($q >> m$).

2) Introduction of the heat bath allows the negative helicity to chirality ratio states to propagate.

3) In the limit $m >> q$ the positive and negative states are indistinguishable.

4) Similar to the case of photons, the imaginary part of the leading order fermion self energy vanishes. This occurs because the plasma frequencies in (1.4.13) are always larger than q, thus there is no way the argument of the logarithm of (1.3.7) can be negative.

Chapter 2

Power Counting at Leading Order

Power counting arguments allow us to determine the order of a given diagram without having to do extensive calculations (such as those performed for the photon and electron self-energies in appendices C2 and C3). In this chapter we consider power counting at leading order in QCD. Note that the rules we develop can be extended to scalar theory and QED. In the first section we consider diagrams that contain only 3-gluon and quark-gluon vertices and develop basic power counting rules. We then consider the 4-gluon vertex and ghost lines. Diagrams with a 4-gluon vertex do not contribute in leading order HTL with one exception (the gluon tadpole). Similarly, there are no HTLs for diagrams with external ghost lines, and at soft momentum we can use the bare ghost propagator. In our notation, K represents a hard momentum (of order T) and Q represents a soft momentum (of order gT).

2.1 Power Counting with 3-Gluon and Quark-Gluon Vertices

In this section we will only consider diagrams consisting of 3-gluon and quark-gluon vertices. The Feynman rules for these vertices are given in [6]. We use the following notation:

$$\begin{aligned}
&\text{Number of vertices} = v \\
&\text{Number of 3 gluon vertices} = v_B \\
&\text{Number of quark gluon vertices} = v_F \\
&\text{Number of propagators} = I \\
&\text{Number of gluon propagators} = I_B \\
&\text{Number of quark propagators} = I_F \\
&\text{Number of external legs} = E \\
&\text{Number of external gluon legs} = E_B \\
&\text{Number of external quark legs} = E_F. \qquad (2.1.1)
\end{aligned}$$

Using (2.1.1) the standard topological constraints are [12],

$$m = I - \sum_{k=3}^{E} v_k + 1, \qquad 2I + E = \sum_{k=3}^{E} k v_k \qquad (2.1.2)$$

where m is the number of loops and v_k is the number of k-point functions. For 1-loop diagrams with only 3-leg vertices, (2.1.2) gives

$$I = v = E. \qquad (2.1.3)$$

Consider a 1-loop diagram with E external momenta labeled $Q_i (i = 1, 2...)$ and I_F fermion propagators. To find the order of this diagram we follow these steps:

1) Obtain an expression for the diagram in terms of the elements of the matrix propagator in (1.2.2), (1.2.3) and (1.2.4) and using vertices in the (1-2) basis (1.2.5). Convert the (1-2) propagators to Keldysh propagators using (1.2.8).

2) There are I terms in the sum, each containing a single symmetric propagator with a different argument. For each term, shift the loop momentum so that all symmetric propagators now depend only on the loop

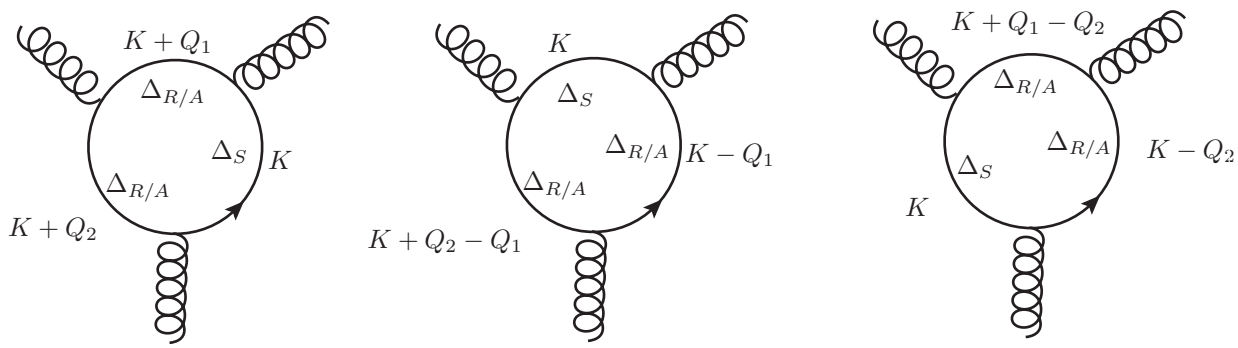

Figure 2.1: Terms in the integrand of a 3-point function after shifting so that all symmetric propagators have the same argument.

momentum K. For example, if the argument of the symmetric propagator is $K + \sum_{i=1}^{j} Q_i$, make the shift $K \to K - \sum_{i=1}^{j} Q_i$. This is illustrated for a 3-point function in figure 2.1.

3) Each additional propagator with argument $K + \sum_{i=1}^{r} Q_i - \sum_{j=1}^{t} Q_j$ appears to contribute a factor $\frac{1}{(K+\sum_{i=1}^{r} Q_i - \sum_{j=1}^{r} Q_i)^2}$. However, any K^2 terms in the integrand vanish upon performing the k_0 integration due to the presence of the $\delta(K^2)$ factor from the symmetric propagator (1.2.9). Thus, $\frac{1}{(K+\sum_{i=1}^{r} Q_i - \sum_{j=1}^{t} Q_j)^2} \sim \frac{1}{K\cdot(\sum_{i=1}^{r} Q_i - \sum_{j=1}^{t} Q_j)}$.

4) Quark propagators have a similar structure to gluon propagators except for multiplication by an operator in the numerator (1.2.14). Since we are only concerned with the leading order result, we can neglect any external momenta in the numerators of quark propagators, thus each quark propagator produces an additional factor of K.

5) Similarly, a 3-gluon vertex contributes a factor of K relative to a quark-gluon vertex.

The results can be summarized as follows:

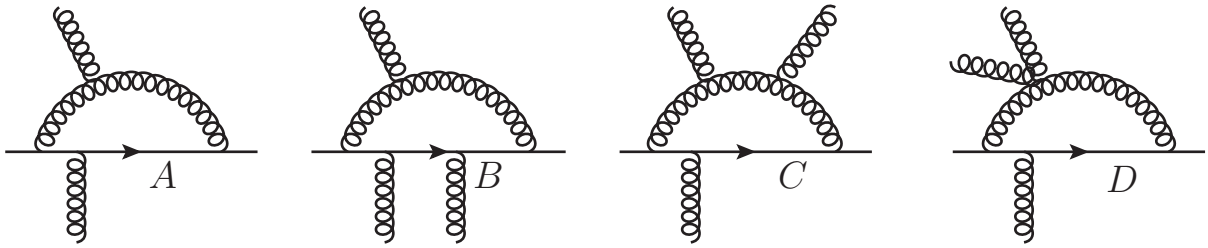

Figure 2.2: The different ways to add a gluon leg to an arbitrary diagram in QCD (note that D is discussed in the next section).

$$\begin{aligned}
&\text{symmetric propagator} \sim \delta(K^2) N_{B/F}(k_0) \\
&\text{non}-\text{symmetric propagators} \sim \frac{1}{K \cdot Q} \\
&\text{numerator of quark propagators} \sim K \\
&3-\text{gluon vertices} \sim gK \\
&\text{quark}-\text{gluon vertices} \sim g.
\end{aligned} \tag{2.1.4}$$

Using (2.1.4), the integral expression for an arbitrary diagram is

$$\begin{aligned}
\Gamma \quad &\sim g^v \int d^4K \frac{K^{I_F+v_G}}{(K\cdot Q)^{I-1}} N_{F/B}(k_0)\delta(K^2) \\
&\sim g^v \int d^4K \frac{K^{v+I_F-v_F}}{(K\cdot Q)^{v-1}} N_{F/B}(k_0)\delta(K^2)
\end{aligned} \tag{2.1.5}$$

where in the last line we used (2.1.3). We deduce the order of Γ starting from (2.1.5) step by step:

1) Use the delta function of the symmetric propagator to integrate over dk_0:

$$\Gamma \sim g^v \int d^3k \frac{N_{B/F}(k)}{k} \frac{k^{v+I_F-v_F}}{(kQ)^{v-1}}.$$

Note that when the k_0 integration is done, $K \cdot Q = k_0 q_0 - k \cdot q \to \sum_{n=\pm 1} \left(nkq_0 - k \cdot q\right) \sim kQ$.

2) Substitute $\int d^3k \sim \int dk k^2$ and use $\int dk k^n N_{B/F}(k) \sim T^{n+1}$ (A.7):

$$\begin{aligned}
\Gamma \quad &\sim g^v \int dk k N_{B/F}(k) \frac{k^{v+I_F-v_F}}{(kQ)^{v-1}} \\
&\sim g^v Q^{1-v} \int dk k^{I_F-v_F+2} N_{B/F}(k) \propto g^v Q^{1-v} T^{I_F-v_F+3}.
\end{aligned} \tag{2.1.6}$$

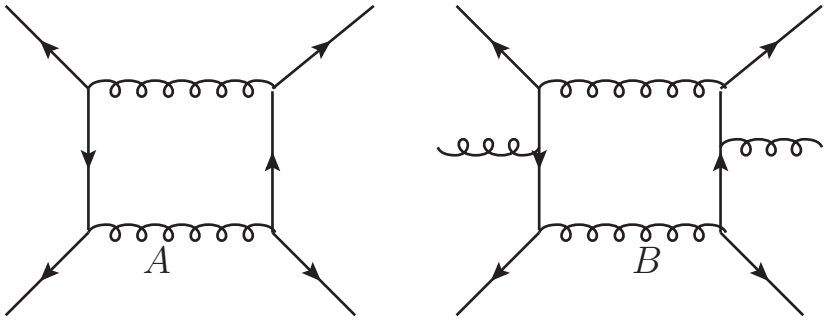

Figure 2.3: Constructing an arbitrary diagram in QCD.

Now consider the relative order of the diagrams in figure 2.2. To get figures 2.2B and 2.2C we added a gluon leg to 2.2A, but connect one to a quark propagator and the other to a gluon propagator. The result is that, compared to figure 2.2A, figure 2.2B has an additional quark propagator and an additional quark-gluon vertex, and figure 2.2C has an additional gluon propagator and 3-gluon vertex. Using (2.1.4):

$$\begin{aligned} 2.2B &\sim g\frac{K}{K\cdot Q}\big(2.2A\big) \\ 2.2C &\sim gK\frac{1}{K\cdot Q}\big(2.2A\big) \\ \rightarrow 2.2B \sim 2.2C &\sim \frac{g}{Q}\big(2.2A\big). \end{aligned} \tag{2.1.7}$$

From (2.1.7), we can conclude that in terms of the order of a diagram, it is equivalent to connect an external gluon leg to a quark propagator or a gluon propagator. For simplicity we will now assume that we always attach external gluon legs to quark propagators.

Now we want to use our power counting arguments to get the order of a diagram in terms of external variables. A 1-loop diagram with E_F and E_B external fermion and gluon legs can be built in the following manner (see figure 2.3):

1) Construct the diagram with E_F quark legs and no gluon legs. Each pair of quark legs contributes a quark propagator, a gluon propagator and two quark-gluon vertices. For $E_B = 0$,

$$v_F = E_F, \quad I_F = I_B = \frac{E_F}{2}. \tag{2.1.8}$$

2) Connect E_B external gluon legs to the quark propagator. Every external gluon leg contributes an addi-

tional quark propagator and quark-gluon vertex. Thus we have in general

$$v_F = E_F + E_B, \quad I_F = \frac{1}{2}E_F + E_B, \quad I_B = \frac{E_F}{2}. \tag{2.1.9}$$

3) Substitute (2.1.9) into (2.1.6):

$$\Gamma_{E_F \neq 0} \sim g^E Q^{1-E} T^{3-\frac{E_F}{2}} \sim g T^{4-E-\frac{1}{2}E_F} \tag{2.1.10}$$

where in the last line we used $Q \sim gT$.

Now we explain the subscript in the first line of (2.1.10). It is important to note (2.1.10) is not correct for diagrams with propagators with all the same statistics, as these diagrams result in integrals in which the leading order term vanishes. To see how this happens, we consider one example in detail. The photon self energy is given by

$$\begin{aligned}
\Pi^{\mu\nu}(P) \quad &\propto g^2 \int d^4K Tr[\gamma^\mu S(K)\gamma^\nu S(K+Q)] \\
&\propto g^2 \int d^4K K_\alpha K_\beta Tr[\gamma^\mu\gamma^\alpha\gamma^\nu\gamma^\beta]\left(\frac{N_F(k_0)\delta(K^2)}{(K+Q)^2} + \frac{N_F(k_0+q_0)\delta((K+Q)^2)}{K^2}\right) \\
&\propto g^2 \int d^4K (K^\mu(K+Q)^\nu + K^\nu(K+Q)^\mu - g^{\mu\nu}K\cdot(K+Q))\left(\frac{N_F(k_0)\delta(K^2)}{(K+Q)^2} + \frac{N_F(k_0+q_0)\delta((K+Q)^2)}{K^2}\right) \\
&\propto g^2 \int d^4K \Bigg[(K^\mu(K+Q)^\nu + K^\nu(K+Q)^\mu - g^{\mu\nu}K\cdot(K+Q))\frac{N_F(k_0)\delta(K^2)}{(K+Q)^2} \\
&\quad + ((K-Q)^\mu K^\nu + (K-Q)^\nu K^\mu - g^{\mu\nu}(K-Q)\cdot K)(\frac{N_F(k_0)\delta(K^2)}{(K-Q)^2})\Bigg].
\end{aligned} \tag{2.1.11}$$

Taking the leading order terms of the numerators of (2.1.11),

$$\Pi^{\mu\nu}(P) \propto g^2 \int d^4K N_F(k_0)\delta(K^2)[2K^\mu K^\nu - g^{\mu\nu}K^2]\left[\frac{1}{(K+Q)^2} + \frac{1}{(K-Q)^2}\right].$$

Following the strategy outlined in section 2.1, $K^2 = 0$ due to the delta function and we neglect the Q^2 terms in the denominator because they are subleading. We obtain

$$\Pi^{\mu\nu}(P) \propto g^2 \int d^3K \sum_{n=\pm 1} \frac{nK^\mu K^\nu N_F(k)}{k}\left[\frac{1}{nkq_0 - k\cdot q} - \frac{1}{nkq_0 - k\cdot q}\right] = 0. \tag{2.1.12}$$

Thus, the term that would give us the order predicted by (2.1.10) vanishes, and the true leading order term is a factor of g smaller. We call this additional factor of g the statistical suppression factor. This cancellation

occurs in any diagram with no external fermion legs. The cancellation is proven for an n-gluon vertex in appendix E, and occurs for quark, gluon and ghost loops. We can adjust the power counting rules given in (2.1.10) by multiplying by a factor of $g^{\delta_{E_F 0}}$, which is equal to g for $E_F = 0$ and 1 for $E_F \neq 0$. Including this factor, (2.1.10) becomes

$$\begin{aligned} \Gamma &\sim g^E g^{\delta_{E_F 0}} Q^{1-E} T^{3-\frac{1}{2}E_F} \\ &\sim g g^{\delta_{E_F 0}} T^{4-E-\frac{E_F}{2}} \end{aligned} \tag{2.1.13}$$

where we have used $Q \sim gT$ in the last line.

An exception to (2.1.13) specific to QED is Furry's theorem, which states that diagrams with an odd number of external photon legs vanishes. A proof of Furry's theorem is included as appendix I. Note that Furry's theorem is not a result of HTL and is valid in zero temperature field theory.

2.2 4-Gluon Vertices and Ghost Contributions

In this section we will discuss power counting involving 4-gluon vertices and ghost lines.

The 4-gluon vertex is proportional to g^2 [2]. We can construct diagrams with a 4-gluon vertex by adding an external gluon leg to a 3-gluon vertex. This is shown in figure 2.2 D. Consider the orders of the diagrams in figures 2.2 B and D relative to A by applying the power counting rules defined in (2.1.4). In figure 2.2 B there is an additional 3-gluon vertex and a gluon propagator relative to A, and in figure 2.2 D there is an additional 4-gluon vertex and one less 3-gluon vertex than in A:

$$\begin{aligned} & 2.2B && \sim \frac{gK}{KQ}(2.2A) \\ & 2.2D && \sim \frac{g^2}{gK}(2.2A) \\ & \frac{2.2D}{2.2B} && \sim \frac{g^2 KQ}{g^2 K^2} \sim \frac{KQ}{K^2} \sim g \\ \rightarrow\ & 2.2D && \sim g(2.2B). \end{aligned} \tag{2.2.1}$$

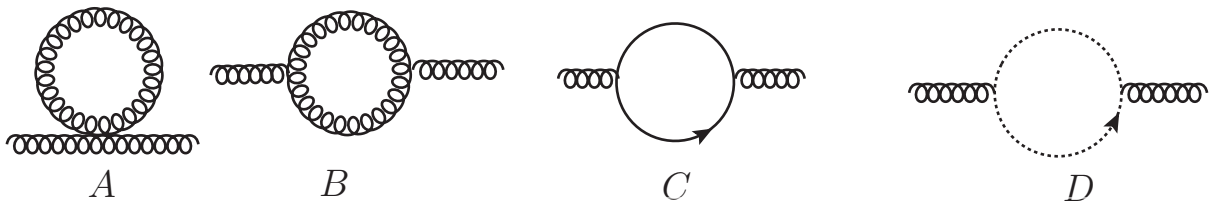

Figure 2.4: The gluon self energy diagrams

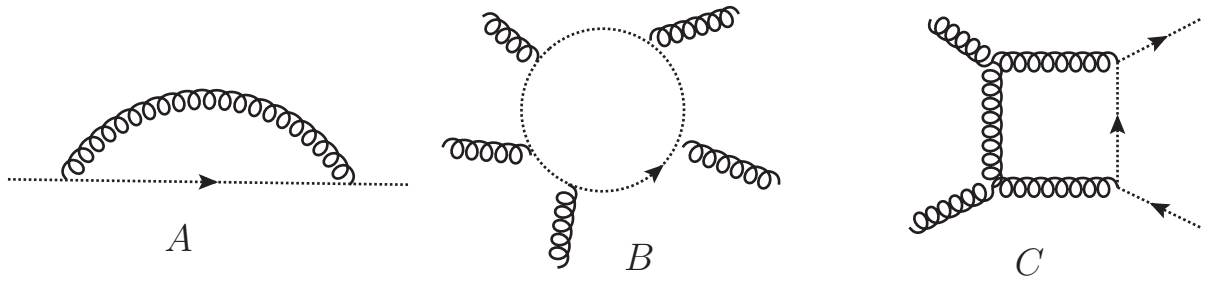

Figure 2.5: Diagrams in QCD involving ghosts.

Thus, we see that diagrams with a 4-gluon vertex are suppressed by a factor of g relative to the corresponding diagrams with two 3-gluon on quark-gluon vertices instead. Therefore, when comparing diagrams with the same numbers of external lines E_F and E_B, diagrams with 4-gluon vertices are subleading.

There is one exception to the above analysis, and that is the gluon tadpole (figure 2.4A), which contains a 4-gluon vertex and contributes at the same order as figures 2.4 B and C. There is a factor of g from the 4-gluon vertex in the tadpole relative to the other gluon self energy diagram, but there is no statistical suppression factor because there is only one propagator. In contrast, in figures 2.4 B, C and D, which do not contain a 4-gluon vertex, all propagators in each diagram obey the same statistics, and as a result there is a statistical suppression factor. Thus, all four diagrams in figure 2.4 must be considered when determining the gluon self energy.

We now consider diagrams with ghost lines (see figures 2.5 A, B and C for examples). Consider the ghost self energy (see figure 2.5A). The bare ghost propagator is given in [2]:

$$G(P) = \frac{\delta^{ab}}{P^2 + i\epsilon}. \tag{2.2.2}$$

The ghost self energy will contribute at leading order in the HTL resummation if it is proportional to the inverse propagator at soft momentum, $G^{-1}(P) \propto g^2T^2$. The ghost vertex is proportional to the incoming ghost momentum [2]. Therefore, the combination of the two ghost-gluon vertices will contribute a factor of order g^2KQ. The ghost self energy is given by

$$\text{ghost self energy} \sim g \times g^2 \int d^4K \frac{QKN_B(k_0)}{K \cdot Q} \sim g^3T^2. \tag{2.2.3}$$

The first g in (2.2.3) is the statistical suppression factor because ghost and gluon lines both carry boson distribution factors. As a result, when constructing the effective propagator from the Dyson equation, even at soft momentum the ghost self energy correction will be suppressed by a factor of g relative to the bare inverse propagator. Therefore, the ghost self energy does not contribute at leading order HTL and we can use bare ghost lines. A similar argument indicates that the 1-loop diagram for the ghost-gluon vertex is subleading relative to the bare ghost-gluon vertex for soft momentum. Therefore, diagrams with external ghost lines do not contribute at leading order. However, diagrams with internal ghost lines and no external ghost legs do contribute at leading order HTL, as at each vertex the incoming momentum is always hard. An example of this is the gluon self energy (figure 2.4 D).

2.3 Determining the Dimensionless Order of a Diagram

The dimensionless order of a diagram is determined in the following manner: if the order of a diagram obtained from (2.1.13) is $\Gamma \sim g^\alpha T^\beta$, we divide the result by $(gT)^\beta$ to obtain $\hat{\Gamma} \sim g^{\alpha-\beta}$. Consider diagrams with different numbers of external fermion lines:

$$\begin{aligned}
\hat{\Gamma}_{E_F=0} &\sim g \times g^E Q^{1-E} T^3 \sim g^2 T^{4-E} \to g^{E-2} \\
\hat{\Gamma}_{E_F=2} &\sim Q^E g^{1-E} T^2 \sim g T^{3-E} \to g^{E-2} \\
\hat{\Gamma}_{E_F=4} &\sim Q^n g^{1-n} T \sim g T^{2-E} \to g^{E-1} \\
\hat{\Gamma}_{E_F\geq 2} &\sim g^E Q^{1-E} T^{3-E-\frac{1}{2}E_F} \sim g T^{4-E-\frac{1}{2}E_F} \to g^{E+\frac{1}{2}E_F-3}.
\end{aligned} \tag{2.3.1}$$

Thus we see that diagrams with $E_F = 0$ and $E_F = 2$ are the same order while diagrams with $E_F \geq 4$

QCD	QED	Scalar ϕ^4 Theory
3-gluon vertex	none	none
4-gluon vertex	none	4-scalar vertex
quark-gluon vertex	electron-photon vertex	none
quark propagator	electron propagator	none
gluon propagator	photon propagator	scalar propagator
ghosts	none	none

Table 2.1: The power counting equivalent quantities in QCD, QED and scalar theory.

are of higher order. Therefore, only diagrams with $E_F = 0$ and $E_F = 2$ contribute at leading order [6].

2.4 Conclusions

The following conclusions can be made from the preceding sections on power counting:

1) Diagrams containing 4-gluon vertices do not contribute at leading order except for the gluon tadpole

2) The bare ghost propagator can be used in leading order HTL, and diagrams with external ghost lines do not contribute

3) Only diagrams with zero quark legs and two quark legs contribute at leading order

4) The leading order term of a diagram is given by (2.1.13):

$$\Gamma \sim g \times g^{\delta_{E_F 0}} g^v Q^{1-v} T^{3-\frac{1}{2}E_F} \sim g^{1+\delta_{E_F 0}} T^{4-E-\frac{1}{2}E_F}.$$

These results can be extended to scalar theory and QED. The analogous quantities are outline in table 2.1. Analogous quantities follow the same power counting rules.

Chapter 3

Hard Thermal Loop Resummation at Next-to-Leading Order

Up to this point, we have only looked at diagrams at leading order, where we are taking the leading order of the momentum ratio $\frac{Q}{K}$. The NLO case is more complicated: reference [1] identifies three potential contributions. However, it is known that inclusion of all three of these terms overestimates the NLO result. The primary goal of this thesis is to develop a set of rules that will accurately identify the diagrams that contribute at NLO. We consider the boson and fermion self energies, as both the real and imaginary parts of these quantities have been studied in great detail and obey simple symmetry relations (see appendix F).

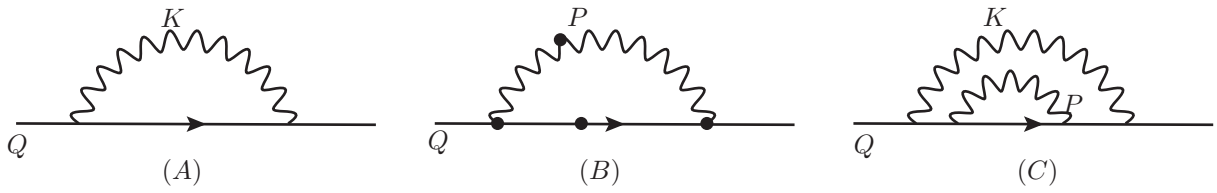

Figure 3.1: Examples of the three different diagrams that contribute at NLO for the fermion self energy. In the second diagram the dots represent effective propagators and vertices.

3.1 Naive NLO Power Counting

In the leading order calculation, there is only one type of term that contributes: the one loop diagram with hard internal momentum expanded at leading order $\frac{Q}{K}$. According to [1], there are three different types of terms that can contribute at NLO (see figure 3.1). We will use the power counting arguments of (2.1.10) to estimate the order of these terms for $\Sigma^{(0)}$ in the limit $q \to 0$. For $\Sigma^{(0)}(q_0, 0)$, the three terms are:

1) (1 loop soft) represents the one-loop diagram with soft internal momentum and requires the use of effective propagators and vertices (constructed from the leading order results). The (1 loop soft) diagram for the fermion self energy is given in figure 3.1B. We consider only the term with the boson statistical factor since it will be the largest at small momentum due Bose enhancement (see A.6). For a soft static fermion the integrand is constructed from the following pieces:

i. g^2 from two effective vertices.

ii. $\frac{N_B(p_0)\delta(P^2)}{2P\cdot Q+Q^2}$ from the propagators. Note that the retarded/advanced propagator is actually of order $(P+Q)^2$, but the P^2 term vanishes due to the presence of the delta function from the symmetric propagator. The Q^2 term is of the same order as $P \cdot Q$ since both P and Q are soft.

iii. $p_0 + q_0$ from the numerator of the fermion propagator.

Constructing the integral from the contributions above and using the soft limit of $N_B(p)$ in the fourth line:

$$\begin{aligned}
(1 \text{ loop soft}) &\sim g^2 \int d^4p \frac{(p_0+q_0)N_B(p_0)\delta(P^2)}{2P\cdot Q+Q^2} \\
&\sim g^2 \int d^3p \frac{N_B(p)}{pQ} \\
&\sim \frac{g^2}{Q} \int dp p N_B(p) \\
&\sim \frac{g^2 T}{Q} \int dp \\
&\sim \frac{g^2 T(gT)}{Q} \sim g^2 T \sim g(LO)
\end{aligned} \tag{3.1.1}$$

where we have used the fact that the leading order term is

$$(\text{LO})\Sigma^{(0)}(q_0, 0) \sim gT \tag{3.1.2}$$

To do the p_0 integration we used (A.15). Note that this result could have been found through simple dimensional analysis: a factor of $Q \sim gT$ for the dimensions, g^2 for the vertices and $\frac{1}{g}$ from Bose enhancement gives g^2T.

2) (1 loop hard correction) represents the one-loop diagram with hard internal momentum expanded to the next order of $\frac{Q}{k}$. The (1 loop hard correction) diagram is figure 3.1 A with the inclusion of NLO $\frac{Q}{K}$. In the leading order calculation we neglected terms that were of order $\left(\frac{q}{k}\right)^2$, $\left(\frac{q_0}{k}\right)^2$ and $\frac{q_0 q}{k^2}$: the (1 loop hard correction) term includes these in the calculation. Consider again a soft static fermion. The integrand contains:

i. g^2 from the two vertices.

ii. $\frac{N_B(k_0)\delta(K^2)}{2K\cdot Q+Q^2} \propto \frac{N_B(k_0)\delta(K^2)}{2kq_0+q_0^2} \propto \frac{N_B(k_0)\delta(K^2)}{kq_0(1+\frac{q_0}{2k})} \sim \frac{N_B(k_0)\delta(K^2)}{kq_0}\left(1-\frac{q_0}{2k}\right)$ comes from the propagators. Note that instead of just taking the leading order term of the denominator, we have expressed it as a power series in $\frac{q_0}{k}$ using the geometric series, and truncated the result after two terms. As in the (1-loop soft) case, the K^2 term of the advanced/retarded propagator vanished due to the presence of $\delta(K^2)$.

iii. $k_0 + q_0$ from the numerator of the fermion propagator $\not{K} + \not{Q}$.

Constructing integral from the contributions above yields

$$\begin{aligned}(1 \text{ loop hard correction}) &\sim g^2 \int d^4k\big(k+q_0\big)\big(1-\frac{q_0}{2k}\big)\frac{N_B(k_0)\delta(K^2)}{kq_0} \\ &\sim g^2 \int d^3k\big(k+q_0\big)\big(1-\frac{q_0}{2k}\big)\frac{N_B(k)}{k^2q_0} \\ &\sim g^2 \int dk\big(k+\frac{q_0}{2}\big)\frac{N_B(k)}{q_0}. \end{aligned} \tag{3.1.3}$$

The leading order term of (3.1.3) is

$$\begin{aligned}(\text{LO}) &\sim \frac{g^2}{q_0}\int dk k N_B(k) \\ &\sim \frac{g^2T^2}{q_0} \sim gT. \end{aligned} \tag{3.1.4}$$

The result of (3.1.4) is in agreement with the result given in (3.1.2). The NLO part is

$$(\text{NLO}) \sim g^2 \int dk N_B(k) \sim g^2T \sim g(LO). \tag{3.1.5}$$

This is the same order as the (1 loop soft) contribution in (3.1.1).

3) (2 loop hard) represents diagrams consisting of 2 loops, both with hard internal momentum. An example

of a (2 loop hard) diagram for the fermion self energy is given in figure 3.1C. The integrand contains:

i. g^4 from the quark-gluon vertices

ii. $\frac{N_B(k_0)N_B(p_0)\delta(K^2)\delta(P^2)}{(K\cdot Q)(P\cdot Q)(P\cdot K)}$ from the propagators. Note that any K^2 and P^2 terms from the retarded/advanced propagators vanish due to the presence of the two delta functions. The Q^2 terms are neglected because they are subleading.

iii. $k_0 P\cdot K$ and similar terms from the numerators of the fermion propagators. There are terms in the trace that vanish due to factors of K^2.

Constructing the integral from the contributions above yields

$$\begin{aligned}(\text{2 loop hard}) &\sim g^4 \int d^4k \int d^4p \frac{(k_0 K\cdot P)N_B(k_0)N_B(p_0)\delta(K^2)\delta(P^2)}{(K\cdot Q)(P\cdot Q)(P\cdot K)} \\ &\sim g^4 \int d^3k \int d^3p \frac{(kN_B(k)N_B(p)}{k^2p^2q_0^2} \\ &\sim \frac{g^4}{Q^2}\int dk \int dpkN_B(k)N_B(p) \\ &\sim \frac{g^4}{Q^2}T^3 \sim g^2T \sim g(LO). \end{aligned} \tag{3.1.6}$$

Thus we see the orders of (3.1.1) (1 loop soft), (3.1.5) (1 loop hard correction) and (3.1.6) (2 loop hard) are all equal and of order $g(LO)$. Therefore, naive power counting predicts that all three of the types of terms discussed in [1] contribute at NLO. Similar arguments can be made for the imaginary parts of the diagrams. However, specific calculations reveal that some of these diagrams do not contribute at NLO. Our goal is to develop a set of rules that allows us to determine immediately which diagrams will contribute at NLO and which are subleading.

3.2 Summary of Explicit Results

In this section we will study the NLO fermion and boson self energies in the real time formalism. The motivation is to understand why the arguments presented in section 3.1 overestimate the NLO results and use this information to obtain more precise power counting rules. Some details of the calculations can be found in appendices at the end of this thesis. Note that when the fermion self energy is decomposed into the form of (1.3.6) the real and imaginary parts of the two components $\Sigma^{(0)}$ and $\Sigma^{(s)}$ obey opposite symmetry

relations. When we discuss the NLO fermion self energy, we will specifically be discussing the $\Sigma^{(0)}$ component since the term with $\Sigma^{(s)}$ vanishes for $q \to 0$. A summary of the results from other papers is presented in table 3.1. In the following sections we discuss the results in greater detail.

3.3 Refined Power Counting

3.3.1 (1 loop hard correction) Terms

The (1 loop hard correction) terms of the fermion and boson self energies are calculated in appendix H. In both cases it is found that these terms are of order $g^2(LO)$, and not $g(LO)$ as predicted in (3.1.5). It is straightforward to see why one always obtains a factor of g^2 relative to the leading order result. From appendix F, the real parts of the boson and fermion self energies are either even or odd under $q_0 \to -q_0$. Consider the calculation of the (1 loop hard correction) term of the NLO fermion self energy described in section 3.1. We see that the leading order term (3.1.4) is odd in q_0, as it should be. However, in (3.1.5), the NLO contribution is even in q_0. Therefore, this term must cancel, and in fact a complete calculation shows that it does (appendix H). A similar argument can be made for the (1 loop hard correction) term of the real part of the boson self energy. Therefore, the (1 loop hard correction) terms for the real parts of the boson and fermion self energy are $g^2(LO)$ and not $g(LO)$ as predicted previously in this chapter.

Due to kinematic constraints, the imaginary part of the (1 loop hard correction) is identically zero. When the imaginary parts of the self energies are calculated, we obtain the difference between the retarded propagator and advanced propagator in the integrand, which gives a delta function that sets a condition $k \sim q_0$, a contradiction for hard loop momentum $k >> q_0$. As a result, there is no expansion, and the integral can be calculated exactly. In the limit $q \to 0$ the leading order part is zero, same as the HTL. The argument is the same as that presented in chapter 1. From (1.3.4), (1.3.5) and (1.3.7), there will only be an imaginary part if the argument of the logarithm is negative. The condition for this to occur is $Q^2 < 0$. The only way this condition is satisfied is if $q > |q_0|$, which cannot occur for $q \to 0$.

Quantity	Term	Result	References
Re Π_g	LO	g^2T^2	[6]
	(1 loop soft)	g^3T^2	[13]
	(hard 2 loop)	g^4T^2	[13]
	(hard 1 loop correction)	g^4T^2	[13]
Re Π_γ	LO	e^2T^2	[6]
	(1 loop soft)	e^4T^2	
	(hard 2 loop)	e^4T^2	
	(hard 1 loop correction)	e^4T^2	
Im Π_g	LO	0	[6]
	(1 loop soft)	g^3T^2	[14], [15]
	(hard 2 loop)	g^4T^2	[13]
Im Π_γ	LO	0	[6]
	(1 loop soft)	$e^5T^2\ln\left(\frac{1}{e}\right)$	[14], [15]
	(hard 2 loop)	$e^5T^2\ln\left(\frac{1}{e}\right)$	[16]
Re Σ	LO	gT	[6]
	(1 loop soft)	g^2T	[17]
	(hard 2 loop)	g^3T	[18]
	(hard 1 loop correction)	g^3T	[19]
Im Σ	LO	0	[6]
	(1 loop soft)	g^2T	[18]
	(hard 2 loop)	g^4T	[17]

Table 3.1: A list of the results for the real and imaginary parts of the NLO boson and fermion self energies. Π_g is the gluon self energy and Π_γ is the photon self energy. Note that logarithms were neglected when the corresponding terms were subleading relative to the NLO result.

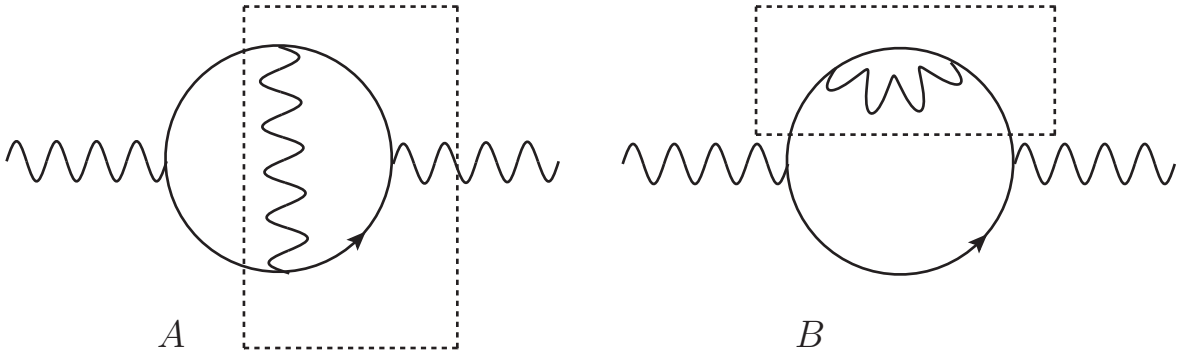

Figure 3.2: Two loop diagrams can be constructed to correspond to an effective vertex (A) or a self-energy insertion (B). The dotted boxes contain the insertions.

It is important to note that the calculation of the imaginary part of the fermion and boson self energies in this manner (where the loop momentum is restricted to be soft) gives the leading order imaginary fermion and boson self energies, and are found to be of order g^3T and g^4T^2 respectively.

3.3.2 (2 loop) Terms

In this subsection we discuss potential contributions from (2 loop hard) diagrams to the real and imaginary parts of the NLO boson and fermion self energies. In section 3.1, naive power counting rules predicted that the (2 loop hard) diagrams are of order $g(LO)$. However, calculations indicate that the (2 loop hard) diagrams are actually of order $g^2(LO)$. The easiest way to understand this is to note that the result of the parity of $\Sigma^{(0)}$ is odd in q_0, a result that contradicts the result of (3.1.6), indicating that a cancellation should occur. In this section we discuss the details of this cancellation. There are two ways in which (2 loop hard) diagrams can be constructed:

1) An additional propagator is added to the diagram such that it separates the external legs, as in figure 3.2 A. In this diagram we treat the loop on the right hand side as an effective vertex. However, since the loop momentum is hard and the external momenta are soft, two of the legs of the vertex will be hard, and the other one will be soft. Therefore, the insertion is not an HTL vertex, and instead has order g^3. As a result, two-loop diagrams that correspond to vertex insertions are of order $g^2(LO)$.

2) An additional propagator is added such that it does not separate the external legs, as in figure 3.2 B. We treat the top loop as a self energy insertion. The additional factor relative to the one loop diagram appears to be

$$\frac{\Sigma(K+Q)(\not{K}+\not{Q})}{K\cdot Q}\sim\frac{k\Sigma(k)}{K\cdot Q}\sim\frac{g^2T^2}{gT^2}\sim g. \tag{3.3.1}$$

Using (3.3.1), we expect the order of the diagram in figure 3.2 B to be $g(LO)$, in agreement with the result in section 3.1. A similar argument can be made when the boson self energy is inserted. We will show that the leading term in (3.3.1) actually vanishes, and as a result the (2 loop hard) diagrams are of order $g^2(LO)$ and subleading relative to $g(LO)$. Note that the insertions $\Sigma(k_0,k)$ and $\Pi(k_0,k)$ are not the leading order HTL self energies that we derived in (1.3.4), (1.3.5) and (1.3.7), as the momentum components k_0 and k are hard. However, the insertion is of the same order and will have the same Dirac or Lorentz structure as the HTL self energy: the fermion insertion can be written as scalar functions times γ_0 and $\vec{\gamma}\cdot\hat{k}$, and the boson self energy insertion obeys the Ward identities. Both insertions obey the symmetry relations of appendix F.

Using figure 3.3 A and taking $q\to 0$, the leading terms are

$$\Sigma^{(0)}(q_0)\sim g^2\int d^4k N_B(k)\mathrm{Tr}[\gamma_0\gamma^\mu\not{K}\gamma^\nu]\Pi_{\mu\nu}(K)\delta(K^2)\left(\frac{1}{k_0q_0}\right)^2\sim g^2T\sim g(LO). \tag{3.3.2}$$

The trace of (3.3.2) gives terms proportional to

$$k_0g^{\mu\nu},\qquad K^\mu g^{\nu 0},\qquad K^\nu g^{\mu 0}. \tag{3.3.3}$$

The first term vanishes upon k_0 integration using the fact that Π is even, and the last two go to zero due to the Ward identity. Thus, this diagram is not of order $g(LO)$ but instead of order $g^2(LO)$. Now consider the leading order term of figure 3.3 B:

$$\Sigma^{(0)}(q_0)\sim g^2\int d^4K N_F(k)\mathrm{Tr}[\gamma_0\gamma_\mu\not{K}\Sigma(k_0,k)\not{K}\gamma^\mu]\delta(K^2)\left(\frac{1}{k_0q_0}\right)^2\sim g(LO). \tag{3.3.4}$$

First consider the insertion of $\gamma_0\Sigma^{(0)}(k_0,k)$ for $\Sigma(k_0,k)$: the trace contains terms proportional to k_0^2 and K^2. Given that $\Sigma^{(0)}(k_0,k)$ is odd in k_0 (F.1), (3.3.4) vanishes upon k_0 integration. There is a similar cancellation for a $\Sigma^{(s)}(k_0,k)$ insertion, as from the trace we get $\frac{k_0^2-K^2}{k_0k}$ times the results for the $\Sigma^{(0)}$ insertion. The change in parity of the trace terms cancels the change in parity from $\Sigma^{(0)}\to\Sigma^{(s)}$, and as such the result

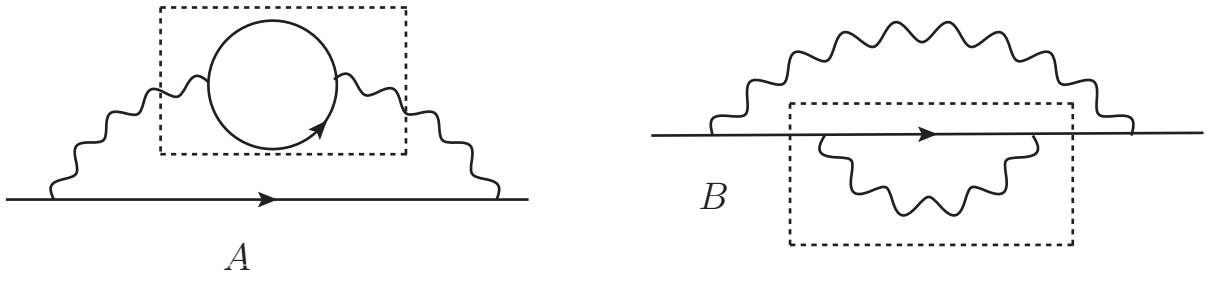

Figure 3.3: The two loop diagrams with self energy insertions that may contribute to the NLO fermion self energy. The boxes highlight the self energy insertions.

is odd in k_0 and vanishes upon integration. Therefore, for the fermion self energy (2 loop hard) diagrams containing self energy insertions contribute at order $g^2(LO)$, not $g(LO)$ as predicted through power counting.

Now consider the 2-loop diagrams in the boson self energy that correspond to self energy insertions. Starting with figure 3.4 A and taking the leading order term,

$$\Pi \sim g^2 \int d^4k N_F(k) \mathrm{Tr}[\gamma_\mu \not{K} \gamma_\nu \not{K} \Sigma(k_0,k) \not{K}] \delta(K^2) \left(\frac{1}{k_0 q_0}\right)^2 \left(\frac{q_0}{k_0}\right) \sim g^3 T^2 \sim g(LO). \tag{3.3.5}$$

The last factor is the statistical suppression factor. The statistical factor of 2-loop diagrams is not obtained in the same manner as in 1-loop diagrams. The statistical factor combinations we end up with for 2-loop boson self energy diagrams have the form

$$N_B(k_0) - N_B(k_0 + q_0) \tag{3.3.6}$$

and a similar one for fermions. We find that (3.3.6) is proportional to $q_0 \times \frac{\partial}{\partial k_0} n_B(k_0)$. This is where the statistical factor appears. We decompose the self energy into the form of (1.3.7). For the $\Sigma^{(0)}(k_0,k)$ term, the elements obtained from the trace are:

$$K^2 k_0 g_{\mu\nu}, \quad K^2 g_{0\mu} K_\nu, \quad K^2 g_{0\nu} K_\mu, \quad k_0 K_\mu K_\nu. \tag{3.3.7}$$

The first three terms of (3.3.7) vanish due to the presence of K^2, and the last term vanishes upon k_0 integration since $\Sigma^{(0)}(k_0,k)$ is odd in k_0. For the $\Sigma^{(s)}(k_0,k)$ term, the elements obtained from the trace are (3.3.7) multiplied by $\frac{(k_0^2-K^2)}{k k_0}$. These terms appear to change parity, however since $\Sigma^{(0)}$ and $\Sigma^{(s)}$ have the opposite parity the result is still odd in k_0 and as a result vanishes upon k_0 integration. Therefore, figure 3.4 A is of

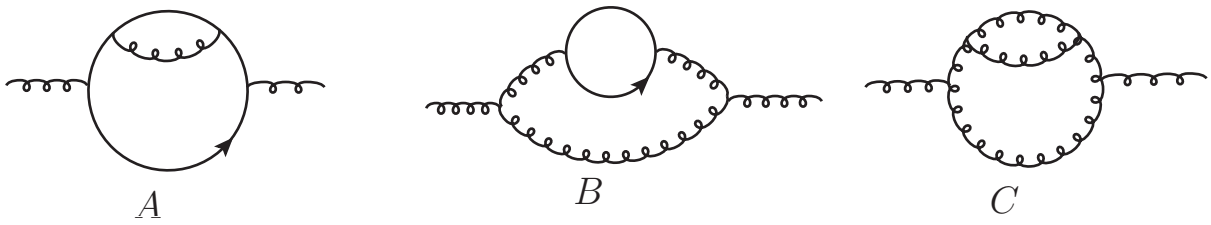

Figure 3.4: The two loop diagrams with self energy insertions that may contribute to the NLO boson self energy. Note that all three are possible for gluons, but only (A) has a photon counterpart.

order $g^2(LO)$ and not $g(LO)$.

Now consider figures 3.4 B and C. Now there are 3-gluon vertices, which have a more complicated structure than the quark-gluon vertices we dealt with before. Let μ and ν be the external indices of the diagram and α and β are the indices of the insertion. There are three main types of terms we get:
1) $g_{\mu\alpha}K_\beta K_\nu$ vanish due to the Ward identity.
2) $g_{\mu\alpha}g_{\beta\nu}K^2$ vanish upon k_0-integration.
3) $K_\mu K_\nu g_{\alpha\beta}$ do not immediately vanish like the other two types of terms. However, this term vanishes when we take the longitudinal and transverse components of $\Pi_{\mu\nu}$. The (00) component and the trace also vanish. These are the quantities that contain the physics of the self energy, thus for our purposes the $g(LO)$ term of this particular term from the trace vanishes.

Therefore, for the boson insertions into boson self energy diagrams, the supposed leading order result obtained by power counting vanishes, and the order of the diagram is $g^2(LO)$.

We conclude that the real parts of the two loop diagrams for the self energy are all of order $g^2(LO)$ and not $g(LO)$.

The imaginary parts are an order g times the corresponding real quantity due to the restriction of phase

space from an additional delta function. In conclusion,

$$\begin{aligned}
&\mathrm{Re}\Pi(\text{2 loop hard}) \sim g^4T^2 \\
&\mathrm{Im}\Pi(\text{2 loop hard}) \sim g^5T^2 \\
&\mathrm{Re}\Sigma(\text{2 loop hard}) \sim g^3T \\
&\mathrm{Im}\Sigma(\text{2 loop hard}) \sim g^4T.
\end{aligned} \tag{3.3.8}$$

In (3.3.8) we have neglected any logarithms that may appear. We will discuss the consequences in the next section.

3.3.3 (1 loop soft) Terms

In this subsection we consider (1 loop soft) terms for the real and imaginary parts of the boson and fermion self energies. In calculations of quantities with hard inner momentum, the only available scales are q_0 and T. However, for 1-loop soft diagrams effective propagators and vertices are used, and as a result two new scales, the effective boson and fermion masses, appear. This makes the development of power counting rules more difficult.

Consider the imaginary parts of (1 loop soft) diagrams. Recall that for hard loop momentum, the imaginary part of the diagram is subleading by a factor of g relative to the real part. The reason is that the delta function that arises in the imaginary part leads to a restriction of the loop momentum to a soft range of phase space. However, for (1 loop soft) terms the loop momentum is already soft, thus there is no additional power of g. This result is not surprising for diagrams with hard loop momentum, as the parity of the real and imaginary parts of the diagram with respect to q_0 are different (appendix F). Since there are no other soft scales the imaginary part must contain a factor of $\frac{q_0}{k}$ relative to the real part. However, for soft loop momentum there are additional soft scales (the effective fermion and boson masses), and as such the parity can be changed without changing the overall order of the diagram through a factor of order $\frac{q_0}{m_{eff}} \sim 1$, where m_{eff} represents an effective mass (either boson or fermion) and shows up in the integral though the use of effective propagators and vertices. Hence, we expect the (1 loop soft) terms for the real and imaginary parts

of the self energy to be of the same order.

For the NLO fermion self energy, the real and imaginary (1 loop soft) terms are calculated in [18] and [17]. We describe here the process in which the (1 loop soft) integrands are obtained:

1) Apply Feynman rules to get the integrand expression for the 1-loop soft diagrams with effective propagators and vertices. Explicit expressions for the HTL propagators can be constructed from the Dyson equation and corresponding self energies (see appendix D).

2) Discard terms that vanish due to the longitudinal and transverse propagators being 4-dimensionally transverse.

3) Terms that contain HTL vertices can be simplified in the following three ways:

i. All vertex components can be written in terms of retarded components using the KMS conditions.

ii. Some terms contain vertices that, upon contraction with leg momenta, can be rewritten in terms of HTL self energies using the Ward identities.

iii. Remaining vertices can be calculated in the HTL approximation in a manner similar to the calculation of the HTL self energies (see appendices C2 and C3).

The relationships used in (i) and (ii) can be found in the appendix of [17].

It is found that the real and imaginary parts of the (1 loop soft) diagrams for the fermion self energy are both proportional to $g^2T \sim g(LO)$, as expected from our naive power counting arguments. Dimensional analysis would have provided the same result, as we have g^2 from the vertices, gT from the dimensions of the diagram and $\frac{1}{g}$ from Bose enhancement.

Similarly, the real and imaginary parts of the (1 loop soft) diagrams for the gluon self energy are calculated in [13] and [14]. Recall that there are four 1-loop diagrams for the gluon self energy: the diagrams with gluon, quark and ghost loops, and the gluon tadpole. The quark loop is subleading: the diagrams with boson propagators will dominate due to Bose enhancement for soft loop momentum. The (1 loop soft) gluon self energy is found to be of order $g^3T^2 \sim g(LO)$. This result could be obtained from dimensional analy-

sis, as we have g^2 from the vertices, $(gT)^2$ from the dimensions of the diagram and $\frac{1}{g}$ from Bose enhancement.

To summarize, for fermions and gluons the (1 loop soft) diagrams give contributions of order (see table 3.1)

$$\begin{aligned} &\mathrm{Re}\Sigma \sim \mathrm{Im}\Sigma \sim g^2 T \sim g(LO) \\ &\mathrm{Re}\Pi_g \sim \mathrm{Im}\Pi_g \sim g^3 T^2 \sim g(LO). \end{aligned} \tag{3.3.9}$$

Comparing the results of (3.3.9) to the results for the (1 loop hard correction) and (2 loop hard) terms, we conclude that for the real and imaginary parts of the fermion and gluon self energies the (1 loop soft) diagrams give the full contribution at NLO.

Now consider the real part of the photon self energy. For photons, there is only one 1-loop diagram that contributes: the diagram with the electron loop, in which there is no Bose enhancement since all the propagators in the loop are fermions. As a result, the real part of the (1 loop soft) diagram for photons is expected to be of order $e^4 T^2 \sim e^2(LO)$ (see table 3.1). This is the same order as the (1 loop hard correction) and (2 loop hard) terms. Therefore, we expect that all three terms must be calculated to determine the complete NLO result for the real part of the photon self energy.

Now we consider the imaginary part of the photon self energy, of which the result is well known and physically interesting [14]. The (1 loop soft) diagrams for the photon self energy are given in figure 3.5. Note that there is no tadpole graph with a 4-photon vertex and internal photon line, as in leading order HTL the 4-photon vertex is proportional to the 3-photon vertex, which is zero by Furry's theorem. When we take the imaginary part of the (1 loop soft) photon self energy, fix q_0 and expand in powers of e, we expect to obtain the 2-loop result from bare perturbation theory [20]. This is not the case, indicating that we missed something in our calculation. The calculation of the (1 loop soft) imaginary photon self energy can be found in appendix G, and the result is found to be of order $e^5 T^2 \ln\frac{1}{e}$. This is a troubling result for two reasons: this result is a factor of $e\ln\left(\frac{1}{e}\right)$ suppressed relative to what we expect from dimensional analysis. The second problem is that the result is only a logarithm times the (2 loop hard) result, and we did not consider

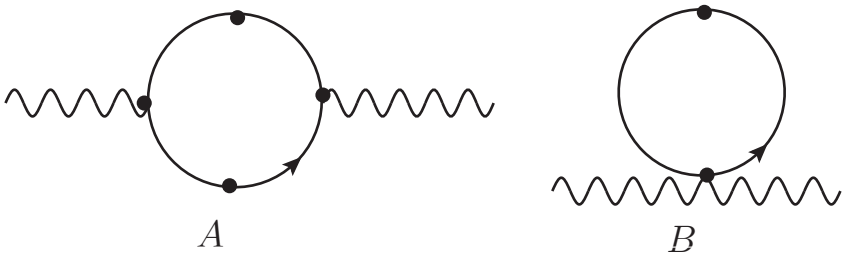

Figure 3.5: The diagrams that can contribute to the (1 loop soft) photon self energy.

potential logarithm terms that may arise in the (2 loop hard) diagrams. Therefore, we need to check the (2 loop hard) diagrams for potential logarithms.

In our previous calculations, we have assumed that momenta can classified as either hard or soft. However, in order to get a logarithm we must integrate over a region that contains both hard and soft momentum:

$$\int_{p_{soft}}^{p_{hard}} \frac{dP}{P} = \ln\frac{p_{hard}}{p_{soft}} \sim \ln\frac{1}{g} \tag{3.3.10}$$

We want to correctly determine if there is a logarithm. Consider the following integrals:

$$\begin{aligned}\int_{k_{soft}}^{k_{hard}} \frac{dK}{K+P} \sim \int_{k_{soft}}^{k_{hard}} \frac{dK}{K} \sim \ln\left(\frac{k_{hard}}{k_{soft}}\right) \sim \ln\frac{1}{g} \\ \int_{p_{soft}}^{p_{hard}} \frac{dP}{P+\frac{P^2}{K^2}} \sim \int_{p_{soft}}^{p_{hard}} \frac{dP}{P} \sim \ln\left(\frac{p_{hard}}{p_{soft}}\right) \sim \ln\frac{1}{g}.\end{aligned} \tag{3.3.11}$$

In the first equation of (3.3.11) the momentum K is assumed to be greater than P but integrated over a range that contains both hard and soft momenta. In this situation, K is said to be logarithmically hard. In the second equation momentum P is assumed to be less than K but is integrated over a range that contains both hard and soft momenta. Here P is said to be 'logarithmically soft'. Integrals of this form can produce logarithms in the final result of the form $\ln\frac{1}{g}$. When considering different momentum regimes, we find that the leading result for the (2 loop hard) diagrams is $e^5T^2\ln\frac{1}{e}$, which is the same order as the (1 loop soft) contribution. Therefore, both must be calculated.

Furthermore, the full $e^5T^2\ln\frac{1}{e}$ comes from the self energy insertion (figure 3.2 B) and the dominant momentum regime is when the electron is hard and the photon is logarithmically soft [14]. Using this

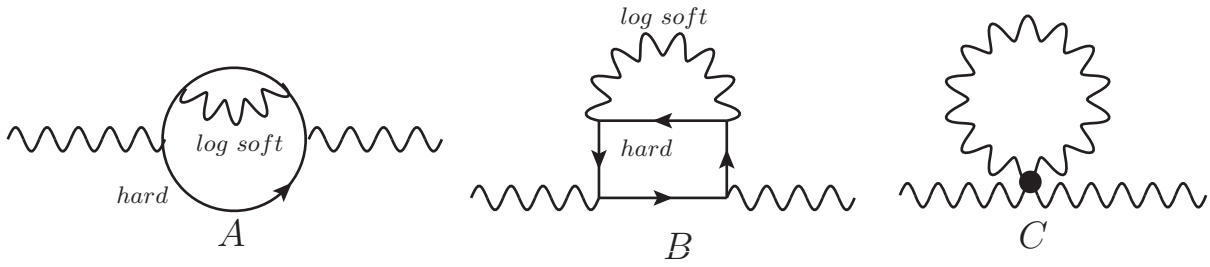

Figure 3.6: The two loop diagram that has the same order as the (1 loop soft) contribution can be drawn as a one loop diagram with an effective vertex.

information, we think about the (2 loop hard) diagram in a different way (see figure 3.6). In figure B the diagram is rearranged. Since the box in B is a hard loop, we can rewrite it as an effective vertex, as shown in figure C. Recall that this tadpole was neglected in the (1 loop soft) case because the 4-photon vertex vanishes in leading order HTL. However, since the result is $e\ln\frac{1}{e}$ less than the power counting prediction, we need to consider the correction to the 4-photon vertex, as it is only proportional to the 3-photon vertex in leading order HTL. From the results of this section, we conclude that the correction is proportional to $e\ln\frac{1}{e}$, and the 4-photon vertex can be written as

$$\Gamma^{htl}_{4\ photon} = g^2\left(0\times 1 + g\ln\frac{1}{g} + ...\right) \tag{3.3.12}$$

where the first term in (3.3.12) is obtained from the power counting rules of (2.1.13) and vanishes due to Furry's theorem. Note that when we include figure 3.6 B in the calculation of the imaginary part of the photon self energy, the result upon fixing q_0 and expanding matches the result of [20]. It is important to note that the diagrams of figure 3.6 B and C illustrate the double counting problem that occurs at NLO: in both diagrams, the external photon momentum is soft and the internal fermion momentum is hard. The difference is that the photon loop is soft for the (1 loop soft) diagram in (C), and logarithmically soft in the (2 loop hard) diagram in (B). Any overlap between these momenta results in double counting. Here we are not concerned with the solution to this problem, as we are concerned merely with determining the orders of diagrams, not the coefficients.

3.3.4 NLO Power Counting Rules

From the results in this section, we can make the following remarks about power counting at NLO:

1) For the real and imaginary parts of the gluon and fermion self energies, the (1 loop soft) diagrams are of order $g(LO)$, the same order we derived using the techniques of power counting. The (2 loop hard) and (1 loop hard correction) are found to be of order $g^2(LO)$ (neglecting any logarithms). Thus, the (1 loop soft) diagrams give the entire NLO result.

2) For the real part of the photon self energy, all three terms must be calculated due to the fact that there is no Bose enhancement. These terms are of order $e^2(LO)$. For the imaginary part of the photon self energy, we found that both the (2 loop hard) and (1 loop soft) contribute at order $e^5T^2\ln\frac{1}{e}$. The logarithm was found to come from the (1 loop soft) diagram with the correction to the HTL 4-photon vertex, and the 2-loop diagram with the self energy insertion with a logarithmically soft internal photon and a hard electron.

Chapter 4

Conclusions

In the second chapter of this thesis we derived a set of power counting rules for leading order HTL's in the real time formalism. This set of rules allows us to predict the order of any diagram at leading order. In particular, we found that diagrams with 4-gluon vertices only contribute in the case of the gluon self energy, where the gluon tadpole must be included. We also showed that diagrams with external ghost lines do not contribute and the bare ghost propagator is sufficient even for soft momentum. It was found that only diagrams with zero or two external fermion lines contribute at leading order.

The third chapter of this thesis involved the derivation of power counting rules at NLO HTL. We only looked at self energies, as these obey particularly simple symmetry relations and are physically interesting. Upon detailed analysis of the three types of terms described in [1] we found that for fermions and gluons, only the (1 loop soft) diagrams need to be calculated in order to determine the full NLO result. However, for photons, we found that all potential types of terms contributed. For the real part, this was due to the lack of Bose enhancement that was present for the gluon self energy diagrams. For the imaginary parts logarithms appeared from the correction to the 4-photon vertex for (1 loop soft) diagrams and for logarithmically soft photon loop momentum (2 loop hard). Refer to table 3.1 for a complete set of results for the self energies at NLO. We accomplished our goal of determining power counting rules at NLO for the boson and fermion self energies and understanding the exceptions to these power counting rules (the photon self energy). We

would like to extend this work to diagrams with an arbitrary number of legs. Looking at our results, we expect that the photon self energy will be the only case in which we get $g^3(LO)$.

Appendix

The first appendix contains important equations that are used in this thesis. The second appendix provides details about the structure of the dressed photon and electron propagators. In the third appendix the leading order self energies in QED are calculated. In the fourth appendix we discuss the spectral function representation of different propagators and derive some well known relationships. The fifth appendix contains the proof of the cancellation of the highest order term in the n-gluon vertex. In the sixth appendix the symmetry relations of the boson and fermion self energies are calculated. The seventh appendix contains the calculation of the (1 loop soft) term for the imaginary photon self energy. In the eight appendix the (1 loop hard correction) terms are shown to be subleading relative to the (1 loop soft) result. The last appendix contains a proof of Furry's theorem.

A Important Formulas

1. The mass scales used are

$$\omega_P^2 = \frac{e^2T^2}{9} \tag{A.1}$$

$$m_F^2 = \frac{e^2T^2}{8} \tag{A.2}$$

$$m_\infty^2 = \frac{e^2T^2}{6}. \tag{A.3}$$

2. The Bose-Einstein and Fermi-Dirac distributions represent the distribution of energies of a system of many identical bosons or fermions at thermal equilibrium. They are defined as follows:

$$\begin{aligned} n_B(k) &= \frac{1}{e^{\beta k}-1} \\ n_F(k) &= \frac{1}{e^{\beta k}+1}. \end{aligned} \tag{A.4}$$

The following quantities and relations are useful in calculations:

$$\begin{aligned} N_B(k_0) &= 1 + 2n_B(k_0) \\ N_F(k_0) &= 1 - 2n_F(k_0) \\ N_B(-k_0) &= -N_B(k_0) \\ N_F(-k_0) &= -N_F(k_0). \end{aligned} \tag{A.5}$$

The soft limits of (A.5) are

$$\begin{aligned} N_B(k_0) &\approx \frac{T}{k_0} \\ N_F(k_0) &\approx \frac{k_0}{T}. \end{aligned} \tag{A.6}$$

The following integrals appear frequently in calculations:

$$\begin{aligned} \int_0^\infty dk k n_B(k) &= \frac{\pi^2k^2}{6} \sim \frac{\pi^2T^2}{6} \\ \int_0^\infty dk k n_F(k) &= \frac{\pi^2k^2}{12} \sim \frac{\pi^2T^2}{12} \\ \int_0^\infty dk k^n N_{B/F}(k) &\sim k^{n+1} \sim T^{n+1}. \end{aligned} \tag{A.7}$$

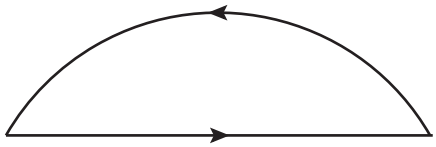

Figure A1: The integration contour used to define equation A.10.

Note that in (A.7) we have assumed that k is hard in the final result of each line.

Given $q_0 = -k_0 - p_0$, the statistical factors satisfy the KMS conditions:

$$N_B(k_0)N_B(p_0) + N_B(k_0)N_B(q_0) + N_B(p_0)N_B(q_0) + 1 = 0 \tag{A.8}$$

$$N_F(k_0)N_F(p_0) + N_F(k_0)N_F(q_0) + N_F(p_0)N_F(q_0) + 1 = 0. \tag{A.9}$$

3. The following equation for contour integration is very useful when performing calculations

$$\begin{aligned} \int \frac{f(x)dx}{x + i\eta} &= P.V. \int \frac{f(x)dx}{x} - i\pi \int f(x)\delta(x)dx \\ \int \frac{f(x)dx}{x - i\eta} &= P.V. \int \frac{f(x)dx}{x} + i\pi \int f(x)\delta(x)dx. \end{aligned} \tag{A.10}$$

It is understood that the integration is over a function $f(x)$, and $f(x)$ is assumed to tend to zero over the arc of the contour of figure A1.

4. The step function in position space is

$$\theta(x_0 - y_0) = \frac{i}{2\pi} \int_{-\infty}^{\infty} d\tau \frac{e^{-i\tau(x_0 - y_0)}}{\tau + i\eta}. \tag{A.11}$$

$$\tag{A.12}$$

A useful relationship involving step functions is

$$\theta(x_0 - y_0) + \theta(y_0 - x_0) = 1. \tag{A.13}$$

5. The following delta function relations are useful:

$$\delta(x^2-\alpha^2) = \frac{1}{2|\alpha|}[\delta(x-\alpha)+\delta(x+\alpha)] \tag{A.14}$$

$$\delta[g(x)] = \sum_{i=1}^{n}\frac{1}{g'(x_i)}\delta(x-x_i) \qquad \text{where } g(x_i)=0 \tag{A.15}$$

$$\delta(K^2) = \frac{i}{\pi}\mathrm{Im}\left(\frac{1}{K^2-i\epsilon}\right). \tag{A.16}$$

6. The geometric series allows for the expansion of denominators with small arguments:

$$\begin{aligned}\frac{1}{1-x} &= \sum_{j=0}^{\infty}x^j \\ \frac{1}{1+x} &= \sum_{j=0}^{\infty}(-1)^j x^j.\end{aligned} \tag{A.17}$$

7. The 2-variable Taylor series for the function $F(x,y)$ expanding around the point (a,b) is

$$F(x,y) \approx F(a,b) + (x-a)\frac{\partial F}{\partial x}(a,b) + (y-b)\frac{\partial F}{\partial y}(a,b). \tag{A.18}$$

B QED Propagators and Self Energies

In this appendix we discuss the bare and dressed photon and electron propagators in QED. The generalization to QCD propagators is straightforward. We remind the reader that we are working in the Feynman gauge.

B1 Photons

The bare inverse photon propagator is obtained from (1.1.8) by taking the Fourier transform of the equation of motion of the free photon part of the Lagrangian. The equation of motion for the photon field A_μ is Maxwell's equation [2],

$$\partial_\mu F^{\mu\nu} = e\bar{\psi}\gamma^\nu\psi = ej^\nu. \tag{B.1}$$

The inverse propagator is then obtained:

$$D_{\mu\nu}^{(0)-1}(Q) = -Q^2 g_{\mu\nu}. \tag{B.2}$$

The zero temperature photon propagator is determined from the inverse propagator:

$$D_{\mu\nu}^{0}(Q) = -\frac{1}{Q^2} g_{\mu\nu} \tag{B.3}$$

where a line in a Feynman diagram is defined to be iD. We define the dressed inverse propagator as

$$D_{\mu\nu}^{-1}(Q) = (D_{\mu\nu}^{0}(Q))^{-1} - \Pi_{\mu\nu}(Q). \tag{B.4}$$

In order to obtain this form for the effective propagator, the self energy is i times the corresponding bubble diagram. It is useful to write the effective photon propagator using projection operators. A set of projection operators P_a and P_b must satisfy the relations

$$\begin{aligned} P_a^2 &= P_a \\ P_a P_b &= 0, \qquad a \neq b. \end{aligned} \tag{B.5}$$

At zero temperature the two projection operators for photons are

$$\begin{aligned} \mathcal{P}_{\mu\nu}^{T}(Q) &= g_{\mu\nu} - \frac{Q_\mu Q_\nu}{Q^2} \\ \mathcal{P}_{\mu\nu}^{L}(Q) &= \frac{Q_\mu Q_\nu}{Q^2}. \end{aligned} \tag{B.6}$$

It is straightforward to show that these obey (B.5). The photon propagator defined in (B.3) can be written

$$D_{\mu\nu}^{0}(Q) = -\frac{1}{Q^2}[\mathcal{P}_{\mu\nu}^{T}(Q) + \mathcal{P}_{\mu\nu}^{L}(Q)]. \tag{B.7}$$

The self energy is decomposed using the projection operators defined in (B.6),

$$-\Pi_{\mu\nu}(Q) = \mathcal{P}_{\mu\nu}^{T}(Q)\Pi_T(Q) + \mathcal{P}_{\mu\nu}^{L}(Q)\Pi_L(Q). \tag{B.8}$$

According to the Ward identity, the photon self energy must be 4-dimensionally transverse ($Q^\mu \Pi_{\mu\nu}(Q) = 0$). Since $\mathcal{P}_T(Q)$ is 4-dimensionally transverse but $\mathcal{P}_L(Q)$ is not, $\Pi_L(Q) = 0$ at zero temperature. Therefore, the self energy is given by

$$-\Pi_{\mu\nu}(Q) = \mathcal{P}_{\mu\nu}^{T}(Q)\Pi_T(Q). \tag{B.9}$$

The finite temperature case is more complicated, as we need another vector to construct the projection operators to account for the heat bath. Using the notation of [21] with $U_\mu = (1,0,0,0)$ defined to be the mean velocity of the plasma, the projection operators are

$$\begin{aligned}
P^T_{\mu\nu}(L) &= \gamma_{\mu\nu} - \frac{\kappa_\mu \kappa_\nu}{\kappa^2} \\
P^L_{\mu\nu}(L) &= g_{\mu\nu} - \frac{L_\mu L_\nu}{L^2} - P^T_{\mu\nu} \\
P^0_{\mu\nu}(L) &= \frac{L_\mu L_\nu}{L^2} \\
\gamma_{\mu\nu} &= g_{\mu\nu} - U_\mu U_\nu \\
\kappa_\mu &= \gamma_{\mu\nu} L^\nu .
\end{aligned} \tag{B.10}$$

These projection operators obey the standard projection operator properties of (B.5) . In the zero temperature limit,

$$\begin{aligned}
P^T_{\mu\nu}(L) &\to \mathcal{P}^T_{\mu\nu}(L) \\
P^L_{\mu\nu}(L) &\to 0 \\
P^0_{\mu\nu}(L) &\to \mathcal{P}^L_{\mu\nu}(L).
\end{aligned} \tag{B.11}$$

Given that $P^0_{\mu\nu}$ is not 4-dimensionally transverse while the other two projection operators are, the self energy has the form

$$-\Pi_{\mu\nu}(Q) = \Pi^T_{\mu\nu}(Q)\Pi_T + \Pi^L_{\mu\nu}(L)\Pi_L. \tag{B.12}$$

Substitution of (B.12) into (B.4) gives the inverse dressed propagator:

$$D^{-1}_{\mu\nu}(Q) = -(Q^2 - \Pi_T)P^T_{\mu\nu}(Q) - (Q^2 - \Pi_L)P^L_{\mu\nu}(Q) - Q^2 P^0_{\mu\nu}(Q). \tag{B.13}$$

We can use (B.5) to determine the effective propagator from (B.13):

$$D_{\mu\nu}(Q) = -\frac{P^T_{\mu\nu}(Q)}{K^2 - \Pi_T} - \frac{P^L_{\mu\nu}(Q)}{K^2 - \Pi_L} - \frac{P^0_{\mu\nu}(Q)}{Q^2}. \tag{B.14}$$

The longitudinal and transverse self energies can be found from (B.14):

$$\Pi_L = \frac{Q^2}{q^2}\Pi_{00} \tag{B.15}$$

$$\Pi_T = \frac{1}{2}(g^{\nu\mu} - \frac{Q^\nu Q^\mu}{Q^2} - P^{\nu\mu}_L)\Pi_{\mu\nu}. \tag{B.16}$$

B2 Fermions

The bare inverse propagator for fermions is found by taking the free fermion part of (1.1.8) and finding the equation of motion. This yields the Dirac equation:

$$(i\gamma^\mu \partial_\mu - m)\psi(X) = 0. \tag{B.17}$$

The bare inverse fermion propagator in momentum space is:

$$S(P) = \frac{1}{\not{P} + i\epsilon}. \tag{B.18}$$

The dressed fermion propagator can be expressed in the same manner as (B.4),

$$S^{-1}(Q) = (S^{(0)})^{-1}(Q) - \Sigma(Q). \tag{B.19}$$

We decompose the fermion self energy into the following form:

$$\Sigma_R(Q) = A(q_0, q)\not{Q} + B(q_0, q)\gamma_0. \tag{B.20}$$

The traces of products of γ-matrices can be used to obtain $A(q_0, q)$ and $B(q_0, q)$:

$$\begin{aligned}
&\mathrm{Tr}[\gamma_0 \Sigma_R(Q)] = \mathrm{Tr}[A\gamma_0 \not{Q} + B\gamma_0^2] = 4Aq_0 + 4B \\
&\mathrm{Tr}[\not{Q}\Sigma_R(Q)] = \mathrm{Tr}[A\not{Q}\not{Q} + B\not{Q}\gamma_0] = 4AQ^2 + 4Bq_0 \\
&A = \frac{1}{4q^2}[q_0 \mathrm{Tr}[\gamma_0 \Sigma_R(Q)] - \mathrm{Tr}[\not{Q}\Sigma_R(Q)]] \\
&B = \frac{1}{4q^2}[q_0 \mathrm{Tr}[\not{Q}\Sigma_R(Q)] - Q^2 \mathrm{Tr}[\gamma_0 \Sigma_R(Q)]].
\end{aligned} \tag{B.21}$$

Another useful representation that can be used to express the fermion self energy is obtained from (B.21):

$$\begin{aligned}
&\Sigma(q_0, q) = \Sigma^{(0)}(q_0, q)\gamma_0 - \Sigma^{(s)}(q_0, q)\vec{\gamma} \cdot \hat{q} \\
&\Sigma^{(0)}(q_0, q) = q_0 A(q_0, q) + B(q_0, q) \qquad , \Sigma^{(s)}(q_0, q) = qA(q_0, q).
\end{aligned} \tag{B.22}$$

Thus, the inverse effective fermion propagator is

$$S^{-1}(Q) = (q_0 - \Sigma^{(0)}(Q))\gamma_0 - (q + \Sigma^{(s)}(Q))\vec{\gamma} \cdot \hat{q}. \tag{B.23}$$

We define the operators

$$\begin{aligned}
P_+ &= \frac{1}{2}(\gamma_0 + \vec{\gamma} \cdot \hat{q}) \\
P_- &= \frac{1}{2}(\gamma_0 - \vec{\gamma} \cdot \hat{q}).
\end{aligned} \tag{B.24}$$

Making the definitions

$$\Sigma_{\pm}(Q) = \Sigma^{(0)}(Q) \pm \Sigma^{(s)}(Q) \tag{B.25}$$

and rewriting (B.23) in terms of these operators, we obtain

$$S^{-1}(Q) = P_{+}(Q)(q_0 - q - \Sigma_{+}(Q)) + P_{-}(Q)(q_0 + q - \Sigma_{-}(Q)), \tag{B.26}$$

P_+ and P_- satisfy the relations

$$\begin{aligned} P_{+}(Q)P_{+}(Q) = P_{-}(Q)P_{-}(Q) = 0 \\ P_{+}(Q)P_{-}(Q) + P_{-}(Q)P_{+}(Q) = 1. \end{aligned} \tag{B.27}$$

Using (B.27), the effective propagator is

$$\begin{aligned} S(Q) \quad &= \frac{1}{q_0 + q - \Sigma_{-}(Q)} P_{+}(Q) + \frac{1}{q_0 - q - \Sigma_{+}(Q)} P_{-}(Q) \\ &= \Delta_{+}(q_0, q) P_{-}(Q) + \Delta_{-}(q_0, q) P_{+}(Q). \end{aligned} \tag{B.28}$$

C Leading Order HTL Self Energy Calculations

In this appendix we calculate the leading order self energies of the scalar in ϕ^4 theory and the photon and fermion in QED. We will start with propagators in the (1-2) basis and substitute the corresponding Keldysh propagators afterwards, allowing us to use the simple vertex structure of the (1-2)-basis. It is also possible to do the calculations directly in the Keldysh basis. The momentum external to the diagram is defined to be Q, the loop momentum K, and on occasion P is some combination of K and Q. We will also use $x = \frac{p_0}{p}$ to simplify the notation. We assume that the masses of particles are much smaller then the momentum components and can be neglected. This assumption is only valid at leading order. It is also important to remember in our notation the self energy is given by i times the corresponding diagram (see appendix B). When we perform the k-integration we neglect the non-thermal parts of the factors $N_B(k)$ and $N_F(k)$. In this appendix we are calculating the retarded self energies.

C1 Leading Order HTL Scalar Self Energy

The scalar self energy involves the calculation of the tadpole diagram (see figure 1.3). Note that there is only one vertex here, so the retarded scalar self energy will simply be given by $\Pi_R = \Pi_{11}$. The self energy is given by i times the tadpole diagram,

$$\Pi = \frac{i\lambda}{2}\int \frac{d^4k}{(2\pi)^4}\Delta_{11} = \frac{i}{2}(\lambda)\int \frac{d^4k}{(2\pi)^4}\left(\frac{1}{K^2 - i\epsilon} - 2\pi i\delta(K^2)\mathrm{sgn}(k_0)n_B(k_0)\right). \tag{C.1}$$

Using the formulas (A.15) and (A.16), we can simplify the integrand. Neglecting the real term of the propagator Δ_{11} because it is temperature independent (1.2.2), we have

$$\Pi = \frac{\lambda}{2}\int \frac{d^3k}{(2\pi)^4}\int dk_0 \frac{2\pi N_B(k_0)}{2k_0}\mathrm{sgn}(k_0)[\delta(k_0 - k) + \delta(k_0 + k)]. \tag{C.2}$$

Performing the k_0 integration and dropping the temperature independent part of $N_B(k)$ gives

$$\Pi = \frac{\lambda}{2}(g^2)\int \frac{d^3k}{(2\pi)^3}\frac{n_B(k)}{k}.$$

Performing the angular integration,

$$\begin{aligned}\int d^3k &= 4\pi\int dk k^2\\ \Pi &= \frac{\lambda}{4\pi^2}\int dk n_B(k)k.\end{aligned} \tag{C.3}$$

Using (A.7), the result for the scalar self energy is then

$$\Pi = \frac{\lambda T^2}{24}. \tag{C.4}$$

C2 Leading Order HTL Photon Self Energy

In this section we calculate the retarded longitudinal and transverse photon self energies in the HTL approximation (see figure 1.4). The photon self energy is given by the integral

$$\begin{aligned}\Pi^{\mu\nu} &= -ie^2\int \frac{d^4k}{(2\pi)^4}\mathrm{Tr}[\gamma^\mu S(K)\gamma^\nu S(K - Q)]\\ &= -ie^2\int \frac{d^4k}{(2\pi)^4}\mathrm{Tr}[\gamma^\mu \not{K}\gamma^\nu(\not{K} - \not{Q})]\tilde{\Delta}(K)\tilde{\Delta}(K - Q).\end{aligned} \tag{C.5}$$

Note that $\Pi^{\mu\nu}$ is a 2×2 matrix in Keldysh space.

C2.1 Longitudinal Photon Self Energy

The longitudinal photon self energy can be obtained from (C.5) using (B.15). Evaluating the trace for $\mu = \nu = 0$ and defining $P = K - Q$ to simplify the calculation yields

$$\mathrm{Tr}[\gamma^0\gamma^\alpha K_\alpha \gamma^0 \gamma^\beta P_\beta] = K_\alpha P_\beta \mathrm{tr}[\gamma^0\gamma^\alpha\gamma^0\gamma^\beta] = 4K_\alpha P_\beta[2g^{0\alpha}g^{0\beta} - g^{\alpha\beta}g^{00}] = 4(k_0p_0 + k\cdot p).$$

Using the first line in (1.2.11) to obtain the retarded self energy, we have

$$\Pi^{00} = -4ie^2 \int \frac{d^4k}{(2\pi)^4}(k_0p_0 + k\cdot p)(\tilde{\Delta}_{11}(K)\tilde{\Delta}_{11}(P) - \tilde{\Delta}_{12}(K)\tilde{\Delta}_{21}(P)). \tag{C.6}$$

Using (1.2.8), the above result can be simplified further since

$$\tilde{\Delta}_{11}(K)\tilde{\Delta}_{11}(P) - \tilde{\Delta}_{12}(K)\tilde{\Delta}_{12}(P) = \frac{1}{2}[\tilde{\Delta}_S(K)\tilde{\Delta}_A(P) + \tilde{\Delta}_R(K)\tilde{\Delta}_S(P)].$$

Note that the propagator combinations $\tilde{\Delta}_R(K)\tilde{\Delta}_R(P)$ and $\tilde{\Delta}_A(K)\tilde{\Delta}_A(P)$ vanish since the poles will be isolated to either the upper half or lower half complex plane, and the contour can be closed to exclude these points. The integral is given by

$$\Pi^{00} = -2ie^2 \int \frac{d^4k}{(2\pi)^4}(k_0p_0 + k\cdot p)(\tilde{\Delta}_S(K)\tilde{\Delta}_A(P) + \tilde{\Delta}_R(K)\tilde{\Delta}_S(P)). \tag{C.7}$$

Shifting $K \to Q - K$ in the first term and using (1.2.10) and (A.5) yields

$$\tilde{\Delta}_S(K)\tilde{\Delta}_A(P) = \tilde{\Delta}_R(K)\tilde{\Delta}_S(P). \tag{C.8}$$

Using (C.8) in (C.7) and substituting in the Keldysh propagators,

$$\Pi^{00} = -4e^2 \int \frac{d^4k}{(2\pi)^3}(k_0p_0 + k\cdot p)\frac{\mathrm{sgn}(k_0)N_F(k_0)\delta(K^2)}{(K-Q)^2 - i\epsilon\mathrm{sgn}(k_0 - q_0)}. \tag{C.9}$$

The next step is to perform the k_0-integration of (C.9):

$$\Pi^{00} = -\frac{e^2}{2\pi^3}\int d^3k \frac{N_F(k)}{k}\sum_{n=\pm1}\frac{2k^2 - nkq_0 - k\cdot q}{-2nkq_0 + 2k\cdot q + Q^2 - i\epsilon\mathrm{sgn}(nk - q_0)}. \tag{C.10}$$

We define $x \to \hat{k}\cdot\hat{q}$, where $\hat{k}$ and $\hat{q}$ represent the unit vectors in the k and q directions. We also take $nk >> q_0$ and use $\int d^3k = 2\pi\int dkk^2\int_{-1}^{1}dx$. Substitution into (C.10) yields

$$\begin{aligned}\Pi^{00} &= -\frac{e^2}{\pi^2}\int d^3k\frac{N_F(k)}{k}\int_{-1}^{1}dx\sum_{n=\pm1}\frac{2k^2 - nkq_0 - kqx}{-2nkq_0 + 2kqx + Q^2 - i\epsilon\mathrm{sgn}(nk)} \\ &= -\frac{e^2}{\pi^2}\int dkN_F(k)k\int_{-1}^{1}dx\frac{1 - \frac{nq_0}{2k} - \frac{qx}{2k}}{-\frac{nq_0}{k} + \frac{qx}{k} + \frac{Q^2}{2k} - in\epsilon}.\end{aligned} \tag{C.11}$$

Take the 2-variable Taylor expansion of (C.11) as given in (A.18) and keep only the leading order terms:

$$\sum_{n=\pm 1} \frac{1-\frac{nq_0}{2k}-\frac{qx}{2k}}{-\frac{nq_0}{k}+\frac{qx}{k}+\frac{Q^2}{2k}-in\epsilon}$$
$$= \sum_{n=\pm 1}\left[\frac{k}{nq_0+qx+ni\epsilon}+\frac{1}{2}\frac{nq_0-qx}{nq_0+qx+ni\epsilon}-\frac{1}{2}\frac{Q^2}{(nq_0+qx+ni\epsilon)^2}\right]. \tag{C.12}$$

The first terms of (C.12) vanish upon the x integration and summation over n. Thus, substitution of (C.12) into (C.10) yields

$$\Pi^{00} = -3\omega_p^2\left[1-\frac{q_0}{2q}\ln\left(\frac{q_0+q+i\epsilon}{q_0-q+i\epsilon}\right)\right]. \tag{C.13}$$

Using (B.15), the longitudinal photon self energy is given by

$$\Pi_L = 3\omega_p^2\frac{Q^2}{q^2}[\frac{q_0}{2q}\ln(\frac{q_0+q+i\epsilon}{q_0-q+i\epsilon})-1]. \tag{C.14}$$

C2.2 Transverse Photon Self Energy

In this subsection we will calculate the retarded transverse photon self energy in the HTL approximation. The transverse photon self energy can be obtained from (C.5) using (B.16). The result is

$$\Pi_T = \frac{1}{2}(g^{\nu\mu}\Pi_{\mu\nu}-\Pi_L). \tag{C.15}$$

Since we already have Π_L (C.14), we only need to calculate Π^μ_μ. Start with the numerator:

$$g^{\mu\nu}\mathrm{Tr}[\gamma_\mu \not{K}\gamma_\nu \not{P}] = g^{\mu\nu}K^\alpha P^\beta \mathrm{Tr}[\gamma_\mu\gamma_\alpha\gamma_\nu\gamma_\beta] = g^{\mu\nu}4K^\alpha P^\beta[g_{\mu\alpha}g_{\nu\beta}+g_{\mu\beta}g_{\nu\alpha}-g_{\mu\nu}g_{\alpha\beta}]$$
$$= 4g^{\mu\nu}[K_\mu P_\nu + K_\nu P_\mu - g_{\mu\nu}K\cdot P] = -8K\cdot P. \tag{C.16}$$

Substitution into (C.5) yields

$$\Pi^\mu_\mu = -4ie^2\int\frac{d^4k}{(2\pi)^4}[-2K^2+2K\cdot Q](\tilde{\Delta}_{11}(K)\tilde{\Delta}_{11}(P)-\tilde{\Delta}_{12}(K)\tilde{\Delta}_{21}(P)). \tag{C.17}$$

Substitution of the Keldysh propagators and dropping the terms with poles in only the upper or lower half planes, we have

$$\Pi^\mu_\mu = 4e^2\int\frac{d^4k}{(2\pi)^3}[-2K^2+2K\cdot Q]\frac{\mathrm{sgn}(k_0)N_F(k_0)\delta(K^2)}{(K-Q)^2-i\epsilon\mathrm{sgn}(k_0-q_0)}. \tag{C.18}$$

The next step is to evaluate the k_0 integral and use $\mathrm{sgn}(k_0-q_0)\to\mathrm{sgn}(k_0)$:

$$\Pi^\mu_\mu = \frac{e^2}{2\pi^3}\int d^3k\frac{N_F(k)}{k}\sum_{n=\pm 1}\frac{nkq_0+k\cdot q}{-2nkq_0+2k\cdot q+Q^2-ni\epsilon}.$$

We define x the same way that we did in the longitudinal self energy calculation:

$$\begin{aligned}\Pi^{\mu}_{\mu} &= \frac{e^2}{\pi^2}\int dkkN_F(k)\int_{-1}^{1}dx\sum_{n=\pm 1}\frac{nkq_0+kqx}{-2nkq_0+2kqx+Q^2-ni\epsilon}\\ &= \frac{e^2}{2\pi^2}\int dkkN_F(k)\int_{-1}^{1}dx\sum_{n=\pm 1}\frac{\frac{nq_0}{k}+\frac{qx}{k}}{-\frac{nq_0}{k}+\frac{qx}{k}+\frac{Q^2}{2k^2}-ni\epsilon}.\end{aligned} \tag{C.19}$$

We take the 2-variable Taylor expansion of the fraction in (C.19) and keep only leading order terms:

$$\Pi^{\mu}_{\mu} = \frac{e^2}{\pi^2}\int dkkN_F(k)\int_{-1}^{1}dx\sum_{n=\pm 1}\frac{nq_0-qx}{-nq_0+qx-ni\epsilon}. \tag{C.20}$$

Note that as in the longitudinal case, the two integrals dk and dx are now separated, and we can do each individually:

$$\begin{aligned}&\int_{-1}^{1}dx\sum_{n=\pm 1}\frac{nq_0-qx}{-nq_0+qx-ni\epsilon} = -4\\ &\int dkkN_F(k) = -\frac{T^2\pi^2}{6}\\ &\rightarrow \quad \Pi^{\mu}_{\mu} = 3\omega_p^2.\end{aligned} \tag{C.21}$$

We use the result (C.21) and substitute it into (C.15) to obtain the transverse photon self energy:

$$\begin{aligned}\Pi_T &= \frac{1}{2}\left[3\omega_p^2+3\omega_p^2\frac{Q^2}{q^2}\left(1-\frac{q_0}{2q}\ln\left(\frac{q_0+q+i\epsilon}{q_0-q+i\epsilon}\right)\right)\right]\\ &= \frac{3\omega_p^2}{2}\left[\frac{q_0^2}{q^2}-\frac{q_0Q^2}{2q^3}\ln\left(\frac{q_0+q+i\epsilon}{q_0-q+i\epsilon}\right)\right].\end{aligned} \tag{C.22}$$

C3 Leading Order HTL Fermion Self Energy

In this section, we calculate the retarded fermion self energy in the HTL approximation (see figure 1.5). The fermion self energy is given by the integral

$$\begin{aligned}\Sigma(Q) &= ie^2 \int \frac{d^4k}{(2\pi)^4}\gamma^\mu(\not{K})\gamma^\nu\Delta(K-Q)(-g_{\mu\nu})\tilde{\Delta}(K)\\ &= 2ie^2\int\frac{d^4k}{(2\pi)^4}\not{K}\tilde{\Delta}(K)\Delta(K-Q)\end{aligned}$$

where we have used $\gamma^\mu\not{K}\gamma_\mu = -2\not{K}$. We obtain the retarded self energy from (1.2.11),

$$\Sigma(Q) = -2ie^2\int\frac{d^4k}{(2\pi)^4}\not{K}[\tilde{\Delta}_{11}(K)\Delta_{11}(K-Q) - \tilde{\Delta}_{12}(K)\Delta_{21}(K-Q)]. \tag{C.23}$$

The next step is to rewrite (C.23) in terms of Keldysh propagators in order to isolate the temperature dependence:

$$\begin{aligned}\Sigma(Q) \quad &= -\frac{ie^2}{2}\int\frac{d^4k}{(2\pi)^4}\not{K}[(\tilde{\Delta}_R(K)+\tilde{\Delta}_A(K)+\tilde{\Delta}_S(K))(\Delta_R(K-Q)+\Delta_A(K-Q)+\Delta_S(K-Q))\\ &-(\tilde{\Delta}_S(K)+\tilde{\Delta}_A(K)-\tilde{\Delta}_R(K))(\Delta_S(K-Q)-\Delta_A(K-Q)+\Delta_R(K-Q))]\\ &= -ie^2\int\frac{d^4k}{(2\pi)^4}\not{K}[\tilde{\Delta}_S(K)\Delta_A(K-Q)+\tilde{\Delta}_R(K)\Delta_S(K-Q)].\end{aligned} \tag{C.24}$$

Shifting $K \to K+Q$ in the second term,

$$\not{K}\tilde{\Delta}_R(K)\Delta_S(K-Q) = (\not{K}+\not{Q})\tilde{\Delta}_R(K+Q)\Delta_S(K). \tag{C.25}$$

Since we have already used the operators out front of the propagators,

$$\Delta_{R,A} = \tilde{\Delta}_{R,A}.$$

Thus, the retarded self energy is

$$\begin{aligned}\Sigma_R(Q) &= -ie^2\int\frac{d^4k}{(2\pi)^4}(-2\pi i)\delta(K^2)[\frac{N_F(k_0)\mathrm{sgn}(k_0)\not{K}}{(K-Q)^2 - i\mathrm{sgn}(k_0-q_0)\epsilon} + \frac{N_B(k_0)\mathrm{sgn}(k_0)(\not{K}+\not{Q})}{(K+Q)^2+i\mathrm{sgn}(k_0+q_0)\epsilon}]\\ &= \frac{e^2}{(2\pi)^3}\int d^4k\delta(K^2)[\frac{N_F(k_0)\mathrm{sgn}(k_0)\not{K}}{(K-Q)^2 - i\mathrm{sgn}(k_0-q_0)\epsilon} + \frac{N_B(k_0)\mathrm{sgn}(k_0)(\not{K}+\not{Q})}{(K+Q)^2+i\mathrm{sgn}(k_0+q_0)\epsilon}].\end{aligned} \tag{C.26}$$

According to (B.21), we need to calculate $\mathrm{Tr}[\gamma_0\Sigma(Q)]$ and $\mathrm{Tr}[\not{Q}\Sigma(Q)]$. We work through both of these in calculations similar to those for the boson self energy. Note that we can set $\mathrm{sgn}(k_0 \pm q_0) \to \mathrm{sgn}(k_0)$ due to

the fact that $k_0 >> q_0$ in (C.26). We start with $\mathrm{Tr}[\gamma_0\Sigma(Q)]$:

$$\begin{aligned}
\mathrm{Tr}[\gamma_0\Sigma(Q)] &= \frac{e^2}{8\pi^3}\int d^4k\delta(K^2)[\frac{N_F(k_0)\mathrm{sgn}(k_0)\mathrm{Tr}[\gamma_0\not{K}]}{(K-Q)^2-i\mathrm{sgn}(k_0)\epsilon}+\frac{N_B(k_0)\mathrm{sgn}(k_0)\mathrm{Tr}[\gamma_0(\not{K}+\not{Q})]}{(K+Q)^2+i\mathrm{sgn}(k_0)\epsilon}]\\
&= \frac{e^2}{2\pi^3}\int d^3k\frac{1}{2k}\sum_{n=\pm1}\int_{-1}^{1}dx[\frac{nkN_F(k)}{-2nkq_0+2kqx-Q^2-in\epsilon}+\frac{(nk+q_0)N_B(k)}{2nkq_0-2kqx+Q^2+in\epsilon}]\\
&= \frac{e^2}{4\pi^2}\int dkk\sum_{n=\pm1}\int_{-1}^{1}dx[\frac{nN_F(k)}{-nq_0+qx-in\epsilon}+\frac{nN_B(k)}{nq_0-qx+in\epsilon}]\\
&= \frac{e^2}{4\pi^2}\int dkk\sum_{n=\pm1}n[N_B(k)-N_F(k)]\int_{-1}^{1}dx\frac{1}{nq_0-qx+in\epsilon}\\
&= \frac{e^2}{4\pi^2}\int dkk\sum_{n=\pm1}n[N_B(k)-N_F(k)]\frac{1}{q}\ln(\frac{nq_0+q+in\epsilon}{nq_0-q+in\epsilon})\\
&= \frac{e^2}{4\pi^2}\int dkk\left[(N_B(k)-N_F(k))\frac{1}{q}\ln(\frac{q_0+q-i\epsilon}{q_0-q-i\epsilon})-(N_B(k)-N_F(k))\frac{1}{q}\ln(\frac{-q_0+q+i\epsilon}{-q_0-q+i\epsilon})\right]\\
&= \frac{e^2}{2\pi^2}\int dkk(N_B(k)-N_F(k))\frac{1}{q}\ln\left(\frac{q_0+q+i\epsilon}{q_0-q+i\epsilon}\right)\\
&= \frac{e^2}{2\pi^2}\frac{\pi^2T^2}{2}\frac{1}{q}\ln\left(\frac{q_0+q+i\epsilon}{q_0-q+i\epsilon}\right)\\
&= \frac{e^2T^2}{4q}\ln\left(\frac{q_0+q+i\epsilon}{q_0-q+i\epsilon}\right).
\end{aligned}\tag{C.27}$$

Now consider $\mathrm{Tr}[\not{Q}\Sigma(Q)]$:

$$\begin{aligned}
\mathrm{Tr}[\gamma_0\Sigma(Q)] &= \frac{e^2}{8\pi^3}\int d^4k\delta(K^2)[\frac{N_F(k_0)\mathrm{sgn}(k_0)\mathrm{Tr}[\not{Q}\not{K}]}{(K-Q)^2+i\mathrm{sgn}(k_0)\epsilon}+\frac{N_B(k_0)\mathrm{sgn}(k_0)\mathrm{Tr}[\not{Q}(\not{K}+\not{Q})]}{(K+Q)^2-i\mathrm{sgn}(k_0)\epsilon}]\\
&= \frac{e^2}{2\pi^3}\int d^3k\frac{1}{2k}\sum_{n=\pm1}\int_{-1}^{1}dx[\frac{N_F(k)(nkq_0-kqx)}{-2nkq_0+2kqx-Q^2+in\epsilon}+\frac{N_B(k)(nkq_0-kqx)}{2nkq_0-2kqx+Q^2}]\\
&= \frac{e^2}{4\pi^2}\int kdk\sum_{n=\pm1}\int_{-1}^{1}dx[\frac{N_F(k)(nq_0-qx)}{-nq_0+qx+in\epsilon}+\frac{N_B(k)(nq_0-qx-in\epsilon)}{nq_0-qx-in\epsilon}]\\
&= \frac{e^2}{4\pi^2}\int kdk(N_B(k)-N_F(k))\sum_{n=\pm1}\int_{-1}^{1}dx\frac{nq_0-qx}{nq_0-qx-in\epsilon}\\
&= \frac{e^2}{4\pi^2}\frac{\pi^2T^2}{2}(4)=\frac{e^2T^2}{2}.
\end{aligned}\tag{C.28}$$

We use the results of (C.27) and (C.28) to obtain $A(q_0,q)$ and $B(q_0,q)$ given in (B.20):

$$\begin{aligned}
A(q_0,q) &= \frac{m_F^2}{q^2}[\frac{q_0}{2q}\ln(\frac{q_0+q-i\epsilon}{q_0-q-i\epsilon})-1]\\
B(q_0,q) &= \frac{m_F^2}{q^2}[q_0-\frac{Q^2}{2q}\ln(\frac{q_0+q-i\epsilon}{q_0-q-i\epsilon})].
\end{aligned}\tag{C.29}$$

Therefore, the retarded fermion self energy is

$$\Sigma_R(Q) = \frac{m_F^2}{q^2}\left[\left(\frac{q_0}{2q}\ln(\frac{q_0+q-i\epsilon}{q_0-q-i\epsilon})-1\right)\not{Q} + \left(q_0 - \frac{Q^2}{2q}\ln(\frac{q_0+q-i\epsilon}{q_0-q-i\epsilon})\right)\gamma_0\right]. \tag{C.30}$$

We rewrite (C.30) in the form given by (1.3.6):

$$\begin{aligned}
&= \Sigma^{(0)}(q_0,q)\gamma_0 - \Sigma(s)(q_0,q)\hat{q}\cdot\vec{\gamma} \\
\Sigma^{(0)}(q_0,q) &= \frac{m_F^2}{q}\left[\frac{1}{2}\ln\left(\frac{q_0+q-i\epsilon}{q_0-q-i\epsilon}\right)\right] \\
\Sigma^{(s)}(q_0,q) &= \frac{m_F^2}{q}\left[\frac{q_0}{2q}\ln\left(\frac{q_0+q-i\epsilon}{q_0-q-i\epsilon}\right)-1\right].
\end{aligned} \tag{C.31}$$

D Spectral Function Calculation

In this section we will study the spectral function and how it relates to different forms of the propagator. We will start by looking at scalars, and later study fermions.

We define ρ in position space:

$$\rho(X-Y) = i(\Delta_R(X-Y) - \Delta_A(X-Y)). \tag{D.1}$$

We use (1.2.1) and (1.2.7) to get:

$$\begin{aligned}
\Delta_R(X-Y) &= \Delta_{11}(X-Y) - \Delta_{12}(X-Y) = -i\langle T(\phi(X)\phi(Y))\rangle + i\langle\phi(Y)\phi(X)\rangle \\
&= -i\theta(x_0-y_0)\langle[\phi(X),\phi(Y)]\rangle \\
\Delta_A(X-Y) &= \Delta_{11}(X-Y) - \Delta_{21}(X-Y) = -i\langle T(\phi(X)\phi(Y))\rangle + i\langle\phi(X)\phi(Y)\rangle \\
&= -i\theta(y_0-x_0)\langle[\phi(Y),\phi(X)]\rangle \\
\rho(X-Y) &= \langle[\phi(X),\phi(Y)]\rangle
\end{aligned} \tag{D.2}$$

where we used (A.13) in the last step. Similarly, we use the anti-commutator and make the definition

$$\bar{\rho}(X-Y) = \langle[\phi(X),\phi(Y)]_+\rangle. \tag{D.3}$$

Using (1.2.1) and (1.2.7) it is straightforward to show:

$$\Delta_S(X-Y) = -i\bar{\rho}(X-Y).$$

From [7] we have,

$$\Delta_R(p_0,p) = \int_{-\infty}^{\infty}\frac{d\omega}{2\pi}\frac{\rho(\omega,p)}{\omega-p_0+i\epsilon}. \tag{D.4}$$

This is a particularly interesting result, as the RHS of (D.4) depends only on the imaginary part of $\Delta_R(p_0,p)$, and therefore the real part of $\Delta_R(p_0,p)$ can be determined from the imaginary part.

We now determine the imaginary part of (D.4). Using (A.10),

$$\Delta_R(p_0,p) = \frac{1}{2\pi}\int_{-\infty}^{\infty} d\omega\rho(\omega,p)\left[P.V.\frac{1}{\omega-p_0} - i\pi\delta(\omega-p_0)\right]. \tag{D.5}$$

The first term in the brackets is real. Therefore,

$$\begin{aligned}
&\mathrm{Im}\Delta_R(p_0,p) = -\frac{1}{2}\int_{-\infty}^{\infty} d\omega\rho(\omega,p)\delta(\omega-p_0)\\
&\frac{1}{2i}(\Delta_R(p_0,p)-\Delta_A(p_0,p)) = -\frac{1}{2}\rho(p_0,p)\\
&\rho(p_0,p) = i(\Delta_R(p_0,p)-\Delta_A(p_0,p))
\end{aligned} \tag{D.6}$$

in agreement with (D.1).

Now we calculate the KMS condition (equation (1.2.10)). We start from the Fourier transforms of (D.2) and (D.3):

$$\begin{aligned}
\rho(X,Y) &= \int d^4(X-Y)e^{iP\cdot(X-Y)}\langle[\phi(X),\phi(Y)]_-\rangle\\
\bar{\rho}(X,Y) &= \int d^4(X-Y)e^{iP\cdot(X-Y)}\langle[\phi(X),\phi(Y)]_+\rangle.
\end{aligned} \tag{D.7}$$

In the Heisenberg representation $\phi(X) = e^{iP\cdot X}\phi(0)e^{-iP\cdot X}$ [22] and we have:

$$\begin{aligned}
\langle\phi(X)\phi(Y)\rangle \quad &= \mathrm{Tr}(e^{-\beta H}\phi(X)\phi(Y))\\
&= \sum_n \langle n|e^{-\beta H}\phi(X)\phi(Y)|n\rangle\\
&= \sum_n \langle n|e^{-\beta H}e^{iP\cdot X}\phi(0)e^{-iP\cdot X}e^{iP\cdot Y}\phi(0)e^{-iP\cdot Y}|n\rangle\\
&= \sum_{n,m} \langle n|e^{-\beta H}e^{iP\cdot X}\phi(0)e^{-iP\cdot X}|m\rangle\langle m|e^{iP\cdot Y}\phi(0)e^{-iP\cdot Y}|n\rangle\\
&= \sum_{n,m} e^{-\beta E_n}e^{iP_n\cdot X}e^{-iP_m\cdot X}e^{iP_m\cdot Y}e^{-iP_n\cdot Y}\langle n|\phi(0)|m\rangle\langle m|\phi(0)|n\rangle\\
&= \sum_{n,m} e^{-\beta E_n}e^{i(P_n-P_m)\cdot(X-Y)}|\langle n|\phi(0)|m\rangle|^2.
\end{aligned} \tag{D.8}$$

Similarly,

$$\langle\phi(Y)\phi(X)\rangle = \sum_{n,m} e^{-\beta E_n}e^{-i(P_n-P_m)\cdot(X-Y)}|\langle n|\phi(0)|m\rangle|^2. \tag{D.9}$$

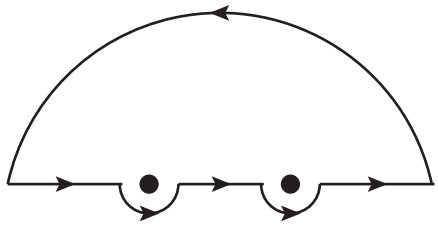

Figure D1: The contour of integration used for (D.14). We integrate around the poles such that they are inside the contour include, hence the presence of the residue term. The dots represent the poles.

Taking the Fourier transform of (D.8) and (D.9),

$$\begin{aligned}
&\int d^4(X-Y)e^{iP\cdot(X-Y)}\langle[\phi(X),\phi(Y)]_\pm\rangle \\
&= \int d^4(X-Y)e^{iP\cdot(X-Y)}\sum_{n,m} e^{-\beta E_n}|\langle n|\phi(0)|m\rangle|^2[e^{i(P_n-P_m)\cdot(X-Y)} \pm e^{-i(P_n-P_m)\cdot(X-Y)}] \\
&= \sum_{n,m}|\langle n|\phi(0)|m\rangle|^2[\delta(P+P_n-P_m)e^{-\beta E_n} \pm \delta(P-P_n+P_m)e^{-\beta E_n}] \\
&= \sum_{n,m}|\langle n|\phi(0)|m\rangle|^2\delta(P+P_n-P_m)[e^{-\beta E_n} \pm e^{-\beta E_m}] \\
&= \sum_{n,m}|\langle n|\phi(0)|m\rangle|^2\delta(P+P_n-P_m)e^{-\beta E_n}(1 \pm e^{\beta p_0}).
\end{aligned} \tag{D.10}$$

In the fourth line of (D.10) we switched the indices m and n in the second term in order to factor out the delta function. Therefore,

$$\frac{\bar{\rho}(p_0,p)}{\rho(p_0,p)} = \frac{1+e^{\beta p_0}}{1-e^{\beta p_0}} = 1+2n_B(p_0). \tag{D.11}$$

Using (D.1) and (D.4),

$$\begin{aligned}
&\frac{\bar{\rho}(p_0,p)}{\rho(p_0,p)} = \frac{i\Delta_S(p_0,p)}{i(\Delta_R(p_0,p)-\Delta_A(p_0,p))} = 1+2n_B(p_0) \\
\rightarrow \qquad &\Delta_S(p_0,p) = (1+2n_B(p_0))(\Delta_R(p_0,p)-\Delta_A(p_0,p)).
\end{aligned} \tag{D.12}$$

Thus we have derived (1.2.10) and shown that the Keldysh propagator has only two independent components.

Now we calculate the spectral function. Integrating (D.1),

$$\int_{-\infty}^{\infty} dp_0\rho(p_0,p) = i\int_{-\infty}^{\infty} dp_0(\Delta_R(p_0,p)-\Delta_A(p_0,p)). \tag{D.13}$$

We start by considering the integration of D_R. The poles of D_R will be in the lower half plane, thus we choose a contour in the upper half plane.

$$\oint dp_0 D_R(p_0,p) = \int_{-\infty}^{\infty} D_R(p_0,p) + \int_C D_R(p_0,p) = 0$$
$$\int_{-\infty}^{\infty} dp_0 D_R(p_0,p) = -\int_C dp_0 \Delta_R(p_0,p). \tag{D.14}$$

The next step is to find the expression for $\int_C dp_0 D_R$. We do this by taking the limit as the imaginary part of the poles approach zero. In this limit, the poles will be on the contour. To use the residue theorem we must detour around the poles. We choose the contour in figure D. We obtain

$$\oint dp_0 D_R(p_0) = 2\pi i \sum Res(\Delta_R)$$
$$\rightarrow \qquad P.V.\big|_R + i\pi \sum Res(\Delta_R) + \int_C \Delta_R(p_0) = 2\pi i \sum Res(\Delta_R) \tag{D.15}$$

where

$$P.V.\big|_R = \lim_{\delta\to 0}\left[\int_{-\delta}^{-\infty} \Delta_R(p_0,p)dp_0 + \int_{\delta}^{\infty} \Delta_R(p_0,p)dp_0\right]$$

and the second term in (D.15) comes from the small semi-circles in figure D. Solving (D.15) for $\int_C \Delta_R(p_0)$ and substituting into (D.14) we obtain:

$$\int_{-\infty}^{\infty} dp_0 \Delta_R(p_0,p) = P.V.|_R - \pi i \sum Res(\Delta_R). \tag{D.16}$$

For $\Delta_A(p_0,p)$, the poles will be in the upper half plane, so we choose a contour in the lower half plane. Performing a similar calculation to the one for $\Delta_R(p_0,p)$ and noting that the orientation of the curve is changed, the result is

$$\int_{-\infty}^{\infty} \Delta_A(p_0,p) = P.V.|_A + \pi i \sum Res(\Delta_A). \tag{D.17}$$

Combining (D.16) and (D.17), the integral of the spectral function will be

$$\int_{-\infty}^{\infty} dp_0 \rho(p_0,p) = i(P.V._R - P.V._A) + \pi[\sum Res(\Delta_R) + \sum Res(\Delta_A)]. \tag{D.18}$$

Now we will consider photons and look at transverse modes. The spectral function can be written using

the photon projection operators,

$$\rho_{\mu\nu} = -P^T_{\mu\nu}\rho_T - P^L_{\mu\nu}\frac{p^2}{P^2}\rho_L$$

$$\rho_T = \Delta^T_R - \Delta^T_A$$

$$\rho_L = \frac{P^2}{p^2}(\Delta^L_R - \Delta^L_A). \tag{D.19}$$

The propagator Δ^T is given in (1.3.3) and the self-energy Π_T in (1.3.5). Note that $P.V.\big|_R \neq P.V.\big|_A$ due to the presence of the logarithm function and the necessity of a cut in the complex q_0 plane to make the function single-valued. Consider the two factors on the RHS of (D.18). We will show that

$$\pi[\sum Res(\Delta_R) + \sum Res(\Delta_A)] = \quad 2\pi \int dp_0[\delta(\omega - p_0) - \delta(\omega + p_0)]Z(p_0, p)) \tag{D.20}$$

$$i(P.V.|_R - P.V.|_A) = \quad 2\pi\beta(p_0, p) \tag{D.21}$$

where

$$Z(p_0, p) = \frac{p_0(p_0^2 - p^2)}{3m_\infty^2 p_0^2 - (p_0^2 - p^2)^2} \tag{D.22}$$

$$\beta(p_0, p) = -\frac{\frac{3}{4p^2}m_\infty^2 \frac{p_0}{p}P^2\theta(-P^2)}{(P^2 - \frac{3}{2}m_\infty^2[\frac{p_0^2}{p^2} - \frac{p_0 P^2}{2p^3}\ln\frac{|p_0+p|}{|p_0-p|}])^2 + \frac{9\pi^2 m_\infty^4 p_0^2 P^2}{16p^6}}. \tag{D.23}$$

We start with the residue terms (D.20). The residues of the propagator are obtained from

$$\mathrm{Res}(\Delta_R) = \lim|_{p_0\to\omega_T}(p_0 - \omega_T)\Delta^T_R(p_0, p)$$

$$= \lim|_{p_0\to\omega}\frac{p_0 - \omega}{\left[(\Delta^T_R(p_0, p)\right]^{-1}}.$$

To evaluate the limit we apply L'Hopitals rule to obtain

$$Z_T(p) = \left(\frac{\partial}{\partial p_0}(\Delta^{-1})|_{p_0=\omega_T(p)}\right)^{-1}. \tag{D.24}$$

Using equations (1.3.3), (1.3.5) and (1.4.3) we obtain (D.20). The calculation is simplified using the following trick: since $\Delta_T^{-1}(\omega_T) = 0$ we have

$$\ln\frac{\omega_T + p + i\epsilon}{\omega_T - p + i\epsilon} = \frac{2\omega_T p}{\omega_T^2 - p^2} - \frac{4p^3}{3m_\infty^2\omega_T}.$$

The advanced self energy is obtained from the retarded self energy by the relation $\Delta_A = \Delta_R(i\epsilon \to -i\epsilon)$. It is easy to see that the residues will follow the same rule.

Recall that there are two poles of the propagator, located at $\pm\omega_T$. Since $Z_T(-\omega_T) = -Z_T(\omega_T)$ the contribution to $\rho(p_0, p)$ from the residues will be

$$\pi(Res(\Delta_R, p_0 = \omega_T) + Res(\Delta_R, p_0 = -\omega_T)) = \pi \int_{-\infty}^{\infty} dp_0[\delta(p_0 - \omega_T) - \delta(p_0 + \omega_T)]Z(\omega_T, p).$$

The advanced case will produce the same result. Therefore, we have reproduced (D.20).

The next step is to calculate $\beta(p_0, p)$. Using (D.21), (1.3.3) and (1.3.5) we have:

$$i[P.V.|_R - P.V.|_A] = i\theta(-P^2) \qquad \Big[\frac{1}{p_0^2 - p^2 - \frac{3m_\infty^2}{2}(\frac{p_0^2}{p^2} - \frac{p_0^3 - p^2 p_0}{2p^3}(\ln\frac{p_0+p+i\epsilon}{p_0-p+i\epsilon}))} - \frac{1}{p_0^2 - p^2 - \frac{3m_\infty^2}{2}(\frac{p_0^2}{p^2} - \frac{p_0^3 - p^2 p_0}{2p^3}(\ln\frac{p_0+p+i\epsilon}{p_0-p+i\epsilon}))}\Big] \tag{D.25}$$

where we set ϵ to zero everywhere except in the argument of the logarithm.

We define the logarithm function with a cut along the negative real axis. To find $\mathrm{Im}\Pi_R$ and $\mathrm{Im}\Pi_A$ we will need to evaluate 4 logs whose arguments are shown in figure D. Using $p > |p_0|$ we have:

$$\begin{aligned}
\ln((p_0 + p) + i\epsilon) &= \ln\big[|p_0 + p|e^{i0^+}\big] = \ln|p_0 + p| \\
\ln((p_0 - p) + i\epsilon) &= \ln\big[|p_0 - p|e^{i\pi}\big] = \ln|p_0 - p| + i\pi \\
\ln((p_0 - p) - i\epsilon) &= \ln\big[|p_0 - p|e^{-i\pi}\big] = \ln|p_0 - p| - i\pi \\
\ln((p_0 + p) - i\epsilon) &= \ln\big[|p_0 + p|e^{i0^-}\big] = \ln|p_0 + p|.
\end{aligned} \tag{D.26}$$

The logarithm will be imaginary if the argument is negative. This occurs when exactly one of the numerator or denominator of (D.26) is negative. Thus, the two situations in which (D.26) will have an imaginary component are

1) $p_0 + p > 0,\ p_0 - p < 0$

2) $p_0 + p < 0,\ p_0 - p > 0$

which means there will be an imaginary component of the logarithm if and only if $p > |p_0|$, i.e. $P^2 < 0$.

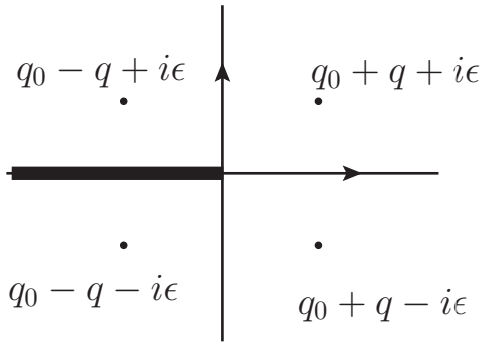

Figure D2: Poles in the complex plane that give (D.26) given that $k > k_0$. The cut is along the negative q_0 axis.

Substituting (D.26) into (D.25) we obtain

$$i[P.V.|_R - P.V.|_A] = i\theta(-P^2) \qquad \Bigg[\frac{1}{p_0^2 - p^2 - \frac{3m_\infty^2}{2}(\frac{p_0^2}{p^2} - \frac{p_0^3 - p^2 p_0}{2p^3}(\ln\frac{|p_0+p|}{|p_0-p|} - i\pi))} \\ - \frac{1}{p_0^2 - p^2 - \frac{3m_\infty^2}{2}(\frac{p_0^2}{p^2} - \frac{p_0^3 - p^2 p_0}{2p^3}(\ln\frac{|p_0+p|}{|p_0-p|} + i\pi))}\Bigg]. \tag{D.27}$$

Defining

$$A = P^2 - \frac{3m_\infty^2 p_0^2}{2p^2} + \frac{3m_\infty^2 P^2 p_0}{4p^3}\ln\frac{|p_0+p|}{|p_0-p|}$$
$$B = \frac{3m_\infty^2 P^2 p_0 \pi}{4p^3}$$

we have

$$\begin{aligned} i[P.V.|_R - P.V.|_A] \qquad &= i\theta(-P^2)\left[\frac{1}{A - iB} - \frac{1}{A + iB}\right] = i\theta(-P^2)\left[\frac{2iB}{A^2 + B^2}\right] \\ &= 2\pi\theta(-P^2)\frac{\frac{-3\omega_p^2 P^2 p_0 \pi}{2p^3}}{(P^2 - \frac{3\omega_p^2 p_0^2}{2p^2} + \frac{3\omega_p^2 P^2 p_0}{4p^3}\ln\frac{|p_0+p|}{|p_0-p|})^2 + (\frac{3\omega_p^2 P^2 p_0 \pi}{4p^3})^2} \end{aligned} \tag{D.28}$$

in agreement with (D.23).

Combining pieces we have shown that the spectral function is given by

$$\rho_T(\omega_T, p) = 2\pi \int dp_0[\delta(p_0 - \omega_T) - \delta(p_0 + \omega_T)]Z(\omega_T, p) + 2\pi\beta(\omega_T, p). \tag{D.29}$$

It is straightforward to take the zero temperature limit of the transverse spectral function. In the limit $m_\infty \to 0$ we have $\beta(\omega_T, p) = 0$ from (D.21). Using $\omega_T \sim p$ (see equation (1.4.3)) we obtain from (D.20)

$Z \sim 1/2p$. Combining we have:

$$\begin{aligned}\rho_0(p_0, p) &= 2\pi sgn(p_0)\frac{1}{2\omega}[\delta(p_0 - \omega) + \delta(p_0 + \omega)] \\ &= 2\pi sgn(p_0)\delta(p_0^2 - \omega^2).\end{aligned}$$

Therefore in the zero temperature limit the free spectral function reduces to the result that would be obtained from (D.6) using bare propagators [6].

E Cancellation of Leading Order Term in n-Gluon vertex

In this appendix we show that the expected leading order term of the n-gluon vertex vanishes, and as such the power counting rules must be modified from (2.1.10). This cancellation produces the statistical factor discussed in section 2 and accounts for the factor $g^{\delta_{E_F 0}}$in (2.1.13).

We define

$$P_i = \sum_{m=0}^{i} Q_m, \qquad P_0 = 0. \tag{E.1}$$

The amplitude of the n gluon vertex is given by

$$\begin{aligned}
\Gamma &= i(-g)^n C_1 \int \frac{d^4k}{(2\pi)^4} C_2 X \\
C_1 &= \mathrm{Tr}[\prod_{i=1}^{n} (t^{a_i})] \\
C_2 &= \mathrm{Tr}[\not{K}(\prod_{j=1}^{n-1} (\gamma^{\mu_j}(\not{K} + \not{P}_i)))\gamma^{\mu_n}] \overset{LOHTL}{\longrightarrow} K^n \\
X &= \tilde{\Delta}(K) \prod_{i=1}^{n-1} \tilde{\Delta}(K + P_i).
\end{aligned} \tag{E.2}$$

The number of gluon legs is n but the number of independent external momenta is $n-1$ (due to conservation of momentum). The t^{a_i} are the QCD generators and have no effect on the order of the diagram, contributing only a multiplicative constant to the amplitude. The trace term containing the momenta can be simplified, but there is no need to do so since we are only interested in the result at leading order. The term X is a product of propagators dependent on the internal momenta of the loop.

We remind the reader that the Keldysh propagators for fermions are (1.2.9):

$$\begin{aligned}
\tilde{\Delta}_S(P) &= -2\pi i N_F(p_0)\delta(P^2) \\
\tilde{\Delta}_{R,A} &= \frac{1}{P^2 \pm i\epsilon}.
\end{aligned} \tag{E.3}$$

Given a 1-loop diagram, the product of n propagators will always contain one symmetric propagator and a combination of $(n-1)$ advanced and retarded propagators. We are only concerned with the real part of the diagram, therefore we only care about the real part of the advanced and retarded propagators. We make

the definition $D(P_j) = \mathrm{Re}(\Delta_{R,A}(P_j))$ and rewrite X:

$$X = \sum_{i=0}^{n-1} \tilde{\Delta}_S(K + P_i) \prod_{j=0, j\neq i}^{n-1} D(K + P_j). \tag{E.4}$$

Substitution of the Keldysh propagators into (E.4) yields

$$X = -2\pi i \sum_{i=0}^{n-1} N_F(k_0 + p_{(i)0})\delta((K + P_i)^2) \prod_{j=0, j\neq i}^{n-1} \frac{1}{(K + P_j)^2}. \tag{E.5}$$

The next step is to perform a shift of variables on each term of the summation of (E.5) in order to factor out the delta function and statistical factor. In the summation, for the i^{th} term, we make the substitution $K \to K - P_i$. The result is

$$X = -2\pi i N_F(k_0)\delta(K^2) \left[\sum_{i=0}^{n-1} \prod_{j=0, j\neq i}^{n-1} \frac{1}{(K + P_j - P_i)^2} \right]. \tag{E.6}$$

Due to the presence of the delta function, all factors of K^2 vanish. We can also neglect any terms of the form $Q_i \cdot Q_j$, as they are sub-leading . Also note that each factor of the product contributes a factor of $\frac{1}{2}$. Therefore:

$$\frac{1}{(K + P_j - P_i)^2} \overset{LO\ HTL}{\longrightarrow} \frac{1}{2K \cdot (P_j - P_i)}. \tag{E.7}$$

Substitution of (E.7) into (E.6) gives

$$X = -(2)^{2-n}\pi i N_F(k_0)\delta(K^2) \left[\sum_{i=0}^{n-1} \prod_{j=0, j\neq i}^{n-1} \frac{1}{K \cdot (P_j - P_i)} \right]. \tag{E.8}$$

We define

$$\begin{aligned} C &= 2^{2-n}\pi g^n C_1 \\ I_C &= N_F(k_0)\delta(K^2)C_2. \end{aligned} \tag{E.9}$$

Using (E.8) and (E.9), (E.2) becomes

$$\begin{aligned} \Gamma &= C \int \frac{d^4k}{(2\pi)^4} I_C \Theta_n \\ \Theta_n &= \sum_{i=0}^{n-1} t_i, \qquad t_i = \prod_{j=0, j\neq i}^{n-1} \frac{1}{K \cdot (P_j - P_i)}. \end{aligned} \tag{E.10}$$

We want to show that the above equation vanishes for any arbitrary n. This will be accomplished using mathematical induction. The first step is to show that the $n = 2$ case vanishes. We have already done this

(see (2.1.12). We repeat the calculation to illustrate the notation of this section:

$$\begin{aligned}\Theta_2 &= \sum_{i=0}^{2} \prod_{j=0, j\neq i}^{2} \frac{1}{K\cdot(Q_j - Q_i)} \\ &= \frac{1}{K\cdot(Q_2 - Q_1)} + \frac{1}{K\cdot(Q_1 - Q_2)} = 0. \end{aligned} \tag{E.11}$$

Therefore, (E.10) is valid for $n = 2$.

Now we will show that $\Theta_{n+1} \propto \Theta_n$. From (E.10),

$$\Theta_{n+1} = \sum_{i=0}^{n} \left[\prod_{j=0, j\neq i}^{n} \frac{1}{K\cdot P_j - K\cdot P_i} \right]. \tag{E.12}$$

We will use the partial fraction relation

$$\frac{1}{AB} = \frac{1}{A-B}\left(\frac{1}{B} - \frac{1}{A}\right). \tag{E.13}$$

Starting from (E.12), we use the following strategy:

1) Separate the last two terms from the remainder of the summation of (E.12).

$$\Theta_{n+1} = \sum_{i=0}^{n-2} t_i + t_{n-1} + t_n. \tag{E.14}$$

2) Partial fraction the last two factors of the terms of the summation term of (E.14) using (E.13).

$$\begin{aligned}\sum_{i=0}^{n-2} t_i &= \sum_{i=0}^{n-2} \left[\prod_{j=0, j\neq i}^{n} \frac{1}{K\cdot(P_j - P_i)} \right] \\ &= \sum_{i=0}^{n-2} \left[\prod_{j=0, j\neq i}^{n-2} \frac{1}{K\cdot(P_j - P_i)} \right] \underbrace{\frac{1}{K\cdot(P_{n-1} - P_i)} \frac{1}{K\cdot(P_n - P_i)}}_{partial\ fraction} \\ &= \sum_{i=0}^{n-2} \underbrace{\left[\prod_{j=0, j\neq i}^{n-2} \frac{1}{K\cdot(P_j - P_i)} \right] \frac{1}{K\cdot Q_n}}_{B(i)} \left[\underbrace{\frac{1}{K\cdot(P_{n-1} - P_i)}}_{A_1(i)} - \underbrace{\frac{1}{K\cdot(P_n - P_i)}}_{A_2(i)} \right] \\ &= \sum_{i=1}^{n-2} \left[A_1(i)B(i) + A_2(i)B(i) \right]. \end{aligned} \tag{E.15}$$

3) Rewrite the last two terms of (E.14).

$$\begin{aligned} t_{n-1} &= \prod_{j=0, j\neq n-1}^{n} \frac{1}{K\cdot(P_j - P_{n-1})} = \frac{1}{K\cdot Q_n} \prod_{j=0, j\neq n-1}^{n-1} \frac{1}{K\cdot(P_j - P_{n-1})} \\ t_n &= \prod_{j=0, j\neq n}^{n} \frac{1}{K\cdot(P_j - P_n)} = -\frac{1}{K\cdot Q_n} \prod_{j=0}^{n-2} \frac{1}{K\cdot(P_j - P_n)}. \end{aligned} \tag{E.16}$$

We will now show that the combination of all the terms of Θ_{n+1} yields a result that depends on Θ_n with different arguments.

$$\Theta_{n+1} = \sum_{i=0}^{n-2} (A_1(i) + A_2(i))B(i) + t_{n-1} + t_n = P_1 + P_2. \tag{E.17}$$

4) Calculate $\sum_{i=0}^{n-2} A_1(i)B(i) + t_{n-1} = P_1$:

$$P_1 = \frac{1}{K \cdot Q_n}\left[\sum_{i=0}^{n-2}\left[\prod_{j=0,j\neq i}^{n-2}\frac{1}{K\cdot(P_j - P_i)}\right]\underbrace{\frac{1}{K\cdot(P_{n-1}-P_i)}}_{\alpha} + \prod_{j=0,j\neq n-1}^{n-1}\frac{1}{K\cdot(P_j - P_{n-1})}\right].$$

The term labeled α is the $(n-1)^{th}$ term of the product in the sum of (E.18), allowing us to write

$$P_1 = \frac{1}{K\cdot Q_n}\sum_{i=0}^{n-2}\left[\prod_{j=0,j\neq i}^{n-1}\frac{1}{K\cdot(P_j-P_i)}\right] + \prod_{j=0,j\neq n-1}^{n-1}\frac{1}{K\cdot(P_j-P_{n-1})}.$$

Finally, we see that the last term is the $(n-1)^{th}$ term of the summation, thus

$$\begin{aligned} P_1 &= \frac{1}{K\cdot Q_n}\sum_{i=0}^{n-1}\left[\prod_{j=0,j\neq i}^{n-1}\frac{1}{K\cdot(P_j-P_i)}\right] \\ &= \frac{1}{K\cdot Q_n}\Theta_n(P_1, P_2, ..., P_{n-2}, P_{n-1}). \end{aligned} \tag{E.18}$$

We have included the arguments of Θ_n to show which momenta it depends on. This will be particularly important in the next part of the calculation.

5) Calculate $\sum_{i=0}^{n-2} A_2(i)B(i) + t_n = P_2$:

$$P_2 = -\frac{1}{K\cdot Q_n}\left[\sum_{i=0}^{n-2}\frac{1}{K\cdot(P_n-P_i)}\left[\prod_{j=0,j\neq i}^{n-2}\frac{1}{K\cdot(P_j-P_i)}\right] + \prod_{j=0}^{n-2}\frac{1}{K\cdot(P_j-P_n)}\right]. \tag{E.19}$$

We can show that (E.10) is equivalent to (E.19) with the relabeling $P_{n-1} \to P_n$. Start by taking (E.10) and take the $n-1$ terms out of the summation and product.

$$\begin{aligned} \Theta_n &= \sum_{i=0}^{n-1}\prod_{j=0,j\neq i}^{n-1}\frac{1}{K\cdot(P_j-P_i)} \\ &= \sum_{i=0}^{n-2}\prod_{j=0,j\neq i}^{n-1}\frac{1}{K\cdot(P_j-P_i)} + \prod_{j=0}^{n-2}\frac{1}{K\cdot(P_j-P_{n-1})} \\ &= \sum_{i=0}^{n-2}\prod_{j=0,j\neq i}^{n-2}\left[\frac{1}{K\cdot(P_j-P_i)}\right]\frac{1}{K\cdot(P_{n-1}-P_i)} + \prod_{j=0}^{n-2}\frac{1}{K\cdot(P_j-P_{n-1})}. \end{aligned} \tag{E.20}$$

Now, define $P_{n-1} \to P_n$ in (E.20):

$$\begin{aligned} P_2 \quad &= \sum_{i=0}^{n-2} \prod_{j=0, j\neq i}^{n-2} \left[\frac{1}{K\cdot(P_j - P_i)}\right] \frac{1}{K\cdot(P_n - P_i)} + \prod_{j=0}^{n-2} \frac{1}{K\cdot(P_j - P_n)} \\ &= -K\cdot Q_n \Theta_n(P_1, P_2, ..., P_{n-2}, P_n). \end{aligned} \tag{E.21}$$

Therefore,

$$\Theta_{n+1}(P_1, P_2, ..., P_{n-2}, P_{n-1}, P_n) = \frac{1}{K\cdot Q_n}\Theta_n(P_1, P_2, ..., P_{n-2}, P_{n-1}) - \frac{1}{K\cdot Q_n}\Theta_n(P_1, P_2, ..., P_{n-2}, P_n). \tag{E.22}$$

We have shown that both terms of Θ_{n+1} can be written as Θ_n with different arguments. Combined with $\Theta_2(P_1, P_2) \to 0$, we have shown by induction the leading order term of the n-gluon loop cancels.

F Symmetries of the Boson and Fermion Self Energies

In this appendix we show that the real and imaginary parts of the boson and fermion self energies $\Pi(p_0, p)$ and $\Sigma(p_0, p)$ obey specific symmetry relations. The results are obtained exactly, and thus do not depend on the HTL limit or perturbation series. However, the symmetries should be obeyed at every order in the HTL resummation. This makes the calculations much easier, as we can use symmetry arguments to argue that certain terms must vanish. We will show that

$$\begin{aligned}
&\mathrm{Re}\Pi_{T,L}(p_0, p) = \mathrm{Re}\Pi_{T,L}(-p_0, p) \\
&\mathrm{Im}\Pi_{T,L}(p_0, p) = -\mathrm{Im}\Pi_{T,L}(-p_0, p) \\
&\mathrm{Re}\Sigma^{(0)}(-p_0, p) = -\mathrm{Re}\Sigma^{(0)}(p_0, p) \\
&\mathrm{Re}\Sigma^{(s)}(-p_0, p) = \mathrm{Re}\Sigma^{(s)}(p_0, p) \\
&\mathrm{Im}\Sigma^{(0)}(-p_0, p) = \mathrm{Im}\Sigma^{(0)}(p_0, p) \\
&\mathrm{Im}\Sigma^{(s)}(-p_0, p) = -\mathrm{Im}\Sigma^{(s)}(p_0, p).
\end{aligned} \tag{F.1}$$

F1 Preliminaries

We start with the effective propagators in the spectral representation in position space (see appendix D). $\phi(X)$ are boson fields, and $\psi(X)$ are fermion fields:

$$\begin{aligned}
D_{ret}(X - Y) &= -i\theta(x_0 - y_0)\langle[\phi(X), \phi(Y)]_-\rangle \\
D_{adv}(X - Y) &= i\theta(y_0 - x_0)\langle[\phi(X), \phi(Y)]_-\rangle
\end{aligned} \tag{F.2}$$

$$\begin{aligned}
S_{ret}(X - Y) &= -i\theta(x_0 - y_0)\langle[\psi(X), \overline{\psi}(Y)]_+\rangle \\
S_{adv}(X - Y) &= i\theta(y_0 - x_0)\langle[\psi(X), \overline{\psi}(Y)]_+\rangle
\end{aligned} \tag{F.3}$$

where the step function is defined in (A.11).

The following relations between propagators are useful [23] and follow from (F.2) and (F.3):

$$D^*_{ret}(X-Y) = D_{adv}(Y-X)$$

$$S^*_{ret}(X-Y) = S_{adv}(Y-X) \tag{F.4}$$

$$D^*_{ret}(P) = D_{adv}(P)$$

$$S^*_{ret}(P) = S_{adv}(P). \tag{F.5}$$

Note that (F.5) are obtained by taking the Fourier transform of the first line of (F.2) and (F.3) and then taking the complex conjugate.

The next step is to rewrite the expectation values of the position space propagators (F.2, F.3) in the spectral representation. We use the Heisenberg representation [22] and take the expectation value by tracing over a complete set of momentum eigenstates $\{|n\rangle\}$ weighted by the Boltzmann operator. We then insert another complete set of momentum eigenstates $\{|m\rangle\}$:

$$\begin{aligned}
\langle\phi(X)\phi(Y)\rangle &= \sum_n \langle n|e^{-\beta H}\phi(X)\phi(Y)|n\rangle \\
&= \sum_n \langle n|e^{-\beta H}e^{iP\cdot X}\phi(0)e^{-iP\cdot X}e^{iP\cdot Y}\phi(0)e^{-iP\cdot Y}|n\rangle \\
&= \sum_{n,m} \langle n|e^{-\beta H}e^{iP\cdot X}\phi(0)e^{-iP\cdot X}|m\rangle\langle m|e^{iP\cdot Y}\phi(0)e^{-iP\cdot Y}|n\rangle \\
&= \sum_{n,m} e^{-\beta E_n}e^{i(P_n-P_m)\cdot(X-Y)}\langle n|\phi(0)|m\rangle\langle m|\phi(0)|n\rangle.
\end{aligned} \tag{F.6}$$

Interchanging X and Y we obtain

$$\langle\phi(Y)\phi(X)\rangle \qquad = \sum_{n,m} e^{-\beta E_n}e^{-i(P_n-P_m)\cdot(X-Y)}\langle n|\phi(0)|m\rangle\langle m|\phi(0)|n\rangle. \tag{F.7}$$

Switching m and n in (F.7) and combining with (F.6) gives

$$\langle[\phi(X),\phi(Y)]_-\rangle = \sum_{n,m}[e^{-\beta E_n} - e^{-\beta E_m}]e^{i(P_n-P_m)\cdot(X-Y)}\langle n|\phi(0)|m\rangle\langle m|\phi(0)|n\rangle. \tag{F.8}$$

The corresponding calculation for fermions is similar:

$$\langle[\psi(X),\overline{\psi}(Y)]_+\rangle = \sum_{n,m}[e^{-\beta E_n} + e^{-\beta E_m}]e^{i(P_n-P_m)\cdot(X-Y)}\langle n|\psi(0)|m\rangle\langle m|\overline{\psi}(0)|n\rangle. \tag{F.9}$$

Our strategy is to use (F.2) and (F.3) to determine if the propagator is even or odd under the transformation $p_0 \to -p_0$. We will then use the Dyson equation to determine the symmetries of the self energies with respect to p_0.

F2 Boson Self Energy

In this subsection we will determine the symmetry of the real and imaginary parts of the boson self energy under $p_0 \to -p_0$. Using (F.4), we take the Fourier transform of the imaginary part of the retarded propagator:

$$\begin{aligned} C_1(p_0) \quad &= 2i\mathrm{Im}D_{ret}(P) = \int d^4(X-Y)e^{iP\cdot(X-Y)}(D_{ret}(X-Y) - D_{adv}(X-Y)) \\ &= -i\int d^4(X-Y)e^{iP\cdot(X-Y)}(\theta(x_0-y_0)+\theta(y_0-x_0))\langle[\phi(X),\phi(Y)]_-\rangle \\ &= -i\int d^4(X-Y)e^{iP\cdot(X-Y)}\sum_{n,m}[e^{-\beta E_n} - e^{-\beta E_m}]e^{i(P_n-P_m)\cdot(X-Y)}\langle n|\phi(0)|m\rangle\langle m|\phi(0)|n\rangle \\ &= -i\sum_{n,m}[e^{-\beta E_n} - e^{-\beta E_m}]\delta^3(\vec{p}+\vec{p_n}-\vec{p_m})\delta(p_0+E_n-E_m)\langle n|\phi(0)|m\rangle\langle m|\phi(0)|n\rangle. \end{aligned} \tag{F.10}$$

Now consider the transformation $p_0 \to -p_0$:

$$\begin{aligned} C_1(-p_0) \quad &= -i\sum_{n,m}[e^{-\beta E_n} - e^{-\beta E_m}]\delta^3(\vec{p}+\vec{p_n}-\vec{p_m})\delta(p_0-E_n+E_m)\langle n|\phi(0)|m\rangle\langle m|\phi(0)|n\rangle \\ &= -i\sum_{n,m}[e^{-\beta E_m} - e^{-\beta E_n}]\delta^3(\vec{p}+\vec{p_n}-\vec{p_m})\delta(p_0+E_n-E_m)\langle n|\phi(0)|m\rangle\langle m|\phi(0)|n\rangle \\ &= -C_1(p_0). \end{aligned} \tag{F.11}$$

Note that in the second line we switched the indices m and n to get back to our original $C_1(p_0)$. We have also made use of the fact that the 3-momentum delta function and matrix elements are not effected by this switch due to rotational symmetry.

Therefore, the imaginary part of the retarded boson propagator is odd with respect to p_0:

$$\mathrm{Im}D_{ret}(p_0,p) = -\mathrm{Im}D_{ret}(-p_0,p). \tag{F.12}$$

Now consider the real part of the boson self energy. This calculation is more complicated than the one for the imaginary part due to the fact that the step functions do not combine as they did for the imaginary

part:

$$
\begin{aligned}
C_2(p_0) \quad &= 2\mathrm{Re}D_{ret}(P) = \int d^4(X-Y)e^{iP\cdot(X-Y)}(D_{ret}(X-Y)+D_{adv}(X-Y)) \\
&= -i\int d^4(X-Y)e^{iP\cdot(X-Y)}(\theta(x_0-y_0)-\theta(y_0-x_0))\langle[\phi(X),\phi(Y)]_-\rangle \\
&= \frac{1}{2\pi}\int d^4(X-Y)e^{iP\cdot(X-Y)}\int_{-\infty}^{\infty}d\tau\big[\frac{e^{-i\tau(x_0-y_0)}}{\tau+i\eta}-\frac{e^{i\tau(x_0-y_0)}}{\tau+i\eta}\big] \\
&\quad\cdot\sum_{n,m}[e^{-\beta E_n}-e^{-\beta E_m}]e^{i(P_n-P_m)\cdot(X-Y)}\langle n|\phi(0)|m\rangle\langle m|\phi(0)|n\rangle \\
&= \frac{1}{2\pi}\int_{-\infty}^{\infty}\frac{d\tau}{\tau+i\eta}\sum_{n,m}[e^{-\beta E_n}-e^{-\beta E_m}]\delta^3(\vec{p}+\vec{p_n}-\vec{p_m})\langle n|\phi(0)|m\rangle\langle m|\phi(0)|n\rangle \\
&\quad\cdot\big[\delta(p_0+E_n-E_m-\tau)-\delta(p_0+E_n-E_m+\tau)\big].
\end{aligned}
\tag{F.13}
$$

Switching the dummy variables m and n in the second energy delta function term of (F.13) and noting that the matrix elements and 3-momentum delta function are not affected,

$$
\begin{aligned}
C_2(p_0) &= \frac{1}{2\pi}\int_{-\infty}^{\infty}\frac{d\tau}{\tau+i\eta}\sum_{n,m}e^{-\beta E_n}\delta^3(\vec{p}+\vec{p_n}-\vec{p_m})\langle n|\phi(0)|m\rangle\langle m|\phi(0)|n\rangle \\
&\quad\cdot\big[\delta(p_0-E_n+E_m-\tau)+\delta(p_0+E_n-E_m+\tau)\big].
\end{aligned}
\tag{F.14}
$$

Note that the sign switch in the second energy delta function is a result of $[e^{-\beta E_n}-e^{-\beta E_m}]$ being odd under the transformation $m \to n$.

Now, consider the effect of substituting $p_0 \to -p_0$ into (F.14):

$$
\begin{aligned}
C_2(-p_0) \quad &= \frac{1}{2\pi}\int_{-\infty}^{\infty}\frac{d\tau}{\tau+i\eta}\sum_{n,m}[e^{-\beta E_n}-e^{-\beta E_m}]\delta^3(\vec{p}+\vec{p_n}-\vec{p_m})\langle n|\phi(0)|m\rangle\langle m|\phi(0)|n\rangle \\
&\quad\cdot\big[\delta(p_0+E_n-E_m+\tau)+\delta(p_0-E_n+E_m-\tau)\big] \\
&= C_2(p_0).
\end{aligned}
\tag{F.15}
$$

Therefore, the real part of the retarded boson propagator is even with respect to p_0:

$$
\mathrm{Re}D_{ret}(p_0,p) = \mathrm{Re}D_{ret}(-p_0,p). \tag{F.16}
$$

Now we will show that the real part of the boson self energy is even and the imaginary part is odd. Using (F.12) and (F.16)we can express the propagator as

$$
D_{ret}(P) = D_{even}(p_0,p) + iD_{odd}(p_0,p) \tag{F.17}
$$

where $D_{even}(p_0, p)$ and $D_{odd}(p_0, p)$ are real functions and the subscript indicates the symmetry with respect to $p_0 \to -p_0$. We define the inverse propagator as

$$D_{ret}(P)^{-1} = R_{even}(p_0, p) + R_{odd}(p_0, p) + iI_{even}(p_0, p) + iI_{odd}(p_0, p) \tag{F.18}$$

where $R_{even/odd}(p_0, p)$ and $I_{even/odd}(p_0, p)$ are real functions. We will suppress the momentum arguments in intermediate calculations for brevity.

Using $D(P)D(P)^{-1} = 1$, we can deduce the symmetry of the real and imaginary parts of the inverse propagator:

$$\begin{aligned} &D_{ret}(P)D_{ret}(P)^{-1} = 1 = (D_{even} + iD_{odd})(R_{even} + R_{odd} + iI_{even} + iI_{odd}) \\ &= [D_{even}R_{even} - D_{odd}I_{odd}] + [D_{even}R_{odd} - D_{odd}I_{even}] \\ &+i[D_{even}I_{even} + D_{odd}R_{odd}] + i[D_{even}I_{odd} + D_{odd}R_{even}]. \end{aligned} \tag{F.19}$$

This gives us the systems of equations

$$\begin{aligned} &D_{even}R_{even} - D_{odd}I_{odd} = 1 \\ &D_{even}R_{odd} - D_{odd}I_{even} = D_{even}I_{even} + D_{odd}R_{odd} = D_{even}I_{odd} + D_{odd}R_{even} = 0. \end{aligned} \tag{F.20}$$

The solutions for $R_{even/odd}$ and $I_{even/odd}$ are

$$\begin{aligned} R_{odd} &= I_{even} = 0 \\ R_{even} &= \frac{D_{even}}{D_{even}^2 + D_{odd}^2} \\ I_{odd} &= -\frac{D_{odd}}{D_{even}^2 + D_{odd}^2}. \end{aligned} \tag{F.21}$$

Therefore, the inverse retarded boson propagator is given by

$$D_{ret}(P)^{-1} = R_{even}(p_0, p) + iI_{odd}(p_0, p). \tag{F.22}$$

Using the Dyson equation,

$$\begin{aligned} R_{even}(p_0, p) + iI_{odd}(p_0, p) \qquad &= P^2 - m^2 - \Pi(p_0, p) \\ &= P^2 - m^2 - \mathrm{Re}\Pi(p_0, p) - i\mathrm{Im}\Pi(p_0, p) \end{aligned}$$

$$R_{even}(p_0,p) = P^2 - m^2 - \mathrm{Re}\Pi(p_0,p)$$
$$I_{odd}(p_0,p) = -\mathrm{Im}\Pi(p_0,p). \tag{F.23}$$

From (F.23), it is clear the $\mathrm{Re}\Pi(p_0,p)$ is even and $\mathrm{Im}\Pi(p_0,p)$ is odd with respect to $p_0 \to -p_0$.

Thus, we have proven the first two relations of (F.1).

F3 Fermion Self Energy

In this section we determine the symmetries of the fermion self energy. The bare propagator, inverse propagator and self energy are decomposed in the usual manner (see appendix B). The symmetry of the propagators can be determined similar to the method used for the boson symmetry relations (F.12) and (F.16). We will start from [6],

$$\mathrm{Re}\Delta_+(p_0,p) = -\mathrm{Re}\Delta_-(-p_0,p)$$
$$\mathrm{Im}\Delta_+(p_0,p) = \mathrm{Im}\Delta_-(-p_0,p). \tag{F.24}$$

The propagator and inverse propagator are

$$S(p_0,p) = \Delta_+(p_0,p)P_-(p) + \Delta_-(p_0,p)P_+(p)$$
$$S^{-1}(p_0,p) = \Upsilon_+(p_0,p)P_-(p) + \Upsilon_-(p_0,p)P_+(p). \tag{F.25}$$

Multiplying the propagator and the inverse propagator and using the relations of P_+ and P_- (B.27) gives

$$S(P)S^{-1}(P) = 1 = 2\big(\Delta_+(p_0,p)\Upsilon_-(p_0,p) + \Delta_-(p_0,p)\Upsilon_+(p_0,p)\big)$$
$$+ 2\gamma_0\vec{\gamma}\cdot\hat{p}\big(\Delta_+(p_0,p)\Upsilon_-(p_0,p) - \Delta_-(p_0,p)\Upsilon_+(p_0,p)\big). \tag{F.26}$$

From (F.26) it is clear that

$$\Delta_+(p_0,p)\Upsilon_-(p_0,p) + \Delta_-(p_0,p)\Upsilon_+(p_0,p) = \frac{1}{2}$$
$$\Delta_+(p_0,p)\Upsilon_-(p_0,p) - \Delta_-(p_0,p)\Upsilon_+(p_0,p) = 0. \tag{F.27}$$

From this point on we will suppress the 3-momentum in the argument, as it will always be p. Breaking down $\Delta_\pm$ and $\Upsilon_\pm$ into the corresponding real and imaginary components and using (F.27), we end up with four

equations:

$$\begin{aligned}
&\mathrm{Re}\Delta_+(p_0)\mathrm{Re}\Upsilon_-(p_0) - \mathrm{Im}\Delta_+(p_0)\mathrm{Im}\Upsilon_-(p_0) + \mathrm{Re}\Delta_-(p_0)\mathrm{Re}\Upsilon_+(p_0) - \mathrm{Im}\Delta_-(p_0)\mathrm{Im}\Upsilon_+(p_0) = \frac{1}{2}\\
&\mathrm{Re}\Delta_+(p_0)\mathrm{Im}\Upsilon_-(p_0) + \mathrm{Im}\Delta_+(p_0)\mathrm{Re}\Upsilon_-(p_0) + \mathrm{Re}\Delta_-(p_0)\mathrm{Im}\Upsilon_+(p_0) + \mathrm{Im}\Delta_-(p_0)\mathrm{Re}\Upsilon_+(p_0) = 0\\
&\mathrm{Re}\Delta_+(p_0)\mathrm{Re}\Upsilon_-(p_0) - \mathrm{Im}\Delta_+(p_0)\mathrm{Im}\Upsilon_-(p_0) - \mathrm{Re}\Delta_-(p_0)\mathrm{Re}\Upsilon_+(p_0) + \mathrm{Im}\Delta_-(p_0)\mathrm{Im}\Upsilon_+(p_0) = 0\\
&\mathrm{Re}\Delta_+(p_0)\mathrm{Im}\Upsilon_-(p_0) + \mathrm{Im}\Delta_+(p_0)\mathrm{Re}\Upsilon_-(p_0) - \mathrm{Re}\Delta_-(p_0)\mathrm{Im}\Upsilon_+(p_0) - \mathrm{Im}\Delta_-(p_0)\mathrm{Re}\Upsilon_+(p_0) = 0.
\end{aligned} \tag{F.28}$$

Now, consider the effect of the substitution $p_0 \to -p_0$ in (F.28). This gives four more equations which, using (F.24), have the form

$$\begin{aligned}
&-\mathrm{Re}\Delta_-(p_0)\mathrm{Re}\Upsilon_-(-p_0) - \mathrm{Im}\Delta_-(p_0)\mathrm{Im}\Upsilon_-(-p_0) - \mathrm{Re}\Delta_+(p_0)\mathrm{Re}\Upsilon_+(-p_0) - \mathrm{Im}\Delta_+(p_0)\mathrm{Im}\Upsilon_+(-p_0) = \frac{1}{2}\\
&-\mathrm{Re}\Delta_-(p_0)\mathrm{Im}\Upsilon_-(-p_0) + \mathrm{Im}\Delta_-(p_0)\mathrm{Re}\Upsilon_-(-p_0) - \mathrm{Re}\Delta_+(p_0)\mathrm{Im}\Upsilon_+(-p_0) + \mathrm{Im}\Delta_+(p_0)\mathrm{Re}\Upsilon_+(-p_0) = 0\\
&-\mathrm{Re}\Delta_-(p_0)\mathrm{Re}\Upsilon_-(-p_0) - \mathrm{Im}\Delta_-(p_0)\mathrm{Im}\Upsilon_-(-p_0) + \mathrm{Re}\Delta_+(p_0)\mathrm{Re}\Upsilon_+(-p_0) + \mathrm{Im}\Delta_+(p_0)\mathrm{Im}\Upsilon_+(-p_0) = 0\\
&-\mathrm{Re}\Delta_-(p_0)\mathrm{Im}\Upsilon_-(-p_0) + \mathrm{Im}\Delta_-(p_0)\mathrm{Re}\Upsilon_-(-p_0) + \mathrm{Re}\Delta_+(p_0)\mathrm{Im}\Upsilon_+(-p_0) - \mathrm{Im}\Delta_+(p_0)\mathrm{Re}\Upsilon_+(-p_0) = 0.
\end{aligned} \tag{F.29}$$

There are eight equations (F.28 and F.29) and eight unknowns ($\mathrm{Re}/\mathrm{Im}\Upsilon_\pm(\pm p_0)$). Solving the system of equations we obtain

$$\begin{aligned}
\mathrm{Re}\Upsilon_+(p_0) &= -\mathrm{Re}\Upsilon_-(-p_0)\\
\mathrm{Im}\Upsilon_+(p_0) &= \mathrm{Im}\Upsilon_-(-p_0)\\
\mathrm{Re}\Upsilon_-(p_0) &= -\mathrm{Re}\Upsilon_+(-p_0)\\
\mathrm{Im}\Upsilon_-(p_0) &= \mathrm{Im}\Upsilon_+(-p_0).
\end{aligned} \tag{F.30}$$

Now we can determine the parity of the components of the self energy from (B.26) and (F.25):

$$
\begin{aligned}
&S^{-1}(p_0,p) = \Upsilon_+(p_0)P_- + \Upsilon_-(p_0)P_+ = \big(p_0 - p - \Sigma_+(p_0)\big)P_+ + \big(p_0 + p - \Sigma_-(p_0)\big)P_- \\
&\Upsilon_+(p_0) = \big(p_0 + p - \Sigma_-(p_0)\big), \qquad \Upsilon_-(p_0) = \big(p_0 - p - \Sigma_+(p_0)\big) \\
&\mathrm{Re}\big(\Upsilon_+(p_0)\big) = p_0 + p - \mathrm{Re}\big(\Sigma_-(p_0)\big) \\
&\mathrm{Re}\big(\Upsilon_-(p_0)\big) = p_0 - p - \mathrm{Re}\big(\Sigma_+(p_0)\big) \\
&\mathrm{Im}\big(\Upsilon_+(p_0)\big) = -\mathrm{Im}\big(\Sigma_-(p_0)\big) \\
&\mathrm{Im}\big(\Upsilon_-(p_0)\big) = -\mathrm{Im}\big(\Sigma_+(p_0)\big).
\end{aligned}
\tag{F.31}
$$

Taking $p_0 \to -p_0$ in (F.31) and using (F.30) gives

$$
\begin{aligned}
&\mathrm{Re}\big(\Sigma_-(-p_0)\big) = -\mathrm{Re}\big(\Sigma_+(p_0)\big) \\
&\mathrm{Re}\big(\Sigma_+(-p_0)\big) = -\mathrm{Re}\big(\Sigma_-(p_0)\big) \\
&\mathrm{Im}\big(\Sigma_-(-p_0)\big) = \mathrm{Im}\big(\Sigma_+(p_0)\big) \\
&\mathrm{Im}\big(\Sigma_+(-p_0)\big) = \mathrm{Im}\big(\Sigma_-(p_0)\big).
\end{aligned}
\tag{F.32}
$$

Using (B.25) and (F.32) it is straightforward to show

$$
\begin{aligned}
&\mathrm{Re}\Sigma^{(0)}(-p_0) = -\mathrm{Re}\Sigma^{(0)}(p_0) \\
&\mathrm{Re}\Sigma^{(s)}(-p_0) = \mathrm{Re}\Sigma^{(s)}(p_0) \\
&\mathrm{Im}\Sigma^{(0)}(-p_0) = \mathrm{Im}\Sigma^{(0)}(p_0) \\
&\mathrm{Im}\Sigma^{(s)}(-p_0) = -\mathrm{Im}\Sigma^{(s)}(p_0).
\end{aligned}
\tag{F.33}
$$

Thus we have proven the last four lines of (F.1).

G NLO Imaginary (1 loop soft) Photon Self Energy

In this appendix we determine the order of the imaginary part of the (1 loop soft) photon self energy (see figure 1.4). The integral is obtained using the Feynman rules. Since the loop momentum is soft, we use dressed propagators, which have the form (appendix D)

$$\rho_{\pm}(\omega,k)=\frac{\omega^2-k^2}{2m_F^2}\Big[\delta(\omega-\omega_{\pm})+\delta(\omega+\omega_{\mp})\Big]+\theta(k^2-\omega^2)\beta_{\pm}(\omega,k). \tag{G.1}$$

Note that we suppress the momentum argument of ω and $\omega_{\pm}$ since it is always k. Using (G.1), the integral for the (1 loop soft) imaginary photon self energy diagram is

$$\begin{aligned}
&\mathrm{Im}\Pi(q_0,q\to 0)=\frac{e^2}{2\pi^2}\int_0^{\infty}k^2dk\int_{-\infty}^{\infty}d\omega\int_{-\infty}^{\infty}d\omega'\big(N_F(\omega)+N_F(\omega')\big)\delta(E-\omega-\omega')\\
&\times\Bigg\{4\bigg(1-\frac{(\omega^2-\omega'^2)}{2kq_0}\bigg)^2\rho_+(\omega,k)\rho_-(\omega',k)+\bigg(1+\frac{(\omega^2+\omega'^2-2k^2)}{2kq_0}\bigg)^2\rho_+(\omega,k)\rho_+(\omega',k)\\
&+\bigg(1-\frac{(\omega^2+\omega'^2-2k^2)}{2kq_0}\bigg)^2\rho_-(\omega,k)\rho_-(\omega',k)+\theta(k^2-\omega^2)\frac{m_F^2}{4kq_0^2}\bigg(1-\frac{\omega^2}{k^2}\bigg)\\
&\times\bigg[\bigg(1+\frac{\omega}{k}\bigg)\rho_+(\omega',k)+\bigg(1-\frac{\omega}{k}\bigg)\rho_-(\omega',k)\bigg]\Bigg\}.
\end{aligned} \tag{G.2}$$

Substitution of $\rho_{\pm}$ into (G.2) leads to cancellations in the integrand. In this calculation we only include the pole-cut terms. The cut-cut terms will contribute at the same order. However, if we want to check our result by expanding in the bare theory, the cut-cut terms correspond to 3-loop terms. Thus, we neglect them here in order to compare our result to bare theory and check to see if terms were missed. Therefore,

$$\begin{aligned}
\rho_+(\omega,k)\rho_+(\omega',k)&\to\frac{\omega^2-k^2}{2m_F^2}\Big[\delta(\omega-\omega_+)+\delta(\omega+\omega_-)\Big]\theta(k^2-\omega'^2)\beta_+(\omega',k)\\
&+\frac{\omega'^2-k^2}{2m_F^2}\Big[\delta(\omega'-\omega_+)+\delta(\omega'+\omega_-)\Big]\theta(k^2-\omega^2)\beta_+(\omega,k)\\
\rho_+(\omega,k)\rho_-(\omega',k)&\to\frac{\omega^2-k^2}{2m_F^2}\Big[\delta(\omega-\omega_+)+\delta(\omega+\omega_-)\Big]\theta(k^2-\omega'^2)\beta_-(\omega',k)\\
&+\frac{\omega'^2-k^2}{2m_F^2}\Big[\delta(\omega'-\omega_-)+\delta(\omega'+\omega_+)\Big]\theta(k^2-\omega^2)\beta_+(\omega,k)\\
\rho_-(\omega,k)\rho_-(\omega',k)&\to\frac{\omega^2-k^2}{2m_F^2}\Big[\delta(\omega-\omega_-)+\delta(\omega+\omega_+)\Big]\theta(k^2-\omega'^2)\beta_-(\omega',k)\\
&+\frac{\omega'^2-k^2}{2m_F^2}\Big[\delta(\omega'+\omega_+)+\delta(\omega'-\omega_-)\Big]\theta(k^2-\omega^2)\beta_-(\omega,k).
\end{aligned} \tag{G.3}$$

We are interested in the limit as k becomes hard, as this provides the maximal order from power counting. In the limit $k >> m_F$, the mode frequencies are (1.4.13):

$$\omega_+ \approx k + \frac{m_F^2}{k}$$
$$\omega_- \approx k + \frac{2k}{e}\exp\left(\frac{2k^2}{m_F^2}\right).$$

The residues of the quasi-particle poles for large values of k are given as (1.4.16) and (1.4.16):

$$Z_+(k) \approx 1 + \frac{m_F^2}{2k^2}\left[1 - \ln\left(\frac{2k^2}{m_F^2}\right)\right]$$
$$Z_-(k) \approx \frac{2k^2}{em_F^2}\exp\left(-\frac{2k^2}{m_F^2}\right).$$

The residues defined in (1.4.16) tend to zero, thus we neglect any terms in (G.2) with a delta function of argument $(\omega \pm \omega_-)$. Substitution of (G.3) into (G.2) and neglecting the mass gives

$$\begin{aligned}
&\mathrm{Im}\Pi(q_0, q \to 0) \approx \frac{e^2}{2\pi^2}\int_0^\infty k^2 dk \int_{-\infty}^\infty d\omega \int_{-\infty}^\infty d\omega' \big(N_F(\omega) + N_F(\omega')\big)\delta(E - \omega - \omega') \\
&\times\Bigg\{4\left(1 - \frac{(\omega^2 - \omega'^2)}{2kq_0}\right)^2\Bigg\{\frac{\omega^2 - k^2}{2m_F^2}\delta(\omega - \omega_+)\theta(k^2 - \omega'^2)\beta_-(\omega', k) \\
&\quad + \frac{\omega'^2 - k^2}{2m_F^2}\delta(\omega' + \omega_+)\theta(k^2 - \omega^2)\beta_+(\omega, k)\Bigg\} \\
&+\left(1 + \frac{(\omega^2 + \omega'^2 - 2k^2)}{2kE}\right)^2\Bigg\{\frac{\omega^2 - k^2}{2m_F^2}\delta(\omega - \omega_+)\theta(k^2 - \omega'^2)\beta_+(\omega', k) \\
&+\frac{\omega'^2 - k^2}{2m_F^2}\delta(\omega' - \omega_+)\theta(k^2 - \omega^2)\beta_+(\omega, k)\Bigg\} \\
&+\left(1 - \frac{(\omega^2 + \omega'^2 - 2k^2)}{2kE}\right)^2\Bigg\{\frac{\omega^2 - k^2}{2m_F^2}\delta(\omega + \omega_+)\theta(k^2 - \omega'^2)\beta_-(\omega', k) \\
&+\frac{\omega'^2 - k^2}{2m_F^2}\delta(\omega' + \omega_+)\theta(k^2 - \omega^2)\beta_-(\omega, k)\Bigg\} \\
&+\theta(k^2 - \omega^2)\frac{\omega'^2 - k^2}{2m_F^2}\frac{m_F^2}{4kE^2}\left(1 - \frac{\omega^2}{k^2}\right)\left[\left(1 + \frac{\omega}{k}\right)\delta(\omega' - \omega_+) + \left(1 - \frac{\omega}{k}\right)\delta(\omega' + \omega_+)\right]\Bigg\}.
\end{aligned} \tag{G.4}$$

The two integrations $d\omega$ and $d\omega'$ can be done using the two delta functions in each term of (G.4). We start by integrating with the delta function from the spectral density:

$$
\begin{aligned}
&\mathrm{Im}\Pi(q_0, q\to 0) \approx \frac{e^2}{2\pi^2}\int_0^\infty k^2 dk \frac{\omega_+^2-k^2}{2m_F^2}\Big[\int_{-\infty}^{\infty} d\omega' \\
&\Big\{4\Big(1-\frac{(\omega_+^2-\omega'^2)}{2kq_0}\Big)^2\theta(k^2-\omega'^2)\beta_-(\omega',k)\big(N_F(\omega')+N_F(\omega_+)\big)\delta(q_0-\omega_+-\omega') \\
&+\Big(1+\frac{\omega_+^2+\omega'^2-2k^2}{2kq_0}\Big)^2\theta(k^2-\omega'^2)\beta_+(\omega',k)\big(N_F(\omega')+N_F(\omega_+)\big)\delta(q_0-\omega_+-\omega') \\
&+\Big(1-\frac{(\omega'^2+\omega_+^2-2k^2)}{2kq_0}\Big)^2\theta(k^2-\omega'^2)\beta_-(\omega',k)\big(N_F(\omega')+N_F(-\omega_+)\big)\delta(q_0+\omega_+-\omega')\Big\} \\
&+\int_{-\infty}^{\infty} d\omega\Big\{4\Big(1-\frac{(\omega^2-\omega_+^2)}{2kq_0}\Big)^2\theta(k^2-\omega^2)\beta_+(\omega,k)\big(N_F(\omega)+N_F(-\omega_+)\big)\delta(q_0-\omega+\omega_+) \\
&+\Big(1+\frac{(\omega^2+\omega_+^2-2k^2)}{2kq_0}\Big)^2\theta(k^2-\omega^2)\beta_+(\omega,k)\big(N_F(\omega)+N_F(\omega_+)\big)\delta(E-\omega-\omega_+) \\
&+\Big(1-\frac{(\omega^2+\omega_+^2-2k^2)}{2kq_0}\Big)^2\theta(k^2-\omega^2)\beta_-(\omega,k)\big(N_F(\omega)+N_F(-\omega_+)\big)\delta(q_0-\omega+\omega_+) \\
&+\theta(k^2-\omega^2)\frac{m_F^2}{4kq_0^2}\Big(1-\frac{\omega^2}{k^2}\Big)\Big[\Big(1+\frac{\omega}{k}\Big)\big(N_F(\omega)+N_F(\omega_+)\big)\delta(q_0-\omega-\omega_+) \\
&+\Big(1-\frac{\omega}{k}\Big)\big(N_F(\omega)+N_F(-\omega_+)\big)\delta(q_0-\omega+\omega_+)\Big]\Big\}\Big].
\end{aligned}
$$

We use the remaining delta function to perform the other frequency integral and drop terms in which the argument of the step function is negative:

$$
\begin{aligned}
&\mathrm{Im}\Pi(q_0, q\to 0) \approx \frac{e^2}{2\pi^2}\int_0^\infty k^2 dk \frac{\omega_+^2-k^2}{2m_F^2} \\
&\big[4\Big(1-\frac{(\omega_+^2-(q_0-\omega_+)^2)}{2kq_0}\Big)^2\theta(k^2-(q_0-\omega_+)^2)\beta_-(E-\omega_+,k)\big(N_F(q_0-\omega_+)+N_F(\omega_+)\big) \\
&+\Big(1+\frac{\omega_+^2+(q_0-\omega_+)^2-2k^2}{2kq_0}\Big)^2\theta(k^2-(q_0-\omega_+)^2)\beta_+(q_0-\omega_+,k)\big(N_F(q_0-\omega_+)+N_F(\omega_+)\big) \\
&+\Big(1+\frac{((q_0-\omega_+)^2+\omega_+^2-2k^2)}{2kq_0}\Big)^2\theta(k^2-(q_0-\omega_+)^2)\beta_+(q_0-\omega_+,k)\big(N_F(q_0-\omega_+)+N_F(\omega_+)\big) \\
&+\frac{m_F^2}{4kq_0^2}\theta(k^2-(q_0-\omega_+)^2)\Big(1-\frac{(q_0-\omega_+)^2}{k^2}\Big)\Big(1+\frac{q_0-\omega_+}{k}\Big)\big(N_F(q_0-\omega_+)+N_F(\omega_+)\big).
\end{aligned}
\tag{G.5}
$$

For small masses and $k >> q_0$, using (1.4.13) in [18],

$$
\begin{aligned}
\beta_+(q_0-\omega_+,k) &\approx \frac{m_F^2}{4k^3} \\
\beta_-(q_0-\omega_+,k) &\approx \frac{m_F^2}{2k^2q_0}.
\end{aligned}
\tag{G.6}
$$

Substituting (1.4.13) and (G.6) into (G.5) gives

$$\mathrm{Im}\Pi(q_0, q \to 0) = \frac{e^2}{8\pi} m_F^2 \int_0^\infty \frac{dk}{k} \theta(2q_0 k - q_0^2 - 2m_F^2)\big(N_F(k) + N_F(q_0 - k)\big). \tag{G.7}$$

We will take the upper limit of the integration to be T since we know that distribution functions will provide an UV cutoff. The lower limit is obtained from the step function of (G.7), as the argument must be positive or else the step function vanishes. Therefore, (G.7) becomes

$$\mathrm{Im}\Pi(q_0, q \to 0) = \frac{e^2 m_F^2}{8\pi^2} \int_{\frac{q_0^2 + 2m_F^2}{2q_0}}^{T} \frac{dk}{k}\big(N_F(k) + N_F(q_0 - k)\big). \tag{G.8}$$

Expanding the statistical factor combination of (G.8) in $\frac{q_0}{k}$, we find that $N_F(k) + N_F(q_0 - k) \approx \frac{q_0}{k}$. Therefore,

$$\begin{aligned} \mathrm{Im}\Pi(q_0, q \to 0) \quad &\approx \frac{e^2 m_F^2 q_0}{8T\pi^2} \int_{\frac{q_0^2 + 2m_F^2}{2q_0}}^{T} \frac{dk}{k} \\ &\approx \frac{e^2 m_F^2 q_0}{8\pi^2 T} \ln\left(\frac{2q_0 T}{q_0^2 + 2m_F^2}\right). \end{aligned} \tag{G.9}$$

Therefore, the imaginary part of the photon self energy is of order $\frac{e^2 m_F^2 q_0}{T} \ln\left(\frac{1}{e}\right)$.

H NLO (1 loop hard correction) Calculations

H1 Real, Fermion

In this appendix we will determine the order of the (1 loop hard correction) term for the real part of the NLO fermion self energy (see figure 1.5). This calculation was done in [18]. We consider $\Sigma^{(0)}$ and take only the term with the boson distribution function:

$$\begin{aligned}
\text{(1 loop hard correction real fermion)} \qquad & \propto g^2 \int d^4k \mathrm{Tr}[\gamma_0 \not{K}] D_{sym}(K) S_{ret}(K+Q) \\
& \propto g^2 \int d^4k \frac{k_0 \mathrm{sgn} k_0 N_B(k_0) \delta(K^2)}{K^2 + 2K\cdot Q + Q^2} \\
& \propto g^2 \int \frac{d^3k}{k} \sum_{n=\pm 1} \frac{nk N_B(k)}{2nkq_0 + q_0^2} \\
& \propto g^2 \int dk N_B(k) k \sum_{n=\pm 1} \frac{nk}{2nkq_0(1+\frac{nq_0}{2k})} \\
& \propto g^2 \int \frac{dk N_B(k) k}{q_0} \sum_{n=\pm 1} (1 - \frac{nq_0}{2k} + \frac{q_0^2}{4k^2} + ...). \qquad \text{(H.1)}
\end{aligned}$$

The leading order term is given by

$$\text{LO} \propto g^2 \int dk \sum_{n=\pm 1} \frac{kN_B(k)}{q_0} \sim \frac{g^2T^2}{q_0} \sim gT \qquad \text{(H.2)}$$

which matches the leading order result we previously derived in appendix C3, and the parity of q_0 is correct.

Now, consider the NLO term. We take the next term from the power series of (H.1):

$$\text{2nd term} \propto g^2 \int dk \frac{kN_B(k)}{q_0} \frac{nq_0}{k} \to 0. \qquad \text{(H.3)}$$

(H.3) vanishes under the sum over n, as does any term in the power series from (H.1) that has a factor of n. It is clear that all terms that have a factor of n vanish under the summation. These terms also contain even powers of q_0. This makes sense from a parity standpoint, as we expect the real part of $\Sigma^{(0)}$ to be odd with respect to q_0. The NLO term is then given by

$$\text{NLO} \propto g^2 \int dk \frac{kN_B(k)}{q_0} \frac{q_0^2}{k^2} \propto g^2 q_0 \int dk \frac{N_B(k)}{k} \sim g^2 q_0 \ln(\frac{1}{g}) \sim g^3 T \ln(\frac{1}{g}). \qquad \text{(H.4)}$$

Therefore, the NLO term is $g^2\ln(\frac{1}{g})(LO)$ and not $g(LO)$ as we expected using naive power counting. This result is subleading relative to the (1 loop soft) result. Similar results can be shown for $\Sigma^{(s)}$ and for terms

involving the fermion statistical distribution. Therefore, we do not have to include the (1 loop hard) term in the calculation of the NLO real fermion self energy.

H2 Real, Boson

In this section we consider the real part of a soft, static boson ($q \to 0$):

$$\text{(1 loop hard correction real boson)} \qquad \propto g^2 \int d^4k \mathrm{Tr}[\gamma_0 \not{K} \gamma_0 (\not{K} + \not{Q})] \left[\frac{\mathrm{sgn}(k_0) N_F(k_0) \delta(K^2)}{(K+Q)^2} + \frac{\mathrm{sgn}(k_0+q_0) N_F(k_0+q_0) \delta((K+Q)^2)}{K^2} \right]. \tag{H.5}$$

Evaluating the trace factor gives

$$\begin{aligned} & g^{\mu\nu} \mathrm{Tr}[\gamma_\mu \not{K} \gamma_\nu (\not{\ell}(K) + \not{\ell}(Q))] \propto g^{\mu\nu} K^\alpha (K+Q)^\beta \mathrm{Tr}[\gamma_\mu \gamma_\alpha \gamma_\nu \gamma_\beta] \\ & \propto g^{\mu\nu} K^\alpha (K+Q)^\beta [g_{\mu\alpha} g_{\nu\beta} - g_{\mu\nu} g_{\alpha\beta} + g_{\mu\beta} g_{\nu\alpha}] \propto g^{\mu\nu} [K_\mu (K+Q)_\nu + K_\nu (K+Q)_\mu - g_{\mu\nu} K \cdot (K+Q)] \\ & \propto K \cdot (K+Q). \end{aligned} \tag{H.6}$$

Substitution of (H.6) into (H.5) gives

$$\begin{aligned} \text{(1 loop hard correction real boson)} \qquad & \propto g^2 \int d^4k \mathrm{sgn}(k_0) N_F(k_0) \delta(K^2) \left[\frac{k_0(k_0+q_0) - k^2}{(K+Q)^2} + \frac{k_0(k_0-q_0) - k^2}{(K-Q)^2} \right] \\ & \propto g^2 \int d^3k \frac{N_F(k)}{k} \sum_{n=\pm 1} \left[\frac{nkq0}{2nkq_0 + q_0^2} + \frac{nkq_0}{2nkq_0 - q_0^2} \right] \\ & \propto g^2 \int dk N_F(k) k \sum_{n=\pm 1} \left[\frac{1}{1 + \frac{nq_0}{2k}} + \frac{1}{1 - \frac{nq_0}{2k}} \right] \\ & \propto g^2 \int dk N_F(k) k \sum_{n=\pm 1} \left[1 - \frac{nq_0}{2k} + \frac{q_0^2}{4k^2} + ... + 1 + \frac{nq_0}{2k} + \frac{q_0^2}{4k^2} + ... \right] \\ & \propto g^2 \int dk N_F(k) k \sum_{n=\pm 1} \left[1 + \frac{q_0^2}{4k^2} + ... \right]. \end{aligned}$$

It is interesting to note that terms with a factor of n vanished due to the fact that both propagators had the same statistical distribution, and would have vanished anyway under the summation. These terms also have a different parity than expected for the real part of the boson self energy.

Consider the leading order self energy from (H.7):

$$\text{LO} \propto g^2 \int dk k N_F(k) \sim g^2 T^2. \tag{H.7}$$

This is the same order we obtained from the leading order calculation of the longitudinal and transverse boson self energies from appendix C2. Now, consider the NLO contribution:

$$\text{NLO} \propto g^2 \int dk N_F(k) \frac{q_0^2}{k} \propto g^2 q_0^2 \ln(\frac{1}{g}) \propto g^4 T^2 \ln\left(\frac{1}{g}\right) \tag{H.8}$$

where we used [19] to obtain the logarithm in (H.8). As with the real part of the fermion self energy, the term of order predicted by [1] vanishes, and as a result the (1 loop hard correction) term is of order $g^2 \ln\left(\frac{1}{g}\right)(LO)$. Since the (1 loop hard correction) term is subleading relative to the result from the (1 loop soft) diagram, we can neglect it at NLO.

I Furry's Theorem

Furry's theorem states that the amplitude for a diagram consisting of an odd number of external photon legs is zero. This can be proven in the following way: consider a diagram with 3 external photon legs (the general case can be deduced in a straightforward manner). We will be following the strategy presented in [24]. Consider two diagrams with the same external momenta but with the internal momenta traveling in the opposite direction.

$$\begin{aligned}\Gamma_1 &= -ig^3 \int d^4k \mathrm{Tr}[\gamma_\mu \not{K} \gamma_\nu (\not{K} + \not{Q}_1)\gamma_\lambda (\not{K} + \not{Q}_1 + \not{Q}_2)]\tilde{\Delta}(K)\tilde{\Delta}(K+Q_1)\tilde{\Delta}(K+Q_1+Q_2) \\ \Gamma_2 &= -ig^3 \int d^4k \mathrm{Tr}[\gamma_\mu (-\not{K} - \not{Q}_1 - \not{Q}_2)\gamma_\lambda (-\not{K} - \not{Q}_1)\gamma_\nu (-\not{K})]\tilde{\Delta}(-K)\tilde{\Delta}(-K-Q_1)\tilde{\Delta}(-K-Q_1-Q_2).\end{aligned} \tag{I.1}$$

Consider the trace in each term. We can bring out the minus sign to make all of the factors in Γ_2 positive:

$$\mathrm{Tr}_2 = \mathrm{Tr}[\gamma_\mu (\not{K} + \not{Q}_1 + \not{Q}_2)\gamma_\lambda (\not{K} + \not{Q}_1)\gamma_\nu \not{K}]. \tag{I.2}$$

Now we will use the charge-conjugation operator to simplify Γ_2, where U_C is the charge conjugation matrix. Application of the charge conjugation on the fermion propagators changes the fermion particles to antiparticles, which travel in the opposite direction of the fermion particles. Note that $U_C U_C^{-1} = 1$ and $\mathrm{Tr}[\Lambda]^T = \mathrm{Tr}[\Lambda]$ for any matrix Λ, and $U_C^{-1}\gamma_\mu U_C = -\gamma_\mu^T$. Plugging in $U_C U_C^{-1}$ into Γ_2 gives:

$$\begin{aligned}\mathrm{Tr}_2 &= \mathrm{Tr}[U_C U_C^{-1}\gamma_\mu U_C U_C^{-1}(K+Q_1+Q_2)^i \gamma_i U_C U_C^{-1}\gamma_\lambda U_C U_C^{-1}(K+Q_1)^j \gamma_j U_C U_C^{-1}\gamma_\nu K^k \gamma_k] \\ &= \mathrm{Tr}(-1)^6[\gamma_\mu^T (K+Q_1+Q_2)^i \gamma_i^T \gamma_\lambda^T (K+Q_1)^j \gamma_j^T \gamma_\nu^T K^k \gamma_k^T] \\ &= \mathrm{Tr}[K^k \gamma_k \gamma_\nu (K+Q_1)^j \gamma_j \gamma_\lambda (K+Q_1+Q_2)^i \gamma_i \gamma_\mu]^T \\ &= \mathrm{Tr}[\gamma_\mu \not{K} \gamma_\nu (\not{K} + \not{Q}_1)\gamma_\lambda (\not{K} + \not{Q}_1 + \not{Q}_2)] \\ &= -\mathrm{Tr}_1.\end{aligned} \tag{I.3}$$

Therefore, $\mathrm{Tr}_1 = -\mathrm{Tr}_1$ and thus $\mathrm{Tr}_1 = 0$.

Bibliography

[1] Eric Braaten and Robert D. Pisarski. Soft Amplitudes in Hot Gauge Theories: A General Analysis. *Nucl. Phys.*, B337:569, 1990.

[2] Michael E. Peskin and Daniel V. Schroeder. *An Introduction to Quantum Field Theory.* Westview Press, United States of America.

[3] Amitabha Lahiri and Palash B. Pal. *A First Book of Quantum Field Theory.* Alpha Science International Ltd., Harrow, United Kingdom.

[4] Markus H. Thoma. New developments and applications of thermal field theory. 2000.

[5] Ashok Das. *Finite Temperature Field Theory.* World Scientific, Singapore, 1997.

[6] Michel Le Bellac. *Thermal Field Theory.* Cambridge University Press, Cambridge, United Kingdom, 1996.

[7] M. E. Carrington and Ulrich W. Heinz. Three-point functions at finite temperature. *Eur. Phys. J.*, C1:619–625, 1998.

[8] C.D. Palmer and M.E. Carrington. A General expression for symmetry factors of Feynman diagrams. *Can.J.Phys.*, 80:847–854, 2002.

[9] M. E. Carrington, T. Fugleberg, D. S. Irvine, and D. Pickering. Real time statistical field theory. *Eur. Phys. J.*, C50:711–727, 2007.

[10] Eric Braaten and Robert D. Pisarski. Calculation of the gluon damping rate in hot QCD. *Phys.Rev.*, D42:2156–2160, 1990.

[11] John David Jackson. *Classical Electrodynamics Third Edition*. Wiley, 1998.

[12] M.E. Carrington and Yun Guo. A new method to calculate the n-Particle Irreducible Effective Action. 2011.

[13] Hermann Schulz. Gluon plasma frequency: The Next-to-leading order term. *Nucl.Phys.*, B413:353–395, 1994.

[14] P. Aurenche, F. Gelis, R. Kobes, and H. Zaraket. Two loop Compton and annihilation processes in thermal QCD. *Phys. Rev.*, D60:076002, 1999.

[15] P. Aurenche, F. Gelis, R. Kobes, and H. Zaraket. Bremsstrahlung and photon production in thermal QCD. *Phys. Rev.*, D58:085003, 1998.

[16] Eric Braaten, Robert D. Pisarski, and Tzu-Chiang Yuan. Production of Soft Dileptons in the Quark-Gluon. *Phys.Rev.Lett.*, 64:2242, 1990.

[17] M. E. Carrington, A. Gynther, and D. Pickering. The fermion mass at next-to-leading order in the HTL effective theory. *Phys. Rev.*, D78:045018, 2008.

[18] M. E. Carrington. The soft fermion dispersion relation at next-to-leading order in hot QED. *Phys. Rev.*, D75:045019, 2007.

[19] Indrajit Mitra. Gauge independence of limiting cases of one-loop electron dispersion relation in high-temperature QED. *Phys. Rev.*, D62:045023, 2000.

[20] T. Altherr and P. Aurenche. Finite Temperature QCD Corrections to Lepton Pair Formation in a Quark - Gluon Plasma. *Z.Phys.*, C45:99, 1989.

[21] P. Aurenche, F. Gelis, and H. Zaraket. Enhanced thermal production of hard dileptons by 3 –¿ 2 processes. *JHEP*, 07:063, 2002.

[22] J. J. Sakurai. *Modern Quantum Mechanics (Revised Edition)*. Addison Wesley, 1 edition, 1993.

[23] Kuang-chao Chou, Zhao-bin Su, Bai-lin Hao, and Lu Yu. Equilibrium and Nonequilibrium Formalisms Made Unified. *Phys.Rept.*, 118:1, 1985.

[24] E M Lifshitz V B Berestetskii and L P Pitaevskii. *Quantum Electrodynamics*. Butterworth-Heinemann, China, 2007.